

**Fibre Modification for Concrete Reinforcement
using a Novel Atmospheric Microwave Induced
Plasma Torch (MIPT)**

Luna Raouf Salh

A thesis submitted in partial fulfilment of the requirements of Liverpool John
Moores University for the degree of Doctor of Philosophy

March 2019

Acknowledgment

First, I would like to express my sincere appreciation and thanks to my supervision team Dr Denise Lee, Dr Andy Shaw and Dr Patryk Kot without their sustained support and guidance this study would not be possible. I will always be in debt to my supervisors for giving as much time as needed for discussion and guidance. Sincere thanks to all the technical staff in the concrete laboratories and workshops at the Liverpool John Moores University.

Finally, I would like to thank my family and friends for their love, guidance and encouragement at all times.

Abstract

This research investigates the design of a novel microwave induced plasma torch for the surface modification of non-corrosive fibres. The system was developed to reduce the equipment cost, and production time needed in the conventional plasma treatment.

To generate a consistent and low-cost microwave plasma jet at atmospheric pressure, a waveguide-based applicator at 5.8GHz was used. The system uses a microwave signal generator connected to a traveling wave tube to provide the required power. The applicator consists of a nozzle section and a tuning section to decrease the reflected power. Argon gas flows through the copper nozzle, and the high electrical field due to the microwave power, between the gas nozzle and an aperture in the waveguide, causes the gas to become a plasma that flows as a jet through the aperture and into the atmosphere. The effect of plasma treatment on surface characterisation of fibres was performed using contact angle measurement, scanning electron microscopy and atomic force microscope and the results are presented and analysed. Thus, the optimised plasma condition for each separate fibre is utilised. Fibres treated with optimised plasma condition were further used in investigating the fibre-matrix interfacial properties. Furthermore, the effect of the plasma treatment on the flexural behaviour of cementitious composites was investigated using three-point bending. The results show some improvement in the fibre surface properties, so there is a potential of using the developed plasma system in the production of construction composites.

List of Abbreviations

AFM	Atomic Force Microscopy
AR	Alkali Resistance
BF	Basalt Fibre
CAM	Contact Angle Measurement
ECC	Engineered Cementitious Composites
FRC	Fibre Reinforced Concrete
FRCC	Fibre Reinforced Cementitious Composite
GF	Glass Fibre
HPFRCC	High Performance Fibre Reinforced Cementitious Composite
ICP	Induction Coupled Plasma
ITZ	Interfacial Transition Zone
MIPT	Microwave Induced Plasma Torch
NACE	National Association of Corrosion Engineers
PP	Polypropylene Fibre
PPF1	Macro polypropylene Fibre
PVA	Polyvinyl Alcohol
RF	Radio Frequency
Rms	Nano Roughness
SEM	Scanning Electron Microscopy
TE	Transverse Electric
TM	Transverse Magnetic
TWTA	Travelling Wave Tube Amplifier
VSWR	Voltage Standing Wave Ratio

W/C Water Cement Ratio

List of Symbols

d	Beam spot diameter (μm)
X	Cantilever deflection (nm)
A_f	Cross sectional area of the fibre (mm^2)
l_e	Embedded length of the fibre in the matrix (mm)
σ	Fibre strength (mm)
D	Fibre's Diameter (mm)
P	Fibre's Perimeter (mm)
σ_b	Flexure strength (MPa)
Rms	Roughness (nm)
F	Force (N)
F_{fr}	Frictional force (N)
h	Height of the beam specimen (mm)
τ_{IFSS}	Interfacial shear strength (MPa)
l	Length of the beam specimen (mm)
θ	Liquid contact angle ($^\circ$)
F_{max}	Maximum force (N)
A	Objective aperture diameter (mm)
M	SEM magnification (μm)
K	Spring constant
γ_{LG}	Surface tension between liquid and gas (N/m)
γ_{SL}	Surface tension between solid and liquid (N/m)
γ_{SG}	Surface tension between solid and gas phase (N/m)
P_u	Ultimate load (N)

b Width of the beam specimen (mm)

Dw Working distance (mm)

Table of Contents

Acknowledgment	i
Abstract	ii
List of Abbreviations	iii
List of Symbols	v
Table of Contents	vii
List of Tables	xiii
List of Figures	xv
Chapter 1 Introduction	1
1.1 Introduction	1
1.2 Research Motivation	4
1.3 Scope	5
1.4 Aim and Objectives.....	7
1.5 Research Contribution.....	8
1.6 Thesis Organisation.....	8
Chapter 2 Review of Literature	10
2.1 Introduction	10
2.2 Fibre Reinforced Cement Composites (FRCC)	10
2.2.1 High Performance Fibre reinforced Cementitious Composites (HPFRCC)	15
2.2.2 Applications and Advantages of HPFRCC	17

2.2.3	Fibres for Reinforcing Cementitious Composites.....	21
2.2.4	Important Factors Affecting the Performance and Characteristics of HPFRCC	24
2.3	Interfacial Transition Zone (ITZ) and Types of Bonding Mechanisms.....	26
2.3.1	Interdiffusion Bonding.....	27
2.3.2	Electrostatic Bonding.....	27
2.3.3	Chemical Bonding.....	28
2.3.4	Mechanical Bonding	28
2.4	Surface Modification of Materials	28
2.4.1	Chemical Modification	31
2.4.2	Physical Modification	32
2.4.3	Mechanical Modification	32
2.4.4	Plasma Modification	34
2.4.4.1	Plasma Definition.....	35
2.3.4.2	Plasma Classifications.....	37
2.3.4.2	Types of Atmospheric Pressure Plasma (Thermal Plasma).....	39
2.3.4.4	Application of Plasma.....	43
2.3.4.5	Performance of Plasma Modified Fibre Reinforced Cementitious Composites.....	45
2.5	Summary	55
Chapter 3 Methodology		57
3.1	Introduction.....	57

3.2 Materials.....	57
3.2.1 Fibres.....	58
3.2.1.1 Macro Polypropylene Fibre (PPF1)	58
3.2.1.2 Glass Fibre (GF).....	59
3.2.1.3 Basalt Fibre (BF).....	59
3.2.2 Cement	61
3.2.3 Limestone Powder.....	61
3.2.4 Superplasticizer	62
3.2.5 Water	63
3.3 Fibre Surface Modification Procedure	63
3.3.1 Plasma Equipment.....	63
3.3.1.1 Signal Generator.....	64
3.3.1.2 Travelling Wave Tube Amplifier (TWTA).....	65
3.3.1.3 Waveguide.....	66
3.3.1.4 Stub Tuner	68
3.3.1.5 Plasma Interaction and Cavity Nozzle	69
3.3.2 Specimen Treatment Conditions	72
3.4 Specimen Characterisation Techniques	74
3.4.1 Surface Characterisation	74
3.4.1.1 Contact Angle Measurement (CAM)	74
3.4.1.2 Scanning Electron Microscopy (SEM)	78

3.4.1.3 Atomic Force Microscopy (AFM)	81
3.4.2 Mechanical Characterization.....	86
3.4.2.3 Tensile Test of Single Fibre	86
3.4.2.1 Single Fibre Pull-Out Test	88
3.4.2.2 Flexural Test.....	95
3.5 Summary	98
Chapter 4 Results and Discussions	99
4.1 Introduction	99
4.2 Plasma Temperature Profile	99
4.3 Surface Characterizations.....	101
4.3.1 Contact angle Measurements	101
4.3.1.1 Macro Polypropylene Fibre (PPF1)	101
4.3.1.2 Glass Fibre (GF).....	107
4.3.2 Scanning Electron Microscopy (SEM)	110
4.3.2.1 Macro Polypropylene Fibre (PPF1)	110
4.3.2.2 Glass Fibre (GF).....	112
4.3.2.3 Basalt Fibre (BF).....	114
4.3.3 Atomic Force Microscopy (AFM) Roughness Analysis.....	116
4.3.3.1 Macro polypropylene Fibre (PPF1)	117
4.3.3.2 Glass Fibre (GF).....	120
4.3.3.3 Basalt Fibre (BF).....	122

4.3.4 General Evaluation of Surface Characterization Variations Affected by Plasma Application on PPF1, GF and BF	124
4.5 Mechanical Characterization.....	126
4.5.1 Fibre Tensile Test.....	126
4.5.1.1 Macro Polypropylene Fibre (PPF1)	127
4.5.1.2 Glass Fibre (GF).....	129
4.5.1.3 Basalt Fibre (BF).....	131
The effect of plasma treatment on tensile strength of basalt fibre were investigated using similar methods to the PPF1 and GF.....	131
4.5.2 Single Fibre Pull-Out Test	132
4.5.2.1 Macro Polypropylene Fibre (PPF1)	133
4.5.2.2 Glass Fibre (GF).....	136
4.5.2.3 Basalt Fibre (BF).....	138
4.5.3 Flexural Test of Fibrous Composites	142
4.5.3.1 Fibre volume optimisation	142
4.5.3.2 28 Days Bending Performance of Plasma Treated PPF1 Composites	147
4.5.3.3 28 Days Bending Performance of Plasma Treated GF Fibre Composites.....	151
4.5.3.4 28 Days Bending Performance of Plasma Treated BF Fibre Composites	154

4.5.4 General Evaluation of mechanical Characterization Variations Affected by Plasma Application on PPF1, GF and BF	156
4.5.4.1 Evaluation of Bending Performances of PPF1 Fibre Composites ...	158
4.5.4.2 Evaluation of Bending Performances of GF Fibre Composites.....	159
4.5.4.3 Evaluation of Bending Performances of BF Fibre Composites.....	160
4.5.5 Summary	161
Chapter 5 Conclusions and Recommendations.....	162
5.1 Introduction.....	162
5.2 Conclusion	163
5.2.1 Surface Characterisation	163
5.2.1.1 Contact Angle Measurement (CAM).....	163
5.2.1.2 Surface Morphology (SEM) and (AFM).....	164
5.2.2 Mechanical Characterisation.....	164
5.2.2.1 Single Fibre Tensile Test	164
5.2.2.2 Single Fibre Pull-Out Test	164
5.2.2.3 Flexural Test.....	165
5.2.3 General Conclusion.....	165
5.3 Recommendations for Future Works	166
References	168

List of Tables

Table 2-1 Properties of structural fibres.....	24
Table 2-2 Current Techniques Used in Fibre Treatments for Cement Based Composites.....	30
Table 2-3 A summary of current plasma systems used in material processing application.....	42
Table 2-4 Contact angle of fibres before and after treatments (Zhang, Gopalaratnam and Yasuda, 1999).....	48
Table 2-5 Composite Mix proportion (Felekoglu, Tosun and Baradan, 2009).....	50
Table 2-6 Current Plasma Techniques Used in Fibre Treatments for Cement Based Composites.....	53
Table 3-1 Mix Design for Fibre reinforced Cement Based Composite (Brandan, Tosun and Felekoglu, 2008).....	57
Table 3-2 Physical and chemical properties of PPF1	58
Table 3-3 Properties of GF.....	59
Table 3-4 Physical and chemical properties of BF	60
Table 3-5 Properties of CEM1-52.5N	61
Table 3-6 Properties of limestone powder	62
Table 3-7 Evaluation of major mods of AFM.....	83
Table 4-1 Selected Plasma Conditions for PPF1	104
Table 4-2 Selected Plasma Conditions for GF.....	108
Table 4-3 PPF1 Tensile Properties before and after Plasma Treatments.....	127
Table 4-4 GF Tensile Properties before and after Plasma Treatments	130
Table 4-5 BF Tensile Properties before and after Plasma Treatments.....	132

Table 4-6 Maximum Force and Interfacial Shear Strength for Untreated and Plasma Treated PPF1	135
Table 4-7 Maximum Force and Interfacial Shear Strength for Untreated and Plasma Treated GF	138
Table 4-8 Maximum Force and Interfacial Shear Strength for Untreated and Plasma Treated BF.....	141
Table 4-9 The 28 Days Flexural Test Results of PPF1 Reinforced Cementitious Specimens	149
Table 4-10 The 28 Days Flexural Test Results of GF Reinforced Cementitious Specimens	152
Table 4-11 The 28 Days Flexural Test Results of BF Reinforced Cementitious Specimens	155
Table 4-12 Tensile Strength Difference	156
Table 4-13 Comparison of plasma effect on the pull-out behaviour of fibres	157
Table 4-14 Comparison between plasma effect on bending strength values for different fibres.....	158
Table 4-15 Comparison of bending strength improvement for different fibres.....	158

List of Figures

Figure 2-1 Loss of fibre diameter as a result of corrosion at the crack cross section (Nordström, 2005).....	11
Figure 2-2 Surface corrosion of steel fibre reinforced concrete (Balouch, Forth and Granju, 2010)	12
Figure 2-3 Failure pattern of corroded steel fibre concrete specimen (Anandan, Vallarasu Manoharan and Sengottian, 2014).....	12
Figure 2-4 Typical stress-strain behaviour of fibre reinforced concrete (Naaman, 1985)	13
Figure 2-5 Effect of fibres on tensile performance of cementitious composites (Naaman and Reinhardt, 1995)	16
Figure 2-6 Applications of fibre reinforced cementitious composites.....	18
Figure 2-7 Shrinkage capability and multiple crack behaviour in bending ECC beams (Brandan, Tosun and Felekoglu, 2008).....	19
Figure 2-8 Plastic joint formation at joint point in reinforced concrete frames: (a) Classic reinforced concrete joint point and (b) reinforced concrete joint point with matrix fibrous micro concrete (ECC) (Brandan, Tosun and Felekoglu, 2008).....	20
Figure 2-9 Summary of the advantages of HPRCC.....	21
Figure 2-10 Characterizations for fibres used in cementitious composites	22
Figure 2-11 Fibre-matrix interfacial bonding mechanisms: (a) molecular entanglement following interdiffusion, (b) electrostatic adhesion, (c) chemical bonding and (d) mechanical interlocking (Zhou, Fan and Chen, 2016).....	26

Figure 2-12 (a) Schematic description for indentation method and (b) pictures of indented fibres (Singh, Shukla and Brown, 2004b)	33
Figure 2-13 Scheme of the states of matter and the processes to change between them	35
Figure 2-14 2D Classification of plasmas (electrons temperature versus electrons density) (Boulos, Fauchais and Pfender, 2013)	37
Figure 2-15 Four different kinds of atmospheric pressure plasma sources (Selwyn et al, 2001).....	39
Figure 2-16 Effect of surface modification of polypropylene (Li and Stang, 1997) .	46
Figure 3-1 Marconi signal generator	64
Figure 3-2 Travelling wave tube amplifier	66
Figure 3-3 Rectangular waveguide TE mode	67
Figure 3-4 Magnetic and electric fields in a TE ₁₀ rectangular cavity.....	68
Figure 3-5 Plasma Test Rig and the Fibre Holder.....	68
Figure 3-6 Schematic diagram of plasma system parts.....	69
Figure 3-7 Microwave Plasma System	71
Figure 3-8 Fibre holder frame	72
Figure 3-9 Modified fibre holder to facilitate larger amount of fibres to be used in flexural test.....	73
Figure 3-10 Examples of different types of wettability: (a) No wettability, completely hydrophobic, contact angle =180° (b) Partial wettability, partially hydrophobic/philic, contact angle=0-180° and (c) Complete wettability, completely hydrophilic, contact angle	75
Figure 3-11 CAM setup	77

Figure 3-12 Three stages of specimen preparation procedure for the SEM analysis: (a) Specimen coating, (b) Placing the specimen on the SEM stage and (c) Vacuuming process.....	80
Figure 3-13 Schematic illustration of the operation of AFM (Guo, Xie and Luo, 2014)	82
Figure 3-14 AFM used in analysing the surface roughness of the fibres.....	84
Figure 3-15 Specimen preparation and testing procedure of fibres: (a) fibres glued to the plates, (b) fibre specimen clamped in the machine	86
Figure 3-16 Typical single fibre pull-out force- displacement graph (Sørensen and Lilholt, 2016)	89
Figure 3-17 Pull-out specimen preparation: (a) casting, (b) curing and (c) gluing fibres in aluminium plates	92
Figure 3-18 Pull-out test set-up for single fibre pull-out specimens: (a) pull-out test rig, (b) schematic diagram of pull-out test rig.....	94
Figure 3-19 Flexural test specimen preparation: (a) dry mix, (b) wet mix with fibre added, (c) moulding, and (d) curing.....	95
Figure 3-20 Three-point bending test setup	96
Figure 4-1 Plasma Temperature Profile	100
Figure 4-2 Wetting Contact Angle of PPF1 before and After Plasma Treatment ...	102
Figure 4-3 PPF1 Failure: (a) Softening of PPF1 at 60 mm, 1 l/min and plasma exposure exceeding 20 sec, (b) Decomposition of PPF1 at 30 mm, 2 l/min, 1 l/min and plasma exposure exceeding 20 sec	103
Figure 4-4 Computer Images and Contact Angle-Time Graph of PPF1: (a) Untreated, (b) Treated at Distance 60mm, Flow Rate 2l/min and Treatment Duration of 120 sec	105

Figure 4-5 Wetting Contact Angle of GF Before and After Plasma Treatment	107
Figure 4-6 Treated at Distance 30 mm, Flow Rate 1 l/min and Treatment Time Exceeding 40 sec.....	108
Figure 4-7 Computer Images and Contact Angle-Time Graph of GF: (a) Untreated, (b) Treated at Distance 30mm, Flow Rate 1l/min and Treatment Duration of 40 sec...	109
Figure 4-8 SEM of PPF1: (a) PPF1-0 (b) PPF1-60-2-120 and (c) PPF1 60-2-200 .	111
Figure 4-9 Effect of Plasma Treatments on GF Surface Morphology: (a) GF--0 (b) GF-30-1-40, (c) GF-60-1-120 and (d) GF-60-1-200	113
Figure 4-10 Effect of Plasma Treatments on BF Surface Morphology: (a) BF--0 (b) BF-30-1-40, (c) BF-60-1-120 and (d) BF-60-1-200	115
Figure 4-11 BF Treated at Distance 30 mm, Flow Rate 1 l/min and Treatment Time Exceeding 40 sec.....	116
Figure 4-12 Effect of Plasma Treatment on Nano Roughness of PPF1 Surface: (a) PPF1-0, (b) PPF1-60-2-120 and (c) PPF1-60-2-200	117
Figure 4-13 Rms Values of PPF1 before and after Plasma Applications	118
Figure 4-14 Effect of Plasma Treatment on Nano Roughness of GF Surface: (a) GF-0, (b) GF-30-1-40, (c) GF-60-1-120 and (d) GF-60-1-200.....	120
Figure 4-15 Rms Values of GF before and after Plasma Applications.....	121
Figure 4-16 Effect of Plasma Treatment on Nano Roughness of BF Surface: (a) BF-0, (b) BF-30-1-40, (c) BF-60-1-120 and (d) BF-60-1-200.....	122
Figure 4-17 Rms Values of BF before and after Plasma Applications	123
Figure 4-18 Contact Angle and Nano Roughness Comparison of Different Fibres	125
Figure 4-19 PPF1 Load-Extension Graph before and after Plasma Treatments.....	127
Figure 4-20 GF Load-Extension Graph	129
Figure 4-21 BF Load-Extension Graph.....	131

Figure 4-22 PPF1 Pull-Out Force-Extension Graph: (a) PPF1-0, (b) PPF1-60-2-120 and (c) PPF1-60-2-200.....	134
Figure 4-23 GF Pull-Out Force-Extension Graph: (a) GF-0, (b) GF-30-1-40, (c) GF-60-1-120 and (d) GF-60-1-200.....	137
Figure 4-24 BF Pull-Out Force-Extension Graph: (a) BF-0, (b) BF-30-1-40, (c) BF-60-1-120 and (d) BF-60-1-200.....	140
Figure 4-25 The Effects of Different Fibre Percentage on the Force-Deflection Curves in: (a) PPF1, (b) GF and (c) BF.....	143
Figure 4-26 Bending Strength of Fibrous Composites: (a) PPF1, (b) GF and (c) BF	144
Figure 4-27 Failure of Composites Prepared with BF	146
Figure 4-28 The 28 Days Force-Deflection Graphs of PPF1 Treated with Optimum Plasma Condition	147
Figure 4-29 Multiple Crack Formation in Case of Optimum Plasma Condition of PPF1	150
Figure 4-30 The 28 Days Flexural Test Results of GF Reinforced Cementitious Specimens	151
Figure 4-31 The 28 Days Force-Deflection Graphs of GF Treated with Optimum Plasma Condition	153
Figure 4-32 The 28 Days Force-Deflection Graphs of BF Treated with Optimum Plasma Condition	154

Chapter 1 Introduction

1.1 Introduction

Currently, fibre reinforced cementitious composites (FRCC) are widely used in numerous civil engineering applications (marine structures (Serna et al, 2009), industrial pavements (Guerrini, 2000), tunnel linings (Li, 2001), earthquake-resistant structures (Marcos-Meson et al, 2018), etc.). By the addition of fibres, plain concrete can be altered from a brittle to a ductile material, consequently improving the resistance to crack initiation and propagation (Vandewalle, 2007). Cementitious materials strengthened with fibres have demonstrated an improvement in tensile and flexural strength, ductility and toughness thus enhanced durability (Yao, Li and Wu, 2003) (Brandt, 2008). Several types of fibres based on their materials are proposed for the application in high performance fibre reinforced cementitious composites (HPFRCC) such as engineering cementitious composite (ECC). The fibres can be categorized as:

- Steel fibres in various forms, shapes, sizes and dimensions.
- Glass fibres (GF), restricted to only alkali resistant (AR) type, due to low durability of glass fibres in alkaline solutions.
- Mineral-based fibres such as asbestos and basalt.
- Synthetic fibres produced with various materials such as polyethylene (PE), polypropylene (PP), nylon (PA), polyvinyl alcohol (PVA) and acrylic (PAN).
- Polyacrylonitrile-based fibres and carbon fibres.
- Natural fibres such as jute, flax, hemp and cellulose.

Due to the advantages of synthetic, glass and basalt fibres over conventional steel and carbon fibres in term of their lower price, lower weight to strength ratio and corrosion resistance, these fibres attracted the attention as an alternative to steel and carbon fibres for fibre reinforced cementitious composites (Alani and Beckett, 2013; Babafemi and Boshoff, 2015; Han et al, 2015; Amin et al, 2017).

Despite the advantages and the wide range of applications of AR glass and synthetic fibres, these fibres exhibit some drawbacks. In particular, glass fibre (GF) and all synthetic fibres excluding PVA and acrylic fibres exhibit low surface free energy, smooth and hydrophobic surface characteristics (Trejbal et al, 2015). Consequently, this leads to poor adhesion with the matrix, poor wettability and vulnerability to slippage from cementitious composites (Skacelova et al, 2011; Tosun, Felekoğlu and Baradan, 2012). Therefore, their contribution in improving flexural strength and post cracking behaviour have been to be limited (Lee et al, 1997; Singh, Shukla and Brown, 2004b). Attempts at overcoming these drawbacks have been made by researchers (Li, Wu and Chan, 1996; Bentur, Peled and Yankelevsky, 1997; Won, Lim and Park, 2006). Several methods have been proposed to alter the surface properties of synthetic fibres to enhance their performance in cementitious composite applications. The methods are based on wet chemical, flame, physical, mechanical and plasma modifications (Gijsbertus and Terlingen, 1993; Massines, Messaoudi and Mayoux, 1998; Pakravan and Memariyan, 2017b).

Wet chemical treatment techniques, for instance acid or any other etching solutions, could result in extreme etching, which consequently causes a loss of the material's mechanical performance. The degree of etching is difficult to measure, and the etching chemical needs to be washed away with extraordinary quantities of washing solutions. Removal of these wastes possibly will furthermore cause environmental harm (Huang

et al, 2006) (Morent et al, 2008). Further, mechanical micro-pitting may possibly cause cross-section damage and be hard to demonstrate on shorter fibres with reduced diameters (Singh, Shukla and Brown, 2004a). In addition, flame or heat treatment, typically results in further brittle structure as stated by (Richaud et al, 2008). Amongst these techniques plasma treatment can be a useful and environmentally friendly alternative for fibre surface modification purposes (Li et al, 2014; Lee, Ohsawa and Takahashi, 2015; Sánchez Serrano et al, 2015; Praveen et al, 2016). Nevertheless, the variety of plasma arrangement brings the possibility of controlled application of treatment, if a suitable gas and treatment condition is designated and no challenging waste will be disposed to the environment post the treatment. Many industrial plasmas operate under vacuum, and are referred to as low-pressure plasma (Shahidi, Ghoranneviss and Mozzenchi, 2012). Low-pressure industrial plasma systems have a broad range of applications and have demonstrated their advantages in terms of quality and consistency. However, vacuum systems are costly, involve difficult and complex fitting and regular maintenance (Li et al, 2016). An Atmospheric pressure plasma system can solve some drawbacks of low-pressure plasma techniques (Liston, Martinu and Wertheimer, 1993; Ren, Wang and Qiu, 2008; Gao et al, 2009). A comprehensive literature review conducted on the plasma treatment of fibres for cementitious composites revealed that there is no previous investigation on using atmospheric pressure plasma treatments. Therefore, in this study a detailed experimental investigation on the effect of microwave plasma treatment on the surface characteristics of commercially used polypropylene, glass and basalt fibres will be undertaken. Moreover, the impact of atmospheric pressure microwave plasma treated fibres on the mechanical performance of cementitious composites will be investigated.

1.2 Research Motivation

Corrosion of steel reinforcement is one of the key features affecting the durability of concrete structures. In an examination of 200 bridge structures in the UK, it was revealed that at least 30% of those investigated were in poor condition because of rusting, spalling and cracking (Wallbank, 1989). Moreover, a comprehensive report released by the National Association of Corrosion Engineers (NACE) in 2016, estimated the overall annual international cost of corrosion at 2.5 trillion euros (Koch et al, 2016).

This indicates that despite preventative efforts and design consideration, steel concrete reinforcement is vulnerable to degradation from corrosion (Adasooriya, Samarakoon and Gudmestad, 2017). The main reasons for this can be summarised as:

- Cracking of concrete;
- Access of moisture and chemicals such as chlorides into concrete over time, reducing alkalinity and encouraging steel corrosion.

To control cracking due to plastic shrinkage and to drying shrinkage, fibres are frequently used in concrete. Fibres act as a crack arrester, which bridge the crack to transfer the stress, thus, preventing the propagation of the crack, hence, protecting the main reinforcement from corrosion. Fibres such as steel have been used widely in the form of longitudinal reinforcement or even as standalone applications. However, steel fibres are vulnerable to corrosion, especially in harsh environments. Non-corrosive fibres such as synthetic fibres (Ababneh et al, 2017), basalt fibres (Włodarczyk and Jędrzejewski, 2016) and glass fibres (Xiaochun, Xiaoming and Xiaopei, 2017) can overcome the corrosion problems of steel fibre. However, these fibres especially synthetic fibres, such as polypropylene (Pakravan and Memariyan, 2017a) and glass

fibres (Anandaraj et al, 2018) exhibit inert and low surface energy which makes them prone to slipping from the concrete. This poor adhesion will affect fibre-matrix interface behaviour, which is a critical parameter, that has a considerable consequence on the mechanical characteristic of fibre-reinforced composites. The fibre-cement adhesion is the nominal parameter in controlling the crack-opening and the energy for propagating the cracks (Li, Wang and Backer, 1987; Mobasher and Cheng Yu, 1996). Therefore, mechanical behaviour of fibre reinforced concrete is critically governed by the degree of fibre-cement adhesion (Chan, 1994; Chan and LI, 1997; Bentur, 2000). Hence, appropriate fibre-cement adhesion lets the stress transfer between the matrix and the fibre (Yan, Jenkins and Pendleton, 2000), improving the fibre-cement interface properties resulting in the composite property enhancement (Pakravan et al, 2012). Therefore, this study aims to develop a new system to modify the surface of these fibres using an electrodeless microwave induced plasma torch.

1.3 Scope

The scope of the project is to design and develop a system that is capable of surface modification of fibres in a continuous way without the requirement of expensive pumps and vacuum equipment.

The new system consists of a microwave induced plasma torch (MIPT). The experimental programme was conducted in three phases. The first phase was aimed at designing and developing the MIPT. The second was to identify the effect of using MIPT treatment on the surface characterisation of fibres such as wetting and surface morphology and to determine the optimum treatment. The aim of surface modification is to modify the surface properties of fibres. Thus, to increase the potential for use in composites.

Fibres were subjected to various plasma conditions. The effect of distance from the plasma torch, the gas flow rate and the treatment duration were investigated. The surface properties of fibres were investigated before and after treatment. The surface energy of the fibres was investigated using static contact angle measurement (CAM) and the best plasma conditions that contributed to the lowest CAM were determined. Physical changes in the surface properties of the fibres due to the application of plasma were evaluated using scanning electron microscopy (SEM) and atomic force microscopy (AFM). Thereafter the tensile strength of the fibres treated using the optimal plasma conditions determined from surface analysis, was examined. The techniques used for this purpose are exhibited in sections 3.4.1 and 3.4.2.3.

In the third phase, the effect of plasma treatment on fibre-cement adhesion was investigated using the single fibre pull-out test for determining the optimum plasma treatment. For this purpose, a test rig was created to hold a cylindrical 40 mm diameter and 50 mm high specimen of cement with a single fibre embedded in the centre. The experimental pull-out set-up is explained in section 3.4.2.1.

Finally, cement-based composites were produced using fibres treated at determined optimum plasma condition and untreated fibres for control purposes. The mix design was out of the scope of this study; therefore, a mix from the literature was used throughout this study. Six rectangular prism $40 \times 40 \times 160$ mm prismatic specimens were prepared using optimum plasma condition for each fibre. The prepared samples were subjected to a three-point bending test at 28 days. The load-deflection relationships were determined from bending tests. Bending strength and flexural performances of the control specimens were compared with plasma treated specimens. The experimental set-up for the flexural test procedure is exhibited in detail in section 3.4.2.2. Experimental results have shown that proper plasma treatment improves the

flexural performance of composites significantly. In addition, the advantages of fibre composite material, modified by the plasma method, and suggestions for possible application areas, are presented.

1.4 Aim and Objectives

The aim of this research is to develop a microwave induced plasma torch that can be used to modify the surface of fibres used in strengthening composites. The objectives were as follow:

1. To investigate design consideration for a plasma system for fibre treatment using literature review.
2. To design a plasma system that could be used continuously for modifying low surface energy fibres in atmospheric pressure.
3. To investigate the effect of various plasma conditions (distance of the fibre from the torch, gas flow rate and treatment duration) on surface characteristics of fibres using contact angle measurements, scanning electron microscope and atomic force microscopy.
4. To characterise the treatment effect on fibre-cement interfacial properties through mechanical testing of single fibre pull-out test and flexural test.
5. To assess the potential of fibre reinforced cementitious composites produced from plasma treated fibres.
6. To address the limitations of the newly designed system and suggest recommendations for future development.

Each of the objectives stated above will be explained in detail in the following chapters of this PhD study.

1.5 Research Contribution

This research will make a significant contribution in the design and development of a MIPT system for the surface modification of hydrophobic fibre. This will contribute in the development of a new and superior product for the fibre industry and building material producing companies. It is possible to produce composite elements with high mechanical properties and post cracking energy absorption capacities with the treatment method used in this project. The extraordinary crack arresting and the limiting feature of the crack width of the material brings the possibility of its being used in concrete structures exposed to harsh environments and for the repair of reinforced concrete structures.

1.6 Thesis Organisation

This thesis is divided into five chapters. Each chapter contains a brief introduction and a summary describing the content of the work. A description of each chapter is presented below:

Chapter -1 Introduction: A brief introduction to FRCC, the fibre types used for producing of concrete fibre composite and their limitations are included. This is followed by a discussion of the current available solutions to overcome these limitations. The scope, objectives and significance of this study are presented.

Chapter -2 Review of Literature: This chapter introduces the literature relevant to FRCC, and detail of HPFRCC are presented. Detailed summaries from its development to its applications, types, factors affecting its performance and fibre types are presented. Types of bonding mechanisms and methods for surface modifications of fibres are briefly explained. The general description of the plasma is made. The properties and applications of plasma technology are introduced. Finally, a few of the

research studies on the performance of surface modified by plasma application in cement-based composites have been summarized.

Chapter -3 Materials and Methodology: Information on the method, test program, analysis method and materials used in the experimental investigations are carried out within the scope of the project are presented. Two different test rigs to hold the fibres at different phases of this study were developed.

Chapter -4 Results and Discussion: Alterations in the surface properties of the fibres due to plasma treatment are discussed. To investigate the fibre-cement interface, the load extension curves of the single fibre pull-out specimens were presented, and detailed evaluations were made. By evaluating the obtained findings, the optimum plasma condition for each different fibre was determined. Furthermore, to investigate the impact of plasma treatment on the flexural performance of FRCC, the load-deflection curves of the three-point bending specimens were presented with detailed evaluations. Possible reasons for the bending behavioural differences in the plasma treated fibre reinforced composites are discussed.

Chapter -5 Conclusion and Recommendations: In this chapter, the findings of this study are made and recommendations for future work are offered.

Chapter 2 Review of Literature

2.1 Introduction

The following section addresses the historical evolution of fibre reinforced cementitious composites (FRCC) and high-performance fibre reinforced cementitious composites (HPFRCC) from the early age (of straw in mud) up to the present. The fundamental idea of mix proportion, physical and mechanical properties, advantages, and applications are discussed. The factors affecting its properties such as fibre type are investigated. The advantages and limitations of typical types of fibres are discussed. The general evaluation of the concept of plasma and the plasma methods used in the modification of fibre surface are introduced. Finally, literature studies are presented on what kind of changes in performance will be brought if fibres are used in cementitious composites after plasma application.

2.2 Fibre Reinforced Cement Composites (FRCC)

Concrete, as an ordinary cement-based composite, is made of a binder such as cement, framework such as coarse aggregate, fine aggregate and additives such as fly ash as filler, as well as water and additional agents. Cracks frequently appear on the surface of concrete when it is subjected to flexural or tensile loading due to its low load carrying capacity property, thus resulting in the failure of the concrete (Lura and Terrasi, 2014). To overcome the brittle nature of concrete, reinforcement may be used in more than one mode. For instance, longitudinal bars are added to provide high tensile strength, thus, the post cracking behaviour of the structure is improved. On the other hand, discontinuous discrete short reinforcement in the form of fibres are added

to provide the mechanical integrity needed of the concrete through bridging the cracks and preventing from further propagation, as these cracks can cause severe damage and corrosion of the longitudinal reinforcements when exposed to harsh environments. These composites are known as fibre reinforced concrete (FRC).

FRC material is one of the most extensively used man-made materials in many fields, such as roadways, buildings, bridges and many more, due to its significantly high hardness and exceptional compression strength post setting (Feng et al, 2017).

Adding a fibre into concrete can improve the performance of the composite in two ways: it enhance the tensile behaviour of the composite and decreases the shrinkage of concrete, which is associated in cracking (Ferrara, 2019).

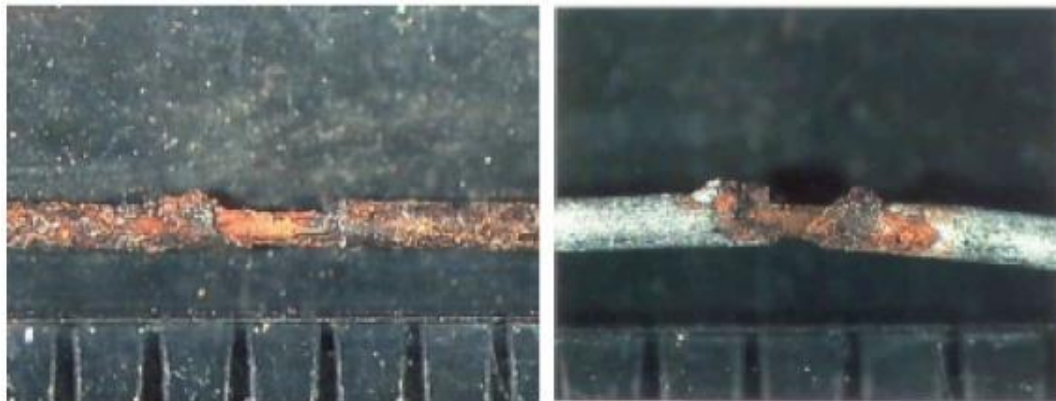


Figure 2-1 Loss of fibre diameter as a result of corrosion at the crack cross section (Nordström, 2005)

To improve these weaknesses, several types of reinforcements have been added into concrete such as steel fibres to. Nevertheless, steel is susceptible to corrosion (see Figure 2-1), which can result in structural failure of the concrete (Tang, 2017; Marcos-Meson et al, 2018).



Figure 2-2 Surface corrosion of steel fibre reinforced concrete (Balouch, Forth and Granju, 2010)

Corrosion of steel fibres in concrete structures can have a negative impact on fibres bridging the cracks. Thus, reducing the strength and the durability of the structures. Moreover, resulting in the presence of corrosion marks on exposed surfaces see (Figure 2-2).



Figure 2-3 Failure pattern of corroded steel fibre concrete specimen (Anandan, Vallarasu Manoharan and Sengottian, 2014)

Figure 2-3 shows the failure of concrete structures as a result of corroded steel fibres. Furthermore, the steel industry consumes a high amount of energy and produces a lot of greenhouse gases, which lead to environmental damage (Yin et al, 2016). In recent

years, chopped synthetic fibres such as, polyvinyl alcohol (PVA) (Sahmaran and Yaman, 2007), polyethylene (PE) (Wang et al, 2016), polyethylene terephthalate (PET) (Foti, 2011), polypropylene (PP) (Anandaraj et al, 2018), glass fibre (GF) (Henriksen, Lo and Knaack, 2016; Rypla and Vořechovský, 2017) and basalt fibre (BF) (Meng and Yan, 2007; Branston et al, 2016) have been added to concrete as reinforcement to enhance the mechanical and engineering properties of concrete.

The idea of using fibres can be traced back to the early civilizations when they used straw in mud to create a composite material that exhibits enhanced post cracking behaviour. Then Portland cement started to be used widely in the construction industry. Although, cement, mortar and concrete are very strong in compression, they are brittle and weak in tension and flexure.

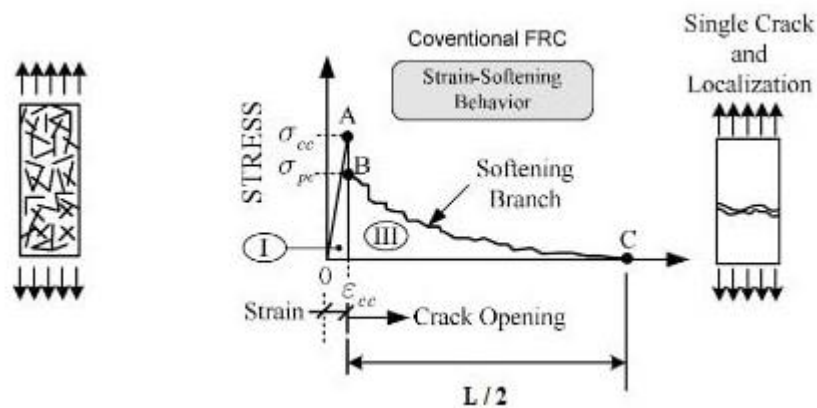


Figure 2-4 Typical stress-strain behaviour of fibre reinforced concrete (Naaman, 1985)

Figure 2-4 shows the comparison between the behaviour of plain concrete and FRC. The deformation of cementitious matrices is initially elastic. Micro cracking will follow the elastic deformation, and then the crack further propagates to form localized macro cracking, and lastly fracture. The fracture or cracking of cementitious material after hardening is expected. This fracture or cracking happens when the tensile stresses exceed the minimum tensile strength of the matrix. This usually occurs due to

shrinkage, load effect or another environmental factor. As cementitious materials are considered brittle with no substantial post-cracking ductility, therefore, as soon as a fracture or crack occurs, the matrix will undergo a sudden, brittle failure. Unless there is engagement of either fibrous or traditional longitudinal reinforcement to enhance the post-cracking behaviour with added tensile strength, the system will fail in a sudden and brittle mode. Engineers and researchers attempted to overcome the main drawbacks of cementitious composites, which were the low tensile strength and the high brittleness. Joseph Lambot, who was a French engineer, thought about the idea of the addition of wires and wire mesh in to the concrete in 1847 (Naaman, 1985). Although, in the early 1950's, investigations into using glass fibres as a reinforcement in concrete were carried out in the USA, UK and Russia, the development FRCC was relatively slow until the 1960's when interest in FRCC increased significantly and many new fibres were introduced. The properties of FRCC rely on the type of the fibre, the properties of the matrix and the interfacial transition zone. In general, fibres in concrete can be defined as discontinuous and discrete with various lengths and diameters.

Referring to the results of early attempts in the development of FRCC, it was observed that the compressive and tensile strength were not increased by a significant value (Naaman, 2008). Therefore, the true significance of fibres as a reinforcement was not an easy task to address. The period of modern FRCC development was during the 1970's and 1980's. During that period, many new pieces of testing equipment and analysis procedures were introduced. Consequently, the most significant improvement, resulting from the presence of fibres in cementitious matrices, is the enhancement in post-cracking behaviour, which is classically evaluated by post cracking energy absorption capacity. A few decades of continuous research in the field

of FRCC has followed, and the major advantage of the addition of fibres is said to be for enhancing the post-cracking behaviour, and crack control which is one of the most common applications of FRCC. The fibres can inhibit larger crack widths that can permit water and contaminant diffusion and lead to corrosion in reinforcing steel (ACI 544 1R-96, 2002). Additional research studies have utilized several types of fibres and cement supplementary materials to develop composites that exhibit improved tensile and compressive strength, beside the fracture toughness. These composites are known as high performance fibre reinforced cementitious composites (HPFRCC). The development of homogeneous and isotropic cement-based material that exhibits higher tensile and compressive strength and significant energy absorption capacity is not an impossible task anymore. The significant amount of research conducted in the field of FRCC has led to the development of HPFRCC that exhibit a combination of outstanding properties compared to the other cementitious composites (Farhat et al, 2007; Li, Luo and Wang, 2014).

2.2.1 High Performance Fibre reinforced Cementitious Composites (HPFRCC)

HPFRCC have a mixture of cementitious materials, sand, fibre reinforcement and admixtures. Low water-to-cementitious materials ratio, high mechanical strengths and ductility and extended service life span due to their refined microstructures are the main features of HPRCC (Meng, Valipour and Khayat, 2017).

The potential of using steel fibre and its ability in controlling the crack width is well recognized in the construction community. Nevertheless, like conventional longitudinal steel reinforcement, steel fibres are susceptible to corrosion (Granju and Ullah Balouch, 2005). The diameter of the fibres is relatively small (0.25-0.75 mm), so any minor corrosion can lead to major loss of cross-sectional dimension (Hwang et

al, 2015). Therefore, an important solution is one that incorporates non-metallic, synthetic and natural fibre systems (Burgoyne, 2001). In the literature, cement-based composites whose properties of toughness are improved by the use of various fibres are called HPFRCC (Abrishambaf, Pimentel and Nunes, 2017). Engineered cementitious composites (ECC) is a form of HPFRCC. ECC has much higher post cracking energy absorption capacities than normal concrete. Additionally, the deformation capacity under tensile and bending stresses is comparatively high. In the literature, ECC with a tensile deformation capacity of up to 2.5-4%, has been reported (Kang et al, 2017).

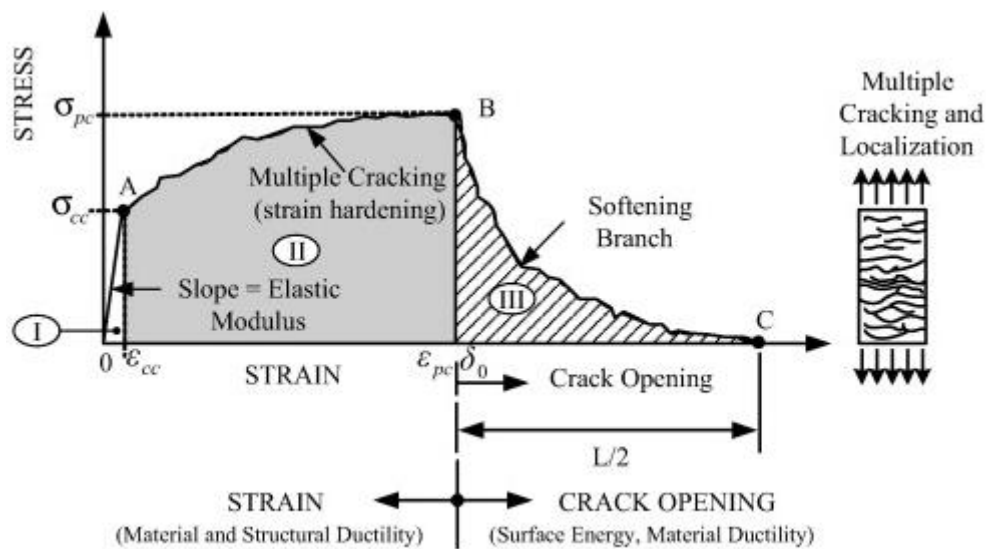


Figure 2-5 Effect of fibres on tensile performance of cementitious composites (Naaman and Reinhardt, 1995)

HPFRCC is a material containing a cement-based matrix and short reinforcing fibres (Ferrara et al, 2017). HPFRCC can be very ductile, presenting several fine cracks and pseudo strain-hardening characteristics when subjected to uni-axial tensile loading (see Figure 2-5). In 1985, Naaman et al. (Naaman, 1985) first introduced the term of HPFRCC to define a composite material that exhibits high strength, toughness and ductility. Strain hardening is a term used commonly in the literature to define the

behaviour of HPFRCC and ECC under tensile stress. Strain hardening can be defined as a process where the microstructure of the material experiences a plastic deformation because of applied strain. Strain hardening processes are not likely in cement matrix composites. Whereas, in HPFRCC and ECC pseudo-ductility is observed and this is due to the ability of the fibre reinforcement to avoid sudden catastrophic failure when the cracking is initiated in the matrix. These materials have a wide range of applications, such as; hydraulic tunnels, bridge decks, building dampers, concrete pipes, retaining walls, and structures exposed to seismic and non-seismic loadings, irrigation channels, roads, and other applications where a lightweight, strong and durable building material is required.

2.2.2 Applications and Advantages of HPFRCC

Fibre reinforced cement and concrete composites have been used in so many applications, both as stand-alone or in arrangement with reinforcing bars. Moreover, they have similarly been used as maintenance materials in restoration and repairing work.

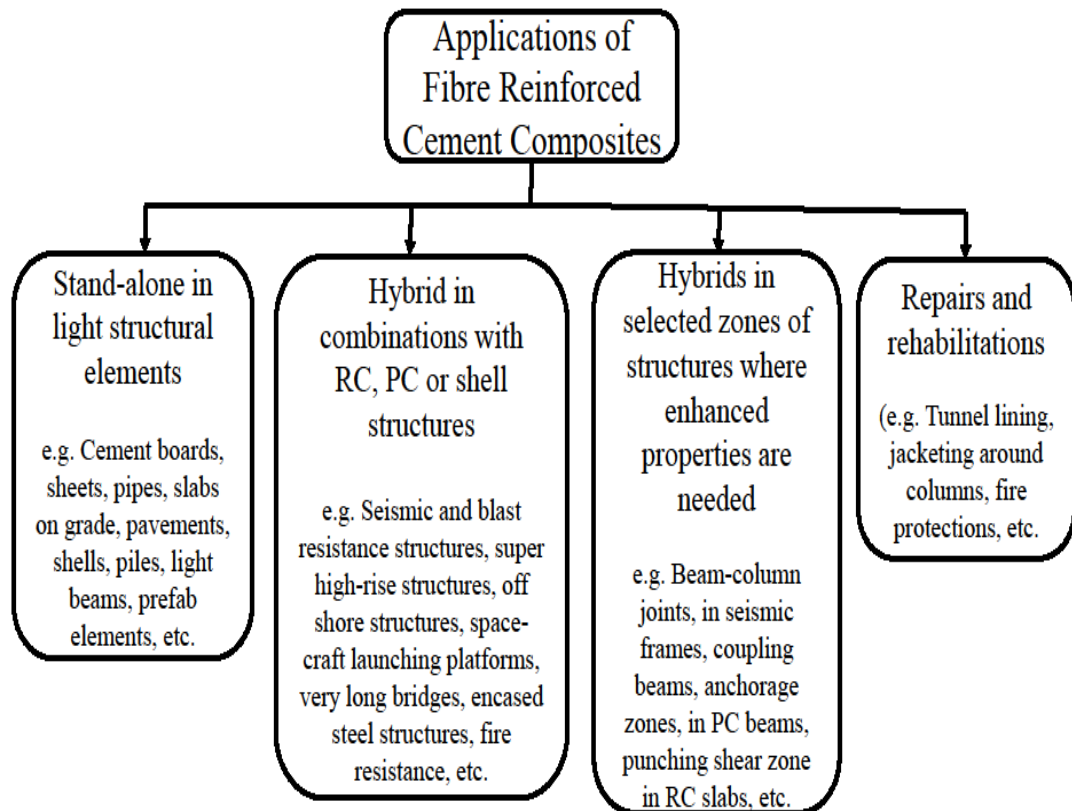


Figure 2-6 Applications of fibre reinforced cementitious composites

Figure 2-6 illustrates the various classes of applications of fibre reinforced cement-based composites (Massicotte and Bischoff, 2000; Naaman, 2003; Naaman, 2008). Stand-alone applications consist of typically thin products such as cement boards, cladding, electrical poles, pipes, and slabs on pavements and grades. Fibres are furthermore used in hybrid applications to support other structural materials such as structural steel, reinforced and pre-stressed concrete. Instances consist of jacketing for repair, impact and seismic resistant structures and strengthening of beams and columns. In the instance of steel, encased beams and trusses to improve ductility and fire resistance. Specific applications of fibre reinforced cement and concrete composites include bridge decks and special structures such as spacecraft launching

platforms, offshore platforms, blast resistant structures, super high-rise structures, bank vaults, and other high-end structures.

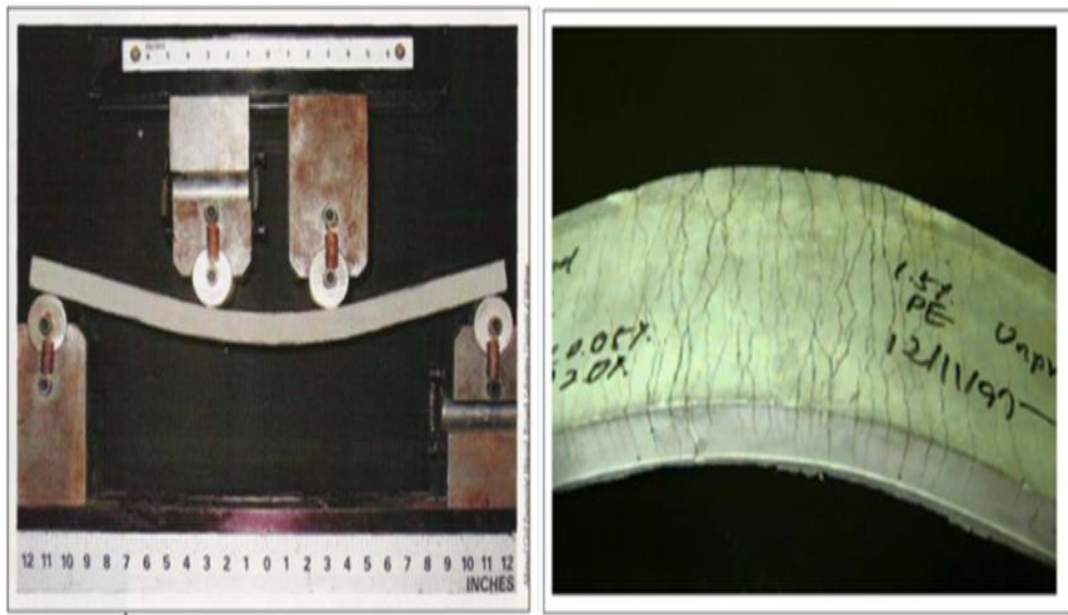
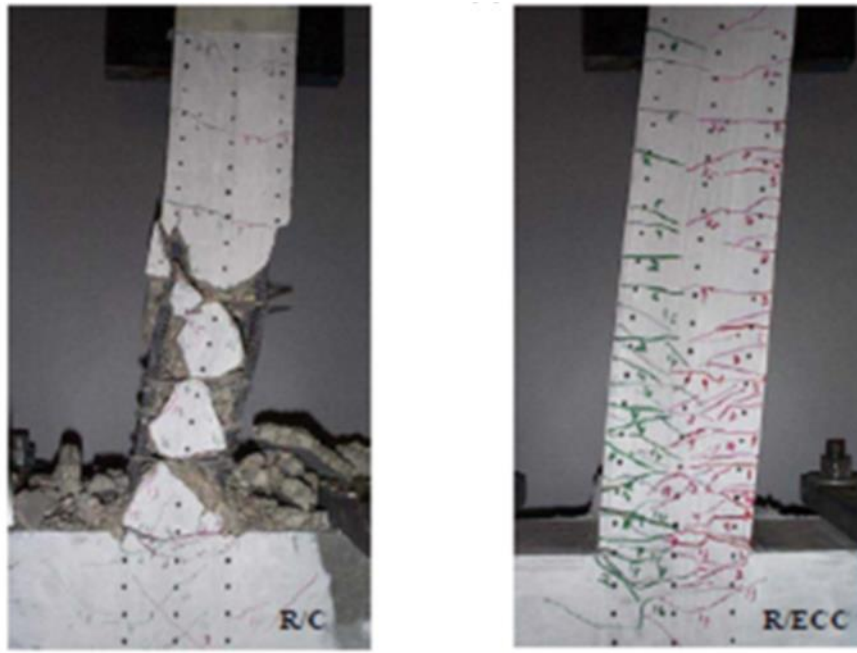


Figure 2-7 Shrinkage capability and multiple crack behaviour in bending ECC beams (Brandan, Tosun and Felekoglu, 2008)

The terms HPRCC and ECC can be used to describe a group of materials industrialised for civil engineering applications. These examples can be summarized as high toughness in bending beams, increased tensile deformation capacity by forming multiple cracks structure member under loading and preventing the plastic joint formation at the joint point in reinforced concrete frames as shown in Figure 2-7 (Brandan, Tosun and Felekoglu, 2008).

In Figure 2-7 the element is deformed and at a visible level. This degree of flexibility is due to the potential of forming multiple cracks in the fibrous composite. There is a similar behaviour under direct uniaxial tensile stress effect. The number of cracks increases without changing the crack width too much, and there is no decrease in the tensile load.



(a)

(b)

Figure 2-8 Plastic joint formation at joint point in reinforced concrete frames: (a) Classic reinforced concrete joint point and (b) reinforced concrete joint point with matrix fibrous micro concrete (ECC) (Brandan, Tosun and Felekoglu, 2008)

Various performances have been reported, especially when using fibre-reinforced micro-concrete in reinforced concrete structures, especially at column beam joints as shown in Figure 2-8 (Brandan, Tosun and Felekoglu, 2008).

In a traditional reinforced concrete system, a plastic joint is formed at the node point in the deformation and the concrete layer in this region is completely spilled as shown in Figure 2-8(a). Whereas, in the use of fibrous micro-concrete matrix, the nodal point maintains its integrity and maintains its load-bearing capacity even at higher beam deformations (10% displacement) Figure 2-8(b).

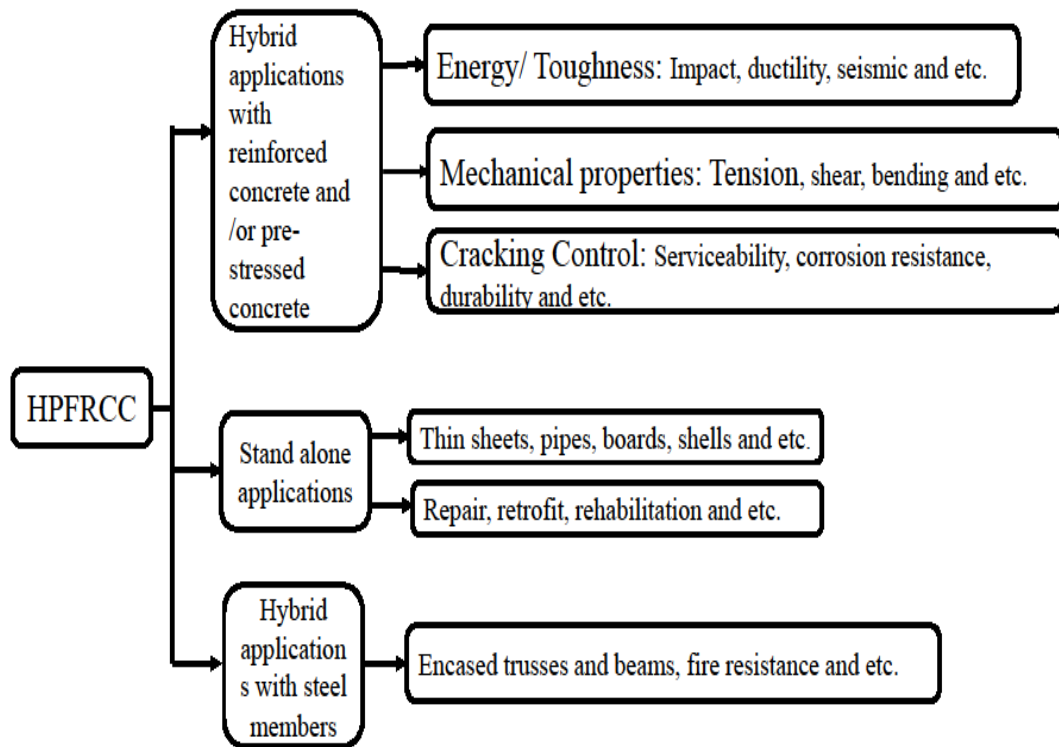


Figure 2-9 Summary of the advantages of HPFRCC

Figure 2-9 summarised advantages of HPFRCC.

2.2.3 Fibres for Reinforcing Cementitious Composites

Discontinuous short discrete fibres used as a reinforcement in cementitious composites can be characterized in various ways. The first classification is based on the fibre material such as, natural organic (examples: cellulose, bamboo, sisal, hair, jute, horsehair, etc.), natural mineral (examples: rock-wool, asbestos, etc.) and artificial fibres such as steel, glass, titanium, carbon, basalt, polymers and other synthetic fibres. The second classification is based on the physical and chemical properties of the fibres such as, surface roughness, density, reactivity with the cement matrix, chemical stability in alkaline environment, fire resistance etc. The third classification is based

on the mechanical properties of the fibres such as modulus of elasticity, tensile strength, ductility, stiffness, surface adhesion properties, elongation to failure etc. The fourth classification is based on the geometric properties of the fibres and this includes fibre length, diameter, longitudinal profile and cross-sectional shape.

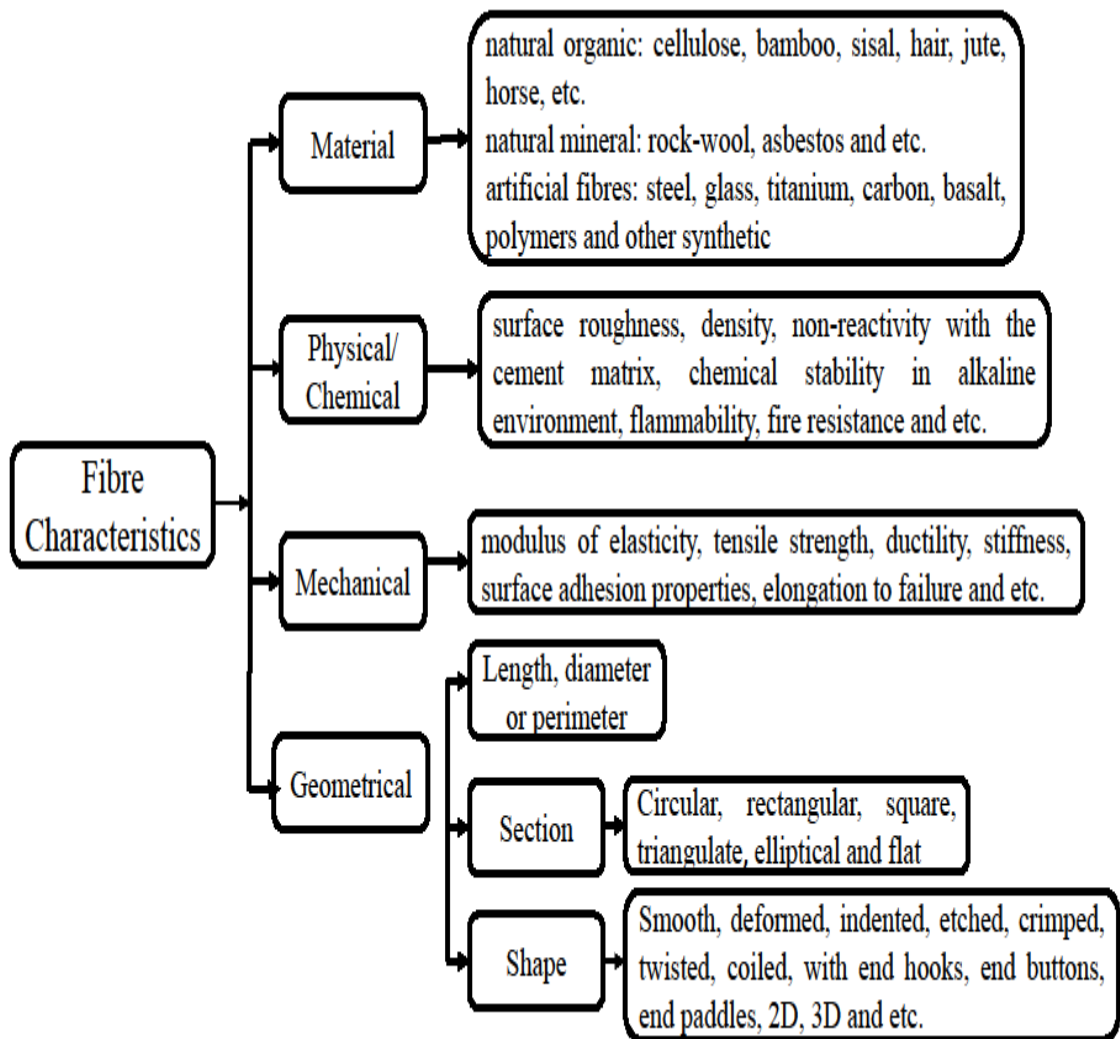


Figure 2-10 Characterizations for fibres used in cementitious composites

The fibre characteristics are illustrated in Figure 2-10. When the material of the fibre (such as steel) has been nominated, an unlimited arrangement of geometric properties associated with its length, diameter, cross sectional shape, or equivalent diameter, and surface deformation can be carefully chosen. In some fibres, the surface of the fibres can be modified such as in etched or plasma treated fibres to increase the bond strength between the fibre and the matrix at the microscopic level. In steel fibres, there is a wide range of cross-sectional selection such as circular, rectangular, square, triangular, diamond, polygonal, flat, or any other shapes. To improve the interfacial zone between the fibre and the matrix and to enhance the mechanical bond, the fibre surface can be modified or deformed lengthwise roughening its surface or introducing mechanical deformations. Therefore, a fibre's surface characteristic can be smooth, indented, deformed, crimped, coiled, and twisted, with end hooks, end paddles, end buttons, or other anchorage systems. Various other forms of steel fibres such as annulus, ring, or clip type fibres have also been used for reinforcing cementitious composites and exhibited considerable improvement in the toughness of concrete in compression. Nevertheless, investigation on such steel fibres did not progress much beyond the research level.

Table 2-1 presents various types of fibre with their respective properties and physical characteristics (Oladele L. and A., 2009).

Table 2-1 Properties of structural fibres

Material	Diameter (μm)	Unit Weight (t/m^3)	Tensile Strength (GPa)	Modulus of Elasticity (GPa)	Ultimate Strain (%)
Steel	5-500	7.85	0.5-2.0	200-210	0.5-3.5
Glass	9-15	2.68	2.0-4.0	70-80	2.0-3.5
PP	20-400	0.93	0.4-0.8	3.5-10	15.0-25.0
Aramid	10-12	1.45	2.3-3.5	63-120	2.0-4.5
PVA	25-40	1.31	1.2-1.6	25-40	7.0-8.0
Carbon	23-400	1.65	2.5-4.0	230-380	0.5-1.5

2.2.4 Important Factors Affecting the Performance and Characteristics of HPFRCC

The scale of the effect of fibres in the post-cracking behaviour of HPFRCC can vary from subtle to substantial, dependent on various factors (ACI 544 1R-96, 2002). The factors are summarized as below (Erdogmus, 2015) :

1. Matrix characteristics: matrix composition, water cement ratio (W/C), aggregate size, strength class, mortar consistency etc., directly affects the properties of fibre-cement transition region and the homogeneity of the mixture. However, the adherence of the interface by physical friction is influenced by the porosity and calcium hydroxide (CH) accumulation in this region.

2. Fibre characteristics: fibre type (elastic modulus, tensile strength, surface bonding characteristics) and fibre geometric (length, diameter, shape, and their ratio, i.e., fibre aspect ratio). The adherence properties related to fibre geometry can be both positive and negative. For instance, when long fibres are used, the adherence is thus positively affected. Nevertheless, long fibres can cause balling and reducing the workability of the mixture, and this can have the opposite effect. Consequently, fibre optimization should be carried out for the size of the fibre and its ratio in the mix. The fibre shape such as twisted, fibrillated, creased etc. can affect the performance of the composite. It has been reported that fibrillated fibres are more advantageous than the other fibres and this is due to the increased surface area of fibrillated fibres.

3. Fibre surface properties: The surface properties of fibres affecting the adherence with the cement-based matrix can be divided into physical surface roughness and chemical surface activation such as reactivity, and hydrophobic or hydrophilic behaviour.

In fibres such as PP and GF which have hydrophobic (water repellent) surface properties and are not capable of reacting with cement mortar, the adherence is gained by friction created by physical surface roughness. The higher the fibre surface area in such fibres, the higher the friction surface will be. If the fibre does not have a rough structure while peeling off from the matrix, the matrix directly slides off. However, if the fibre is rough, the roughness may increase even more during the matrix peeling and this occurs due to the damage of the rough area. In this case, strain hardening or slip hardening may be observed. In some other fibres, particularly in polymer-based fibres, besides the physical effect, the formation of covalent bonds with cement mortar using hydroxide (OH⁻) bonds occurs. These bonds reveal a strong adherence between the matrix and polymer fibre.

2.3 Interfacial Transition Zone (ITZ) and Types of Bonding Mechanisms

The interfacial transition zone (ITZ) of the composite material is where the applied load is transferred from the matrix to the fibre reinforcement. The mechanical properties of the composites are strongly dependant on the ITZ which represents the bond between the fibre reinforcement and the matrix (Zong and Grubb, 1994). Hence the fibre reinforcement must have a tremendous bond to enhance the matrix strength and stiffness, and to guarantee the transfer of the load from the matrix to the fibre reinforcement (Matthews and Rawlings, 1999). In order to accomplish a high-quality bond, good wetting of the fibres by the liquid matrix is required. When the reinforcement is wetted by the matrix, bonding will take place.

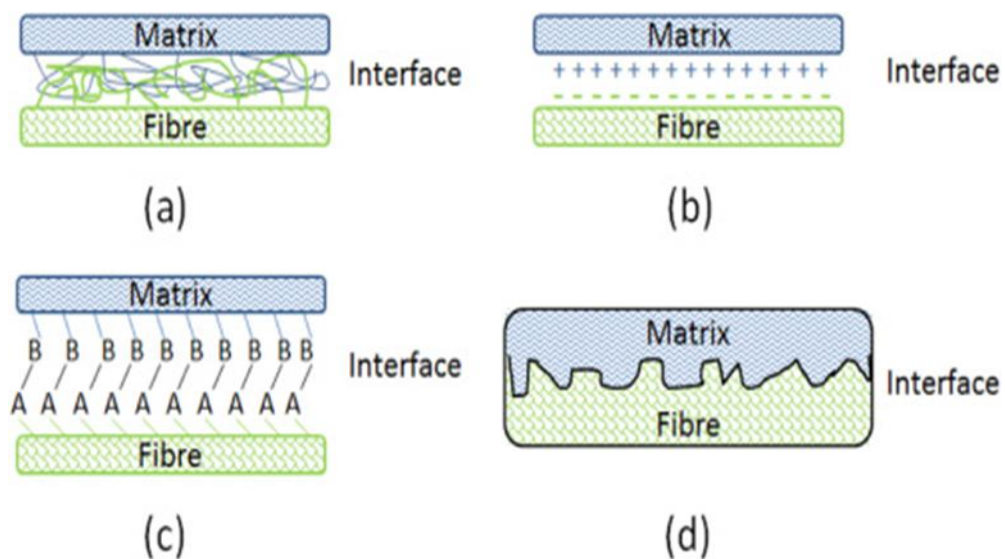


Figure 2-11 Fibre-matrix interfacial bonding mechanisms: (a) molecular entanglement following interdiffusion, (b) electrostatic adhesion, (c) chemical bonding and (d) mechanical interlocking (Zhou, Fan and Chen, 2016)

In general, the bonding mechanisms between the fibre and the matrix include four different types as shown in Figure 2-11 (Zhou, Fan and Chen, 2016). Fibre/matrix

adhesion is controlled by these mechanisms and commonly one of these mechanisms plays a dominant role. These four mechanisms are presented in the following sections:

2.3.1 Interdiffusion Bonding

The Interdiffusion mechanism happens once the intermolecular interaction between the molecule of the fibre and matrix occurs due to hydrogen bonding or Van der Waals force (Liu et al, 2012). In fact, this adhesion mechanism is attributed to two phases, namely adsorption and diffusion. In the initial phase, an intimate contact between the fibre and the matrix should be available, which is in turn governed by two actions including spreading and penetration.

As soon as good wetting occurs, permanent adhesion is established through molecular attractions (for instance, covalent, electrostatic and Van der Waals). In addition, sufficient wetting between the fibre and the matrix leads to the interdiffusion of molecules between the constituent. The degree and the extent of the diffusion is predominantly governed by the chemical compatibility between the fibre and the matrix and porosity of the fibre (Kuk and Kaushik, 2011)

2.3.2 Electrostatic Bonding

The electrostatic bonding mechanism takes place if the surface of the matrix or the reinforcement is positively charged, and the other is negatively charged. Electrostatic bonding is involved in the creation of opposite charges on the surface of fibre and the matrix. Consequently, an interface involving two layers of different charges is created. This interface is responsible for the adhesion between fibre and the matrix (Liu et al, 2012).

2.3.3 Chemical Bonding

The chemical mechanism occurs when a chemical bond is formed between the chemical groups on the reinforcement and matrix surface. The strength of the bond governed by the type of chemical bond and bonds formed per unit area. Chemisorption take place when chemical bonds (atomic and ionic) are formed between the fibre surface and the matrix because of chemical reactions. Existing physical and chemical bonds rely on the surface chemistry of the fibre and this is defined as thermodynamic adhesion.

2.3.4 Mechanical Bonding

The mechanical mechanism, similarly, known as interlocking, is influenced by the surface roughness of the reinforcement. The greater the reinforcement's roughness the more effective the mechanical bonding is.

2.4 Surface Modification of Materials

PP and GF are extensively used in reinforcing fibre for cementitious composites due to their chemical and mechanical properties, easy handling, corrosion resistance and low cost (Karihaloo and Wang, 2000; Trejbal et al, 2015). Due to the low surface energy of glass and synthetic fibres such as polypropylene, polyethylene and nylon fibres, the bonding strength with the cement-based material is poor (Borcia, Anderson and Brown, 2006; Kan and Yuen, 2013). In the light of previous works undertaken by researchers, surface modification of fibres can be categorized as physical, chemical, mechanical and plasma treatment, which are briefly discussed in the following section. Plasma surface modification technique was used in this study. Therefore, only plasma was discussed here in detail. Table 2-2 shows a summary table of current techniques

used in surface modifications of fibres for cementitious applications with their properties and limitations.

Table 2-2 Current Techniques Used in Fibre Treatments for Cement Based Composites

Surface Modification Technique	Properties and Limitations	References
Wet chemical treatment such as acid and etching solutions	<ol style="list-style-type: none"> 1. Leads to disproportionate etching with consequences in loss of mechanical performance of the fibre. 2. The degree of etching is difficult to measure and etching chemical need to be carefully disposed of with great quantities of cleaning solutions. 3. Washing out of these wastes may also cause environmental problems. 	<ol style="list-style-type: none"> 1. (Huang et al, 2006) 2. (Morent et al, 2008) 3. (Morent, 2011) 4. (Gao, Mäder and Plonka, 2004)
Mechanical treatment	<ol style="list-style-type: none"> 1. Leads to cross-section loss of the fibres. 2. Difficulty applying on shorter and thinner fibres 	<ol style="list-style-type: none"> 1. (Singh, Shukla and Brown, 2004b) 2. (Hannant, Zonsveld and Hughes, 1978) 3. (Bentur, Peled and Yankelevsky, 1997) 4. (Li, Wang and Backer, 1990) 5. (Peled, Guttman and Bentur, 1992)
Flame or heat treatment	Frequently leads to further brittle structure of the fibres	<ol style="list-style-type: none"> 1. (Richaud et al, 2008)
Low pressure plasma treatment	<ol style="list-style-type: none"> 1. Flexible method 2. Environmentally friendly nature 3. <u>High vacuum equipment and maintenance cost</u> 4. <u>Low productivity only applicable on smaller batch treatments, and hence very difficult to implement in a continuous way</u> 	<ol style="list-style-type: none"> 1. (Li, Wu and Chan, 1996) 2. (Zhang, Gopalaratnam and Yasuda, 1999) 3. (Hawai-Chung and Victor, 1999) 4. (Feldman et al, 2000) 5. (Tosun, Felekoğlu and Baradan, 2012) 6. (Felekoglu, Tosun and Baradan, 2009) 7. (Felekoglu et al, 2014)
Atmospheric pressure plasma treatment	<ol style="list-style-type: none"> 1. High productivity 2. No vacuum equipment cost 3. Dry process without releasing any harmful chemicals to the environment 	<ol style="list-style-type: none"> 1. (Favia et al, 2001) 2. (Kim et al, 2016) 3. (Yang and Yin, 2007) 4. (Wolf, 2012)

2.4.1 Chemical Modification

Chemical modification generally consists of a direct chemical reaction of the substrate with a specific chemical substance. The two main chemical treatments used in surface modifications are wet treatment and surface grafting. To modify the chemical composition of the material surface especially on polymer surfaces, wet treatment was first used. This was achieved by exposing the surface to a direct chemical reaction with a specific solution. Various chemical solutions were used for the purpose of surface treatment such as acid solutions, organic solutions, and specific solutions that oxidize the polymer surface (Goddard and Hotchkiss, 2007). Surface grafting is another technique for chemical modification, which is used in the surface treatment of material surfaces through covalent bonding of suitable macromolecular chains to the surface of the material. The essential steps consist of the formation of reactive groups on the surface of the material and the diffusion of a monomer onto the surface (Garbassi, Morra and Occhiello, 1998).

To enhance the bonding strength between fibres and the surrounding cementitious matrix, several researchers have treated fibres with chemical agents. Payrow et al. (Payrow, Nokken and Banu, 2011) used two types of chromic acid, potassium permanganate and hydrogen peroxide solutions to treat fibres. Their results indicated that in general fibre reinforced concrete specimens containing treated fibres exhibit higher residual strength in comparison with specimens created with untreated fibres. An investigation on improving the bond strength between the fibre and the cement matrix was made by Lovata and Fahmy (Lovata and Fahmy, 1987). In their investigation polypropylene fibres were treated with a mild organic oleic and a commercial alkali solution. They observed that chemical treatment of fibres improved the compressive strength due to increasing the wettability of fibres after treatment.

2.4.2 Physical Modification

Material physical surface modification can be classified into two groups. In the first group, high energy media is applied to the surface layer of the material. Whereas, the second group involved depositing a layer on the top surface of the material. The most common physical surface modifications used are flame treatment, corona treatment, X-ray and Gamma ray (γ), ultra violet (UV) treatment and plasma treatment (Lippert, 2005; Farris et al, 2010; Morent, 2011; Tuominen, Lahti and Kuusipalo, 2011).

Flame treatments are commonly used to introduce oxygen-containing species to the surface of treated material. The species are generated by high-temperature flame treatment include radicals, ions and molecules in excited states.

Corona treatment (it is also known as air plasma) is a technique that is used for the surface modification purpose of materials using low temperature corona discharge plasma.

UV treatments include active photons which are generally energetic species that have relatively low wavelength to activate numerous chemical reactions on material surfaces. X-ray and γ -ray treatment both involve high energy photons which initiate the development of radical species at the material surfaces and mainly involve crosslinking of polymeric coatings on surfaces.

2.4.3 Mechanical Modification

In mechanical modifications, fibres are modified along their length by introducing mechanical surface deformations and roughness. Consequently, the contact surface area between the fibre and the cement matrix is increased to provide a better mechanical anchorage (Pakravan and Memariyan, 2017b). A study by Singh et al. (Singh, Shukla and Brown, 2004b) investigated the possibility of mechanical

modification of macro polypropylene fibre for enhancing the interfacial bond between the fibre and the matrix.

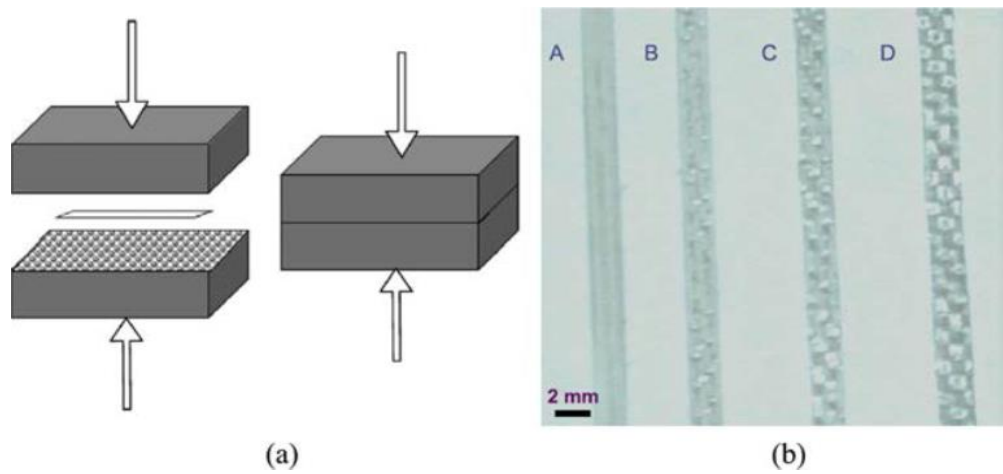


Figure 2-12 (a) Schematic description for indentation method and (b) pictures of indented fibres (Singh, Shukla and Brown, 2004b)

Figure 2-12 shows a mechanical technique which was proposed by pressing the fibres between two hardened steel surfaces having projections to induce mechanical indentations

The new indented surface of the treated fibre leads to improvement in the mechanical interlocking between fibre and surrounding matrix. They reported that even though the level of surface indentation increased the bond strength between the fibre and the surrounding cement matrix, it caused a reduction in fibre tenacity.

Hannant et al. (Hannant, Zonsveld and Hughes, 1978) reported that by converting polypropylene fibre to fibrillated fibres the mechanical interface with the surrounding cement matrix can be enhanced. They observed that the hydration products of a cementitious matrix may enter gaps between fibrillated bundles and be responsible for bonding strength improvement. Similarly, Bentur et al. (Bentur, Mindess and Vondran, 1989) also reported a similar conclusion on the effectiveness of converting

polypropylene fibres into fibrillated form, which can enhance the bonding strength between the fibre and the surrounding cement matrix. The results indicated that the mechanical treatment could improve the frictional bond between fibre and the cement matrix.

2.4.4 Plasma Modification

Plasma treatment is potentially promising method to modify the properties of the fibre surface. Due to its flexibility and environmentally friendly nature compared to other surface treatment techniques, plasma treatment is used widely to enhance the mechanical characteristics of FRC (Denes et al, 1999). This method was shown to be effective in improving the compatibility between hydrophilic cementitious matrix and hydrophobic fibre reinforcement. The ionised gas in the plasma can alter the surface characteristics of fibres by introducing new polar groups on the surface of fibres, increasing the surface roughness of fibres and improving the fibre's surface wettability (Chen et al, 2008). Low-pressure plasma treatment has been investigated by a few researchers in the past. However, the literature revealed that there are no previous studies conducted on the effect of atmospheric pressure plasma treatment to enhance the interfacial adhesion between the fibres and the cement-based matrix.

2.4.4.1 Plasma Definition

Irving Langmuir (1926) first studied plasma in the early 20th century. Plasma can be defined as an electrically conducting medium which normally contains negatively charged electrons, positively charged ions and neutral atoms or molecules or both (Li, Ye and Mai, 1997). Plasma is known as the fourth fundamental state of matter after solid, liquid and gas since it exhibits rather different properties from those of common substances in the gaseous, liquid or solid states. It is believed that over 99% of the matter in the universe is plasma, typically in numerous massive stellar stars. Due to its higher energy intensity compared to the other three states of matter, plasma is rarer than the other three states; therefore, it becomes the fourth on our planet.

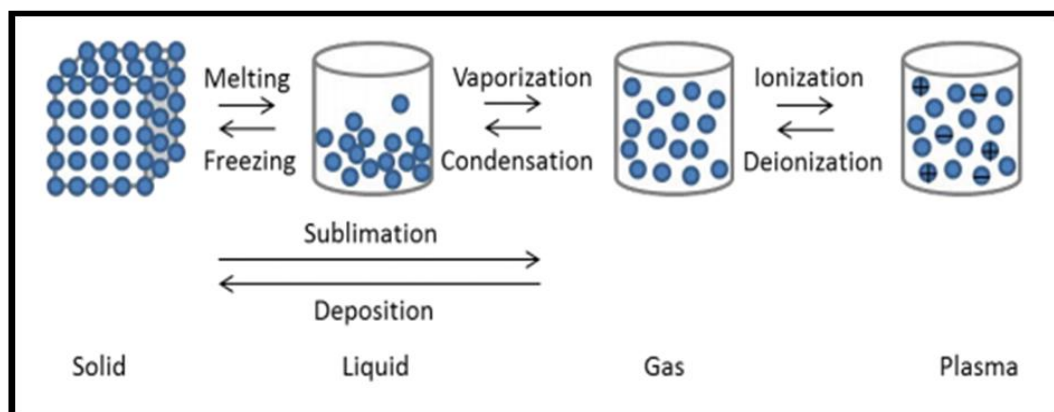


Figure 2-13 Scheme of the states of matter and the processes to change between them

If sufficient energy is employed in a system, a state transformation will take place as matter changes to a higher active state (Figure 2-13). Beginning with matter in solid state, if sufficient energy is applied, a solid can melt and convert to a liquid state. If further energy is applied to the system, the liquid will ultimately vaporise and convert to a gas state. Lastly, if further energy is applied in the system, a level will be attained where electrons breakaway from the neutral gas atoms leading to gas ionization. Once

the number of electrons/ions is sufficient, the gas is considered to have become a plasma. The energy required to form a plasma depends on the gas composition. For instance, a temperature of up to $\sim 20,000$ K is required to ionise helium, however half of this temperature is required for ionizing argon (Jeroen Jonkers et al, 2002). Furthermore, plasma can be produced by applying an electric field too. These types of plasma are known as electrical discharges, in which energy is transferred mainly to electrons, as a result they are excited and heated to tens of thousands of kelvins, however neutral gas molecules remain at ambient temperature since they are not affected by the electric field applied. A spreading of electrons with a temperature reaching up to $11,600$ K ($\sim 1\text{eV}$) have a major fraction of electrons with enough energy ($1\sim 15\text{eV}$) to separate molecules of the gas into reactive species such as free radicals, atoms and excited species, and to create plasma by ionizing them. An eV is the amount of kinetic energy gained or lost by a single electron accelerating from rest through an electric potential difference of one volt in vacuum. Temperature in kelvins is a measurement of the average kinetic energy of the molecules in a system.

2.3.4.2 Plasma Classifications

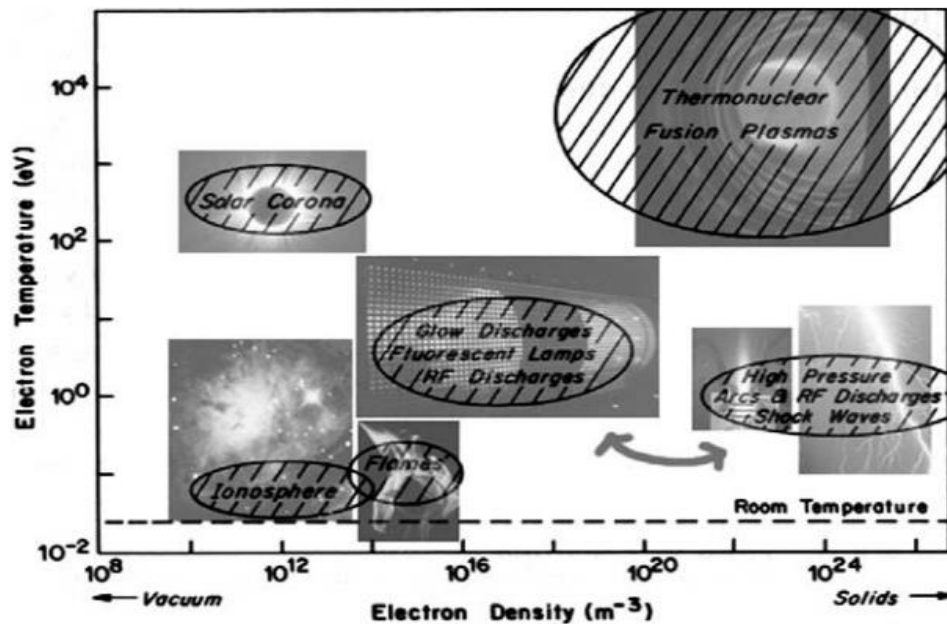


Figure 2-14 2D Classification of plasmas (electrons temperature versus electrons density) (Boulos, Fauchais and Pfender, 2013)

The properties of plasma in terms of temperature or electronic density varies according to the energy supplied and the amount of energy transferred to the plasma. These two parameters differentiate plasmas into categories such as solar corona, ionosphere, glow discharge, thermonuclear, high pressure arc, RF discharges etc., as shown in Figure 2-14. The atmospheric plasma used in this study is thought to be situated close to the glow discharges and the arcs.

According to the methods of activating the plasmas and the activation energies applied, plasma can be classified as:

- High-temperature plasma: When the gas temperature is higher than 10^6 K. This type representing most of the universe.
- Low-temperature plasma: When the gas temperature is lower than 10^6 K. This type is more prevalent on Earth. It can be further divided into:

(1) Cold plasma (non-thermal plasma), when the gas temperature is lower than 1000 K. Such as various glow discharges at low pressure. Cold plasma is also called non-thermal or non-equilibrium plasma because there is a large difference between the temperature of electrons, ions and neutrals ($T_e > T_i \approx T_n$). Energy of the ions could be lost through collision, because the electrons are tremendously light, they travel quickly and have practically no heat capacity (Denes and Manolache, 2004). Therefore, in this type of plasma, ionization is sustained by electrons impacting with neutral species, resulting in generating other ions and electrons. Generally, cold plasmas are sustained by passing electrical current over a gas. Cold plasmas are very suitable for material processing. Nevertheless, they require to be operated at low pressure, thus, expensive vacuum equipment is needed (Selwyn et al, 2001).

(2) Hot plasma (thermal plasma), when the gas temperature is higher than 1000 K and close to 100% degree of ionization. In addition, it can be called near equilibrium plasmas because of similar temperatures of plasma electron, ions and neutral gas molecule ($T_e \approx T_i \approx T_n$). Such as lightning, electrical arc discharge, plasma spraying, nuclear explosion and other high-power discharges. The range of operating pressure is around 10 mBar to more than atmospheric pressure. These plasmas have applications in waste treatment and sintering, they are not well suited for most materials processing applications because of their destructive nature. Atmospheric pressure plasma was used in this study; therefore, it will be further discussed in the following section.

2.3.4.2 Types of Atmospheric Pressure Plasma (Thermal Plasma)

Further to the applications of cold plasmas in vacuum settings, a number of plasmas operating at atmospheric pressure are also available (Schutze et al, 1998).

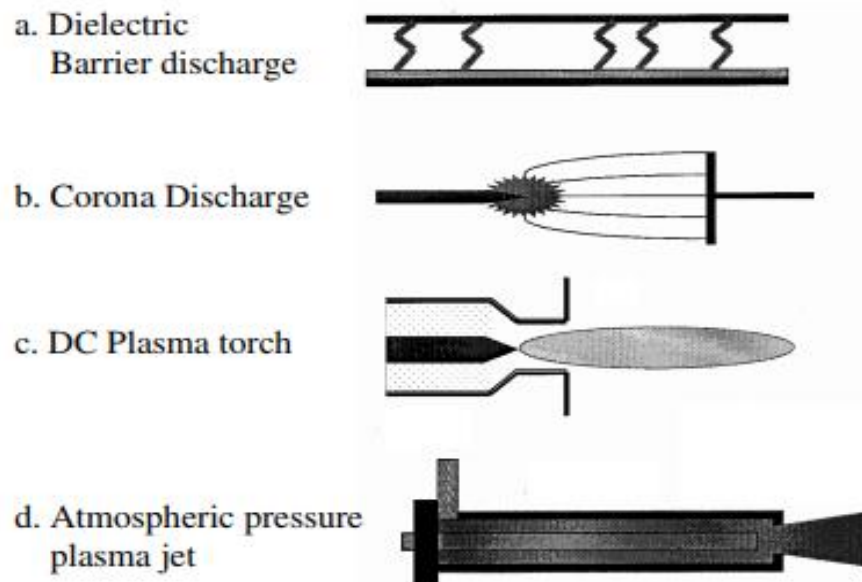


Figure 2-15 Four different kinds of atmospheric pressure plasma sources (Selwyn et al, 2001)

Figure 2-15 shows a selection of atmospheric pressure plasma systems. Dielectric barrier discharge shown in Figure 2-15(a), employs a dielectric layer over one or both electrodes. Normally one of them is AC driven or low frequency (radio frequency), whereas the other is grounded. The reason for the dielectric film is to control and promptly extinguish the arcs that generate in the latent field between the two electrodes. The discharge involves a gathering of fast generating and equally fast extinguished arcs, which occupy the space between the electrodes (Selwyn et al, 2001). Therefore the plasmas are not uniform throughout the volume (Eliasson and Kogelschatz, 1991).

The corona discharge shown in Figure 2-15(b) is non-uniform and non-arcing plasma which ignites the area of the high electric field produced by the sharp points of the electrodes. No grounded surface can be near these field emission points, to avoid arcing, thus, the discharge is non-uniform. Furthermore, plasma density drops off quickly when the distance from the electrode is increased (Goldman and Sigmond, 1982).

The DC plasma torch shown in Figure 2-15(c) is usually mixed with the atmospheric pressure plasma jet. In contrast with the other plasma systems presented in Figure 2-15, the DC plasma torch is a thermal plasma defined by $T_i \approx T_e$. Hence, it has high gas temperatures, which makes it suitable for materials processing applications, mainly for plasma spraying, chemical waste destruction and ceramic coatings deposition applications. Besides the DC plasma torch, other designs are also available which operate by radio frequency or microwave frequency. The application of the DC plasma for processing conducting materials is limited due to the charge being transferred to the material both negatively and positively (Al-Shamma'a et al, 2001).

The atmospheric pressure plasma jet (APPJ) shown in Figure 2-15(d), is similar to the DC plasma torch in some respects, however, it is non-thermal plasma, as verified by the massive temperature differences between the electrons and the ions. The APPJ system generates a steady, regular and constant discharge at atmospheric pressure with no need for any dielectric electrode cover; nevertheless, it is free of streamers and arcing. However, electrodes of the arc plasma jet oxidize very fast, which is attributable to the oxygen molecules in air.

To increase the electrode lifetime to a few hundred hours, water-cooled metallic electrodes have been used in some arc plasma systems. However, there are some safety

concerns arising in this case, since the leak of water into the plasma may cause an explosion (Leis and broekaert, 1984). Graphite electrodes have been introduced in some other plasma systems and are operated only in non-oxidizing environments (Uhm, Hong and Shin, 2006). In this circumstance, there is a new method for producing an electrodeless thermal plasma torch that can be used for various processing applications, such as the radio frequency (RF) and induction coupled plasma (ICP). The ICP thermal plasma system is currently used in the cases where contamination cannot be accepted such as the elemental analysis, fibre optics industries and semiconductors. However, the discharged RF power from the induction coil necessitates protective shielding for safety, and to avoid the probability of combining RF torches to increase power. In addition, high power RF induction torches usually have coupling efficiencies of less than 50% (Uhm, Hong and Shin, 2006).

Therefore, the conventional thermal plasma jets cannot be used effectively in so many environmental applications (Hong and Uhm, 2001). One of electrodeless plasma torches is microwave plasma which can generate plasma in large quantities. This study aims to develop a new system to solve the above-mentioned problems. The system developed consists of a thermal plasma torch operating without electrodes at atmospheric pressure. Unlike, the conventional electrodeless microwave plasma system, which operates at frequency 2.45 GHz, the system developed operates at microwave frequency 5.8 GHz. Table 2-3 summarises the current plasma systems used for material processing applications with their properties and limitations. In contrast, developed MIPT has been put in the lower row for comparison.

Table 2-3 A summary of current plasma systems used in material processing application

Type	properties	
Low pressure plasma system	Vacuum systems are expensive and require maintenance. Load locks and robotic assemblies must be used to shuttle materials in and out of vacuum. Also, the size of the object that can be treated is limited by the size of the vacuum chamber	(Schutze et al, 1998)
Atmospheric-pressure plasm:		
1. Corona Discharge	To prevent arcing and lower the gas temperature, several schemes have been devised, such as the use of pointed electrodes in corona discharge. Therefore, the plasmas are not uniform throughout the volume. Therefore, its application in material processing is limited.	(Goldman and Sigmond, 1982)
2. Dielectric Barrier Discharg	1. Diearectric Barrier Discharge To avoid arcing insulating inserts between the electrodes. Therefore, the plasmas are not uniform throughout the volume. Can only be used for non-conductive material processing. Therefore, its application in material processing is limited.	(Eliasson and Kogelschatz, 1991)
3. DC Plasma Torch	The application of the DC plasma for processing conducting materials is limited due to the charge being transferred to the material both positively or negatively.	(Al-Shamma'a et al, 2001)
4. (2.45 GHz) Microwave induced plasma Torch	Electrodes of the arc plasma torches oxidize very quickly due to the oxygen molecules in air. That is why the conventional thermal plasma torch cannot be used in environmental applications	(Hong and Uhm, 2001)
5. The Developed (5.8 GHz) Microwave Induced Plasma Torch (Electrodeless)	Has very motivating characteristic, which are in direct relationship with the excitation frequency. This is down to the ease to get to high electron density, which itself has an impact on the density of additional formed particles like radicals, ions, excited molecules and atoms or UV light. It is electrodeless, therefore, the problematic of electrode vapour contamination that formerly extremely affected the stability and properties of the plasma torch was avoided, and thus, the processing quality is improved.	

2.3.4.4 Application of Plasma

Plasma particles lead to chemical and physical interactions between the plasma and the treated substrate surface. These interactions depend on so many factors, such as plasma condition, type of gas used, power, pressure, distance from the flame and treatment duration. Despite the wide use of plasma in many different industries, its application and benefits to date are poorly realised in the field of civil engineering. Therefore, in this research study, the effect of atmospheric pressure plasma on the enhancement of the properties of fibre reinforced concrete has been investigated.

The enhancement of the (ITZ) between the cement matrix and the plasma treated reinforcement fibres is caused by both physical and chemical modifications. The physical modifications can be achieved by surface roughening of the fibres, producing a larger surface area for bonding. Thus, the friction between the matrix and the fibre is increased. The chemical modification is included in the implantation of active polar groups on the surface of the fibre, increasing the surface energy of the fibre. Thus, the chemical bonding between the matrix and the fibre is enhanced.

Depending on the power and duration of the plasma, it is possible to classify the changes that the material will bring to the table in three main groups:

- Activation or Modification of the Substrate Surface with Plasma

If a material is held in a plasma environment under certain conditions, the material can have very different functional surface properties from those of the substrate itself. The surface properties to be obtained may vary depending on the type of plasma to be used and on some other parameters such as treatment duration, frequency, pressure, amount of energy applied, etc.

Argon and oxygen plasma generally increase the surface energy of the surface of polymer-based materials. The energy of the polymer surface treated with argon and oxygen plasma increases the water wetting capacity. On the other hand, the argon - carbon tetrafluoride plasma gives a hydrophobic property to the surface of polymer materials. However, the impact of all these effects varies with the duration of the plasma treatment and other parameters. Surface activation does not change mechanical properties if the internal structure is not applied for an extended period.

In terms of ensuring the wettability of polymers, not all plasma gases show the same activity. In 1998, Weiming et al. (Weiming Lu, Fu and Chung, 1998) compared the ozone (O₃) plasma and other chemical etching methods in an investigation of the performance of cement matrix composite by increasing the wettability of steel, carbon, and polyethylene fibres. Their results have shown that (O₃) plasma affects the wettability of steel and carbon fibres positively but is not effective on polyethylene fibres.

In another study by Lai et al. (Lai et al, 2006) to improve the wettability properties of fibres, polycarbonate (PC), polypropylene (PP), polyethylene terephthalate (PET) fibres were exposed to microwave frequency argon gas plasma. They observed that all fibres have increased wettability. In addition, changes in both surface element and bond composition and surface micro-roughness of the fibres have been reported.

- Plasma Polymerization or Cross-Linking

Plasma technology is used to increase adherence with the substrate to which the coating materials will be applied. Under plasma action, bonds on the substrate surface are broken off to form free molecules with covalent bonding capacity. The open bonds increase surface reactivity. If free radicals are present in the plasma, they are connected

to these bonds to change the surface properties. For example, the O₂ plasma forms carbonyl and hydroxyl groups on the polyethylene surface. These groups are highly reactive and it is possible to form covalent bonds with any matrix phase (Pasquariello et al, 2000).

Plasma polymerisation can be used in the enhancement of the performance of polymer adhesives such as epoxy, methyl methacrylate and others (Gabouze, 2002; Oláh et al, 2006). Plasma applications aimed at increasing metal polymer binding are also found in the literature (Hozbor, 1993). Another interesting application of plasma polymerisation is in the field of biotechnology. The surface properties that allow the attachment of protein molecules on the surface of metals can be formed by the plasma method. Thus, it is possible for the body to accept biocompatible parts.

- Plasma Cleaning

Sterilization and cleaning of the surface of biomedical materials is nevertheless an additional application of plasmas in which the properties of the particular surface are changed (microbes and toxins are removed) without the bulk mechanical properties of the substrate being affected. In addition, sensitive systems such as microchips and polymers are cleaned by cold atmospheric plasma as they are affected by high temperatures (Tendero et al, 2006).

2.3.4.5 Performance of Plasma Modified Fibre Reinforced Cementitious Composites

Although the plasma technique is widely used in surface modifications of fibres in many industries (Denes et al, 1999), there are a limited number of studies, in which fibres modified by plasma methods, are used in cement-based composites. These studies mainly focused on low-pressure plasma systems. This method was known to

be very effective in establishing compatibility between the hydrophobic and hydrophilic nature of fibre and cement matrix respectively (Pakravan and Memariyan, 2017b). The positive and negative radical species in plasma introduce a new polar groups to the surface of the treated fibre (Wang et al, 2015). Thus the surface wettability is improved (Chen et al, 2008). Atmospheric pressure plasma surface modification is comparatively new and theoretically promising method for altering the characteristics of the surface of the fibre. It is economical to operate and a simple system to setup with no vacuum equipment requirements (Tyata et al, 2012). Therefore, in this study the atmospheric pressure plasma technique was used to enhance the performance of FRCC. Below is a summary of some research studies that used the plasma technique for improving the performance of FRCC.

(A) Polypropylene Fibre (PP)

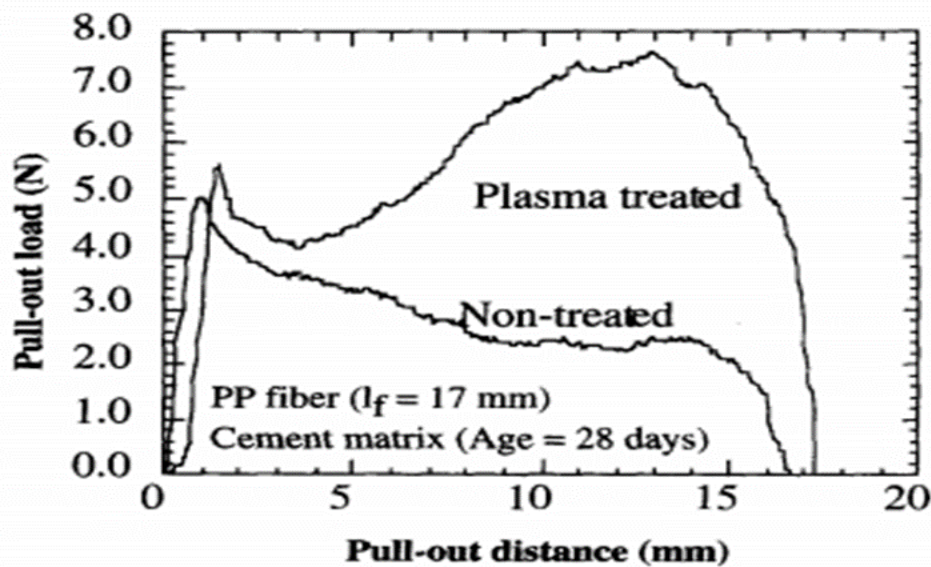


Figure 2-16 Effect of surface modification of polypropylene (Li and Stang, 1997)

The results of an experimental work shown in Figure 2-16 by Li and Stang (Li and Stang, 1997) plasma technique were used in surface modification of PP Fibre. They

used the plasma method to increase the adherence between the cement-based matrix and the fibres. The pull-out load of the plasma-treated fibres was improved by 20%, and a significant improvement in the amount of slip hardening can be seen. The increase in pull-out distance and the increase in load are attributed to the etching effect on the surface of the plasma treated PP fibre. Micro-roughness on the surface increased the matrix's adherence and the load level increased while the fibres were pulled out.

In another investigation using low-pressure plasma by Hawaii and Victor (Hawaii-Chung and Victor, 1999) the tensile strength of PP fibre was modified using three various types of gases were employed such as ammonia (NH_3), carbon Dioxide (CO_2) and argon (Ar). The results indicated that the specimens prepared with plasma modified fibres exhibit higher composite tensile strain as compared to as received. The tensile strain capacity was 5.8%, 5.8% and 6.75% for Ar, CO_2 , and NH_3 respectively. Whereas, the tensile strain capacity of specimens made with untreated fibres was recorded as 5.5%. To confirm that the improvement in strain capacity of the composite was due to the plasma treatment, single fibre pull-out tests were carried out too. The results indicated that all the plasma-treated fibres exhibited enhanced interfacial bonding strength between the fibre and cement matrix. The results showed that the plasma modified polyethylene fibres exhibit higher frictional bond and required higher energy throughout the pull-out test in comparison to specimens prepared with as received fibres. The observed interfacial bonding strength improvements were 21%, 32% and 35% for NH_3 , CO_2 and Ar respectively.

An investigation was undertaken in 1999 by Zhang et al. (Zhang, Gopalaratnam and Yasuda, 1999) on the effect of low temperature cascade arc plasma with various gases on the mechanical performance and toughness of a fibre reinforced cement matrix. Three different types of gases were used, argon, methane + oxygen and air (Ar,

CH₄+O₂ and Air). The fibres used in this study were fibrillated polypropylene and monofilament polyolefin fibres. The contact angle was measured before and after plasma treatment. The results indicated that the wettability of polypropylene fibre after various treatments was enhanced (Table 2-4). It was observed that among the three different treatments they investigated, argon treatment delivered the best performance in all flexure tests. In their investigation they concluded that the effectiveness of the plasma treatment on the mechanical performance of fibre reinforced concrete can be a function of fibre type, parameters and treatment environment.

Table 2-4 Contact angle of fibres before and after treatments (Zhang, Gopalaratnam and Yasuda, 1999)

Fibre Type	Untreated	Ar	CH₄+O₂	Air
Fibrillated	90°	78°	58°	33°
Monofilament	108°	70°	62°	53°

In 2000 an investigation was carried out by Feldman et al. (Feldman et al, 2000) on the effect of SiCl₄ low-pressure cold plasma treatment of polypropylene fibres on the mechanical properties of cementitious composites. The results of the surface analysis indicated few facts such as SiCl₄ plasma treatment-initiated surface roughness of polypropylene fibre and the water contact angles was reduced compared to untreated fibres. The presence of the C-O and C=O functional groups on the surface of the plasma treated fibres was confirmed from the results obtained by XPS and ATR-FTIR analysis. For evaluating the effect SiCl₄ plasma treatment on the interfacial adhesion characteristics, tensile strength of cement composites reinforced with plasma treated polypropylene fibres were demonstrated. The results indicated that the composites reinforced with plasma treated fibres exhibit higher tensile strength than the composite reinforced with untreated fibres by 82%. They concluded the existence of covalent linkages between the fibres and the cement matrix, and the increased surface

roughness are in charge for this enhancement of the mechanical properties of the composite.

Another study was carried out by Wei in 2004 (Wei, 2004) on the surface characterization of low pressure plasma treated polypropylene fibre. This analysis confirmed the presence of oxygen-containing functional groups on the surface of the fibres after plasma treatment. Also, it revealed different surface morphologies under different surface treatment. An improvement in the contact angle measurement was confirmed using a Philips Environmental Scanning Electron Microscopy (ESEM).

In 2006 (Huang et al, 2006) investigated the surface characterization of polypropylene fibres treated with low-pressure argon and oxygen plasma. They observed that the nanoscale grooves (etching) induced by argon plasma were higher compared to oxygen plasma treatment. They observed that the contact angle is reduced significantly with both Argon and oxygen plasma treatment.

In 2009 (Felekoglu, Tosun and Baradan, 2009) carried out an investigation on the effect of low pressure cold plasma surface modification of polypropylene fibre on the flexural behaviour of fibre reinforced cementitious composite. In their study low frequency (40kHz) argon and oxygen plasma at various power levels (60, 120 and 180 W) were used for treating the fibres. The plasma treatment was optimized based on surface characteristic of treated fibres such as Scanning Electron Microscopy (SEM) and contact angle measurement. Based on SEM and contact angle measurement of treated fibres, fibres treated with 60W-8min, 120W-2min, 180W-2min and 180W-30min of argon and oxygen plasma were chosen to demonstrate flexural performance of fibre reinforced cementitious composites. Specimens of 40 mm × 40 mm × 160 mm were produced using a mix ratio in kg/m³ is showed in Table 2-5:

Table 2-5 Composite Mix proportion (Felekoglu, Tosun and Baradan, 2009)

Material	(kg/m ³)
Cement (CEMI42.5)	854
Water	380
Limestone Powder	854
Superplasticizer%	1
PP Fibre %	1%

The results indicated that plasma treatment with both argon and oxygen significantly improved the flexural characteristics of polypropylene fibre reinforced cementitious composites. However, they observed that for treating polypropylene fibres, the efficiency of the argon plasma was much greater than for the oxygen plasma.

A similar conclusion was observed by (Tosun, Felekoğlu and Baradan, 2012) when they investigated the effect of low frequency (40 kHz) argon and oxygen plasma surface treatment of polyethylene fibres on the flexural performance of similar fibre reinforced cementitious composites.

In summary, surface structures of fibres can be physically and chemically modified by using the plasma technique, and the matrix performance can be improved by adjusting the fibre matrix interface adherence.

(B) Glass Fibre (GF)

Although there are no previous studies of the performance of plasma treated glass fibre in cementitious composite, low-pressure plasma treatment was used to enhance the adhesion of glass fibre epoxy resin composites. In an attempt made by Kusano et al. (Kusano et al, 2007) glass fibre reinforced polyester composite plates were modified

with an low pressure plasma. Their results indicated that the wettability measurement of air plasma treated specimens dropped remarkably. Furthermore, X-ray photoelectron spectroscopy analysis demonstrated that aluminium and oxygen contents on the surface of the plasma treated fibres were greater than before. Thus, the adhesion strength of plasma treated specimens was significantly higher in comparison to that achieved by control specimens.

In a study carried out by (Yang et al, 2016), the effects of various treatment durations on the surface energy of E-glass fibre were investigated. Their results indicated that the oxygen contained on the surface of the glass fibre was greater compared to untreated ones. The surface hydrophilicity was improved, and so the adhesion with the matrix was significantly improved.

(C) Basalt Fibre (BF)

Even though the plasma treatment is an alternative environmentally effective method compared to the wet process using silane solution, alkaline and acid, limited studies have been made to consider the surface modification of basalt fibre. (Wang et al, 2007) reported that using low temperature plasma is an effective technique to improve the wettability of basalt fibres, but investigation was limited to analysing chemical alterations on the surface of single basalt fibres and did not investigate the physical and mechanical impact induced by the plasma treatment. In another study carried out by Kim et al. (Kim et al, 2011), low-temperature atmospheric oxygen plasma was used to modify the surface of woven-type basalt fibres, and the influence on the interlinear fracture performance of basalt/epoxy woven composites was investigated. Contact angle measurements of the basalt fibre surface were used to examine the changes in wettability resulting from the plasma treatment. The chemical and

morphological changes to the basalt fibres was evaluated using XPS and FE-SEM. Basalt/epoxy woven composites were created with and without oxygen plasma treatment, and their respective interlinear fracture toughness was compared. The results indicated that the wettability values of the basalt fibre were significantly greater than before, followed by physical etching and by the development of chemical functional groups comprising oxygen and nitrogen on the fibre surface. The interlinear fracture toughness of basalt/epoxy woven composites was enhanced by 16% by oxygen plasma treatment. SEM results on the fractured surface showed epoxy resin adhered well around the surface of basalt fibres in the specimens treated by oxygen plasma, compared to that of the untreated specimen. An adhesive force between fibre/resin interfaces was enhanced by oxygen plasma treatment, thus the interlinear fracture toughness of basalt/epoxy woven composites was increased. Table 2-6 shows a summary table of current research with plasma in cementitious material applications and what has been achieved so far in this field.

Table 2-6 Current Plasma Techniques Used in Fibre Treatments for Cement Based Composites

Plasma Technique used in Cementitious Applications	Achievements	References
Radio frequency (RF) (30 kHz) SiCl ₄ -plasma conditions in a stainless steel, parallel plate, capacitive coupled reactor	<ol style="list-style-type: none"> 1. Enhanced wettability and decreased CAM. Surface morphologies using AFM showed the existence of a rough surface structure for the plasma-treated fibres. 2. The FRC strengthen plasma treated fibre demonstrated improved flexural strength and toughness than those containing untreated fibres. 	(Denes et al, 1999)
Radio frequency Ar, CO ₂ and NH ₃ plasma condition in a small chamber size. Initial pressure 6.38 * 10 ² Pa, and power 58 W.	<ol style="list-style-type: none"> 1. All plasma treated fibres enhanced fibre/cement interfacial bonding strength. From the 2. plasma treated polyethylene fibre has a much higher frictional bond value and consumed additional energy throughout the pull-out process. 	(Li, Wu and Chan, 1996)
Low-temperature, cascade arc plasma polymerization apparatus. Ar was used as the carrier gas. NH ₃ , O ₂ , and air were used as the reactive gases. A steel chamber with a pressure of 36 Pa and power 240-280 W	<ol style="list-style-type: none"> 1. Wettability improvement of fibres. 2. Improvement in flexural performance of the composite. 	(Zhang, Gopalaratnam and Yasuda, 1999)
Ar Plasma 100 and 300 W CH ₄ Plasma 100 and 300 W O ₂ Plasma 300 and 300 W Air Plasma 100 and 300 W	Improvement in fibre/cement interfacial bonding strength by six-fold.	(Hawai-Chung and Victor, 1999)

Radio frequency (RF) (30 kHz) SiCl ₄ Pyrex glass electrodeless plasma reactor with 6.6 Pa and 200W	<ol style="list-style-type: none"> 1. Lower CAM. 2. Enhanced surface roughness of fibres. 3. Existence of C–O functional group on the surface of treated fibres. 4. Improvement of composites tensile strength by 82%. 	(Feldman et al, 2000)
O ₂ Plasma	<ol style="list-style-type: none"> 1. Introduction of O₂ functional groups on the surface of treated fibres from XPS. 2. Improved surface morphology from AFM. 3. Wettability improvement and reduction of CAM. 	(Wei, 2004)
Low temperature vertical plasma machine at a pressure of 15 Pa and a power of (35-75) W.	<ol style="list-style-type: none"> 1. Roughness improvement from SEM and AFM. 2. Considerable reduction in CAM of fibres. 	(Huang et al, 2006)
Low frequency (40 kHz) cold Ar and O ₂ plasma (0-200) W in a vacuum chamber.	<ol style="list-style-type: none"> 1. Improvement in wetting properties and reduction in CAM of fibres. 2. Improvement of surface roughness from SEM and AFM. 3. Enhancement of composites performance in terms of flexural strength and toughness. 	(Felekoglu, Tosun and Baradan, 2009)
Low frequency (40 KHz) cold Ar and O ₂ plasma (0-200) W in a vacuum chamber.	<ol style="list-style-type: none"> 1. Enhanced roughness and surface morphology of fibres from SEM and AFM. 2. Introduction of O₂ containing functional groups on the surface of fibres from XPS. 3. Improvement in flexural strength and toughness by (15-35 %). 	(Tosun, Felekoğlu and Baradan, 2012)

2.5 Summary

In summary, adding fibres to concrete can control the development of cracks and the post crack performance of the concrete (ductility) can be enhanced. Metal fibres for reinforcing concrete has been considerably industrialised in the last 5 decades. Consequently, different types of concrete have been developed, from the conventional fibre reinforced concrete to concrete with an exceptionally dense microstructure, which eventually allowed high strength fibre reinforced concrete to be developed. This concrete allows the production of different types of concrete that are predominantly innovative in favour of design and mechanical characteristics. However, the use of metal fibres is also associated with a number of problems such as the corrosion of the fibres at the concrete surface.

Non-metallic fibres have been industrialised, including polymer fibres, glass fibres and basalt fibres. Many studies have been aimed at investigating the use of non-metallic fibres for reinforcing concrete. Despite the numerous advantages of these fibres such as, high tensile strength, low production cost, low weight to volume ratio and corrosion resistance, but the hydrophobic surface characteristic of these fibres resulted in poor adhesion with the cementitious matrix.

Many techniques for surface modification of these fibres have been developed. Among them, plasma treatment is an attractive method for modifying the fibre surface due to its environmentally friendly nature and effective treatment effects without altering the bulk mechanical properties of the fibres in comparison to chemical, mechanical and physical surface treatments. Surface treatments of polymer fibres using low pressure plasma showed a significant improvement in the performance characteristic of fibre reinforced concrete, however, vacuum systems are expensive, and limit batch sizes.

An atmospheric pressure plasma system can resolve disadvantages of the low-pressure plasma system. Although, there are no previous studies on the effect of plasma treated glass and basalt fibre on the performance of the cementitious composites, however, plasma treated glass and basalt fibres have showed an enhancement in the overall performance of the composites. Therefore, a detailed study on the effect of atmospheric pressure plasma treatment of polypropylene, glass and basalt fibre and its effect on the performance of fibre cementitious composites is required.

Chapter 3 Methodology

3.1 Introduction

This chapter presents a brief description about the plasma system that was developed and used in this study. The properties of the fibres used, and the mix constituent are also presented, as well as a description of the experiments undertaken is presented in this chapter.

3.2 Materials

The same mixture of ingredients was used for making the cement mix throughout this study. The cement mix composition was optimized from the view point of workability, homogeneity and surface finishing (Brandan, Tosun and Felekoglu, 2008). This mix was selected to achieve a comparison between the effects of previous plasma treatment (low-pressure) and the plasma treatment developed in this study. The mix is given in Table 3-1:

Table 3-1 Mix Design for Fibre reinforced Cement Based Composite (Brandan, Tosun and Felekoglu, 2008)

Material	(kg/m³)
Cement (CEMI42.5)	854
Water	380
Limestone Powder	854
Superplasticizer%	1
Fibre %	Optimized for each fibre by total volume as follow:
	PPF1 % 1.25
	GF % 1.5
	BF % 1.25

A brief description of each material used in the mix is presented in the following section:

3.2.1 Fibres

Despite the advantages of synthetic, glass and basalt fibres over conventional steel and carbon fibres in terms of their lower price, lower weight and corrosion resistance, these fibres exhibit low surface energy, thus, poor adhesion with the matrix. The properties of each type of fibres are presented in section 3.2.1.1, 3.2.1.2 and 3.2.1.3.

3.2.1.1 Macro Polypropylene Fibre (PPF1)

The macro PPF1 used was Durus S400 provided by Sika UK. The fibre's physical and chemical properties are presented in Table 3-2. These macro synthetic fibres are specially designed to substitute conventional steel reinforcement for an extensive range of construction applications. Generally when the control of concrete cracking is important, such as in industrial pavements, precast structural elements, tunnel lining, etc (Buratti, Mazzotti and Savoia, 2011), these fibres can significantly improve the performance of the composite, reduce the cost and give health and safety advantages. The physical and chemical properties of the Durus S400 fibres are as follows: Average cross section of 10 specimens was 0.54×1.2 mm.

Table 3-2 Physical and chemical properties of PPF1

Physical and Chemical Properties	
Appearance	Solid
Colour	Natural
Fibre Length	10 mm
Melting Point	160°C
Specific Gravity	0.91
Solubility in Water	Insoluble
Surface	Smooth

3.2.1.2 Glass Fibre (GF)

Alkali resistant GF provided by Oscrete Construction Products was used. The fibre is known as Oscrete 67/36, which is a high-performance alkali resistant glass macro fibre, designed to improve thermal, plastic, and drying shrinkage cracking. It enhances flexural strength and ductility, and improves toughness, and impact and fatigue resistance to the concrete. In addition, it can similarly be used as secondary reinforcement and in particular applications also as primary reinforcement. Oscrete 67/36 has been specifically designed to replace secondary and primary reinforcement (welded wire reinforcement, light rebar, steel and synthetic fibres) in residential, commercial and industrial slabs on ground, compression layers, pavements and precast concrete. Table 3-3 presents the general properties of Oscrete 67/36.

Table 3-3 Properties of GF

Properties	
Nature	AR Glass Fibre
Colour	Opaque
Specific Gravity	2.68
Fibre Length	10.0 mm
Chemical Resistance	Very High
Modulus of Elasticity	72 GPa
Tensile Strength	1700 MPa
Melting Point	860°C

3.2.1.3 Basalt Fibre (BF)

Basalt fibre provided by BASALTEX was used. Basalt fibres are very fine fibres exhibiting properties similar to glass fibres but having a better performance in alkaline solution. Basalt fibre is considerably cheaper compared to carbon fibre, it is estimated to be around 1/10 of the price of carbon fibre (Deák and Czigány, 2009; Lipatov et al, 2015) and lighter in weight

compared to steel fibres (Lopresto, Leone and De Iorio, 2011; Borhan, 2012). Basalt is an igneous rock formed by the rapid cooling of lava. It is found under the earth's crust and solidifies in the open air (Singha, 2012). Basalt has numerous advantages such as, high tensile strength, high resistance to temperature, corrosion resistance, light weight, high chemical stability especially in alkaline environment and it is a waste and renewable material. The physical and chemical properties of the basalt fibres are presented in Table 3-4.

Table 3-4 Physical and chemical properties of BF

Physical and Chemical Properties	
Appearance	Solid
Colour	Green-Brown
Filament Diameter	19 μm
Fibre Length	12.7 mm
Melting Point	1450°C
Specific Gravity	2.67
Solubility in Water	Insoluble

3.2.2 Cement

In order to design a HPFRCC mix, high strength cement 42.5N – 52.5N is required. Due to the difficulty in obtaining cement type CEM1 with a strength class 42.5N, which was used in the original literature mix, a high strength Portland cement type CEM1 with a strength class of 52.5N was used. The cement was blue circle Procem cement provided by Tarmac. The physical and chemical properties are shown in Table 3-5.

Table 3-5 Properties of CEM1-52.5N

Properties	
Mean particle size	5-30
Solubility in water (T=20°C) g/l	Slight 0.1-1.5
Density g/cm ³	2.75-3.20
Ph (T= 20°C in water)	11-13.5
Boiling/melting point	>1250°C

3.2.3 Limestone Powder

A large amount of ordinary Portland cement is required for producing HPFRCC; and an enormous quantity of CO₂ is formed during the manufacturing process (Moon et al, 2017). To decrease the CO₂ emission level, several investigations on the mineral addition of silica fume, ground granulated blast-furnace slag, fly ash or limestone powder to ordinary Portland cement have been carried out. Specifically, limestone powder is commonly used as a mineral admixture in concrete due to its economic and technical advantages in conjunction with natural availability (Baron, 1987) (Singh, Ransinchung and Kumar, 2017)

Limestone powder was used in this study as a micro aggregate. The limestone powder was supplied by Intra Laboratories in the UK. The properties are shown in Table 3-6.

Table 3-6 Properties of limestone powder

Properties	
Weight median (d50) μm	18
Top cut (d98) μm	150
Moisture content (%)	0.05
Loss on ignition (% @ 1000°C)	43.60
Bulk density (loose) (t/m ³)	1.20
Bulk density (compact) (t/m ³)	1.75
Specific gravity	2.65

3.2.4 Superplasticizer

Superplasticizers, similarly identified as high range water reducers, are chemical admixtures made from various organic polymers, used in concrete. The fundamental reason for using a superplasticizer is to reduce the water to cement ratio and to produce a flowing concrete. Before the introduction of superplasticizers, a great quantity of water had to be added to the concrete mixture. Generally, the water/cement ratio ranged between 0.6-0.70. Consequently, the compressive strength of the resulting concrete was limited to around 20-40 MPa. With the introduction of superplasticizers, the water/cement ratio could be reduced significantly, 0.25-0.40, and keeping the same strength (Shah and Ribakov, 2011). The polycarboxylate-based superplasticizer known CSP 340, available at the LJMU concrete laboratory, was used. The material was supplied by Cemex.

3.2.5 Water

Potable tap water from Liverpool John Moores University concrete laboratory was used for mixing. The water supply to this area comes from the River Dee and from Lake Vyrnwy. The water supply to this area can vary in hardness from soft to slightly hard. The supply is low in naturally occurring fluoride and is not artificially fluoridated.

3.3 Fibre Surface Modification Procedure

3.3.1 Plasma Equipment

Plasma is generated when a gas breakdown process occurs under a suitably high voltage. This is similarly true if the electric field has been formed by an electromagnetic wave. Breakdown of the initially non-conducting gas creates a conducting path between the electrodes. The path of an electrical current over the ionised gas causes a collection of phenomena identified as gaseous discharges. These gaseous discharges are the most frequently used but are not the only method for generating plasmas. For various applications, plasmas are generated by electrodeless RF discharges, shock waves, microwaves and by laser or high-energy particle beams. Lastly, increasing the gas temperature (vapour) in a high-temperature furnace can similarly generate plasmas. Due to characteristic temperature limitations, this technique is limited to metal vapour with low ionisation capacities.

In this study a novel electrodeless 5.8 GHz microwave induced plasma system was developed for the purpose of surface modifications of fibres. The 5.8GHz microwave plasma has an appropriately encouraging characteristic, which is directly proportional with the excitation frequency. This is attributed to the easy ability to achieve a high

electron density, which consequently has an influence on the density of further generated species like radicals, ions, excited molecules and atoms or UV light. The developed system is electrodeless, hence the challenging difficulties, of electrode vapour contamination that previously tremendously affected the stability and properties of the plasma torch, were avoided, and therefore the processing feature is enhanced.

Microwaves are electromagnetic waves that have a frequency range from (0.3-300) GHz, and usually comprise distinguishing wavelengths of 30 cm to 0.3 mm (Zhang, Li and Wang, 2015).

In the following sections (3.3.1.1) to (3.3.1.5), the pieces of equipment used in developing the new system are described:

3.3.1.1 Signal Generator



Figure 3-1 Marconi signal generator

Figure 3-1 shows the Marconi 6200A signal generator used in this study. The 6200A is a device combining several measurement functions in a portable and compact set.

Its portability and high specification make it correspondingly appropriate for both field and bench applications. The 6200A is more flexible and practical than an assembly of separate disconnected devices. It is a complete test system; in an individual unit the facilities of an accurate produced arc generator, power meter, four input scalar analysers with colour display, programmable voltage source and frequency counter are combined. The Marconi signal generator cannot produce enough power for the plasma system, it is limited to 10 or 20mW, so a travelling wave tube amplifier (TWTA) is used as a power amplifier.

3.3.1.2 Travelling Wave Tube Amplifier (TWTA)

A travelling wave tube amplifier (TWTA), is vacuum tube that is used in electronics to amplify radio frequency (RF) signals in the microwave range (Gilmour, 2011). In the TWTA a wave is amplified by absorbing power from a beam of electrons while it passes through the tube. Even though there are several forms of TWTA, the two main classes are:

1. Helix TWTA: when the waves interact with the electron beam as travelling through a wire helix, which surrounds the beam. These have extensive bandwidth, but output power is narrowed to a few hundred watts (Abe et al, 2000).
2. Coupled cavity TWTA: when the wave interacts with the beam in a sequence of cavity resonators as the beam passes. These function as an amplifier for narrowband power.

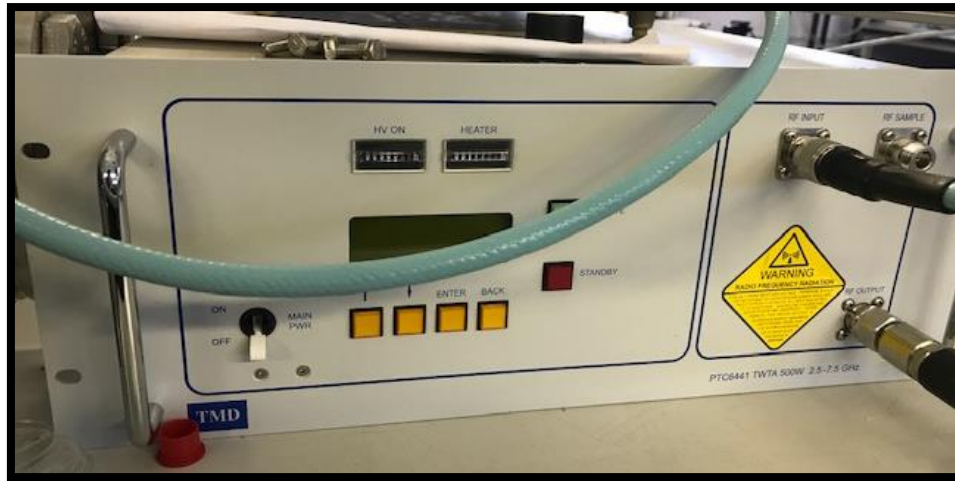


Figure 3-2 Travelling wave tube amplifier

As shown in Figure 3-2, a series PTC6441 TWTA produced by TMD Technologies was used. The TWTA offers an exceptional level of power with decent constancy over a frequency range between 2.5 GHz to 7.5 GHz.

3.3.1.3 Waveguide

A waveguide involves a rectangular or a cylindrical metallic tube that guides microwaves or any other waves with high efficiency and negligible loss of energy by limiting wave expansion to one to two dimensions.

An electromagnetic wave can propagate through the waveguide in several ways. The two common mode types are transverse magnetic (TM) and transverse electric (TE). In the TM mode, the magnetic field component is perpendicular to the axis of the propagation. However, in the TE mode, the electric field component is perpendicular to the axis of the propagation. The electromagnetic field cannot propagate, if the waveguide's cross section is too narrow with respect to (the wavelength).

The waveguides are unable to carry the signal if the frequency is below the cut-off frequency. Therefore, the cross-sectional dimension of the waveguide needs to be of the same order of value as the wavelength of the carried signal.

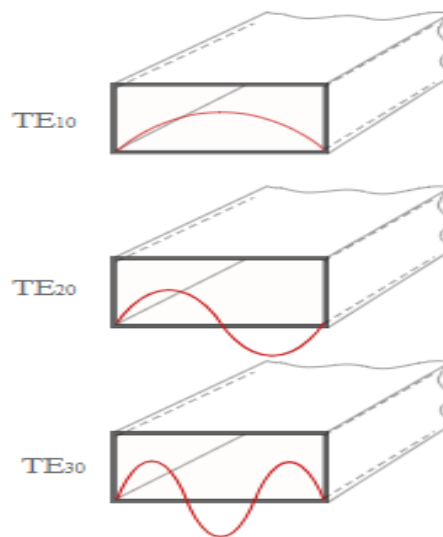


Figure 3-3 Rectangular waveguide TE mode

Figure 3-3 illustrates the diagram of the transverse electric field in the rectangular cross section waveguide. The lowest frequency that can fit into the waveguide will be propagated by a mode.

TE_{10} or TM_{10} are the very fundamental modes for the two different types of propagation. In general, for propagating microwaves for generating plasma, it is a common practice to use the TE_{10} mode. Limiting the waveguide dimension so that only the fundamental mode can propagate mean that the wave pattern is predictable. Primarily, for rectangular waveguides, the TE_{10} mode has the lowest cut-off frequency and therefore, is termed the dominant mode. All other modes have higher cut-off frequencies. This indicates that at the operation frequency-band only the dominant mode is propagating, whereas all higher-order modes are cut-off.

TE model (TE₁₀) was used in the developed plasma system, since the electron energy in the plasma induced by the electric field was of interest.

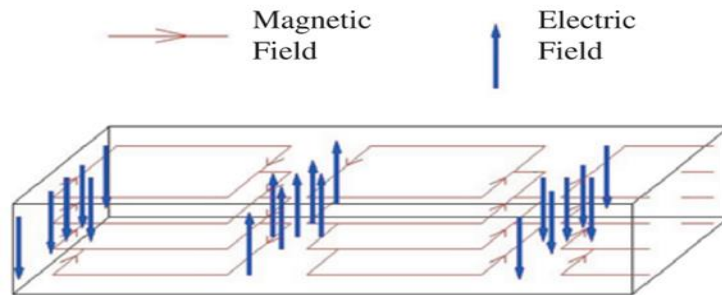


Figure 3-4 Magnetic and electric fields in a TE₁₀ rectangular cavity

Figure 3-4 shows the magnetic and electric field in the TE₁₀ mode.

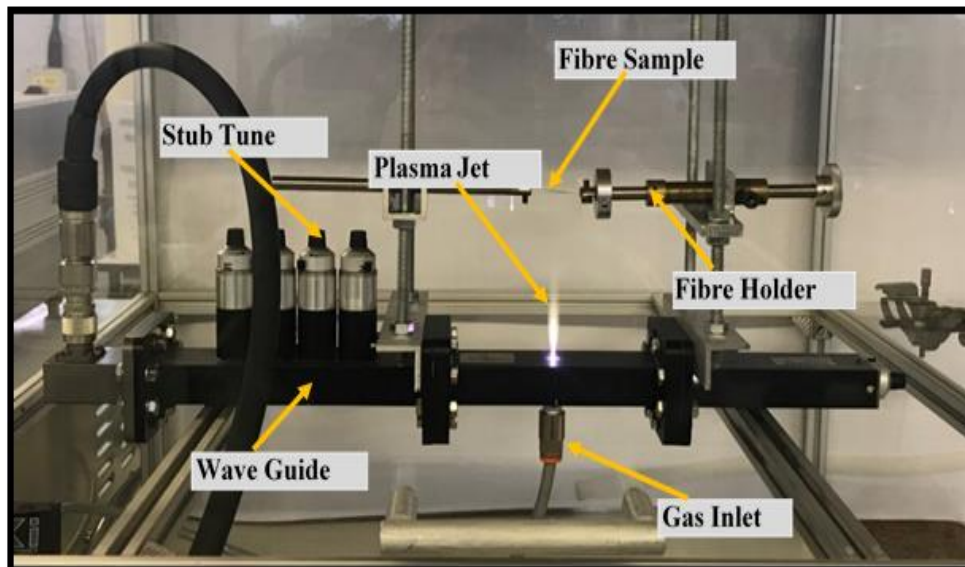


Figure 3-5 Plasma Test Rig and the Fibre Holder

As shown in Figure 3-5, a rectangular waveguide section was used.

3.3.1.4 Stub Tuner

A stub tuner is an impedance matching device used to transform the impedance of the load to match that of the source. If the impedances are matched then maximum power

is transferred to the load as there are no reflections, i.e. the $VSWR=1$ where $VSWR$ is defined as the voltage standing wave ratio. The technique of a single stub impedance matching could be used to match any random, non-zero, finite load impedance to the typical impedance of a waveguide. Nevertheless, the single stub technique necessitates that the stub be placed on the waveguide at a precise point, which varies as the operating frequency or load impedance is changed. This requirement frequently presents practical complications as the specified implantation point might occur at an unwanted position from a mechanical viewpoint or, more significantly, the impedance of the plasma varies with each operating condition. A substitute technique to single stub impedance matching is to use two or more short circuited stubs at fixed, yet not specified, positions. A triple or four stub tuner permits a larger range of impedances to be matched than a two-stub tuner (Mahendra, 2017).

3.3.1.5 Plasma Interaction and Cavity Nozzle

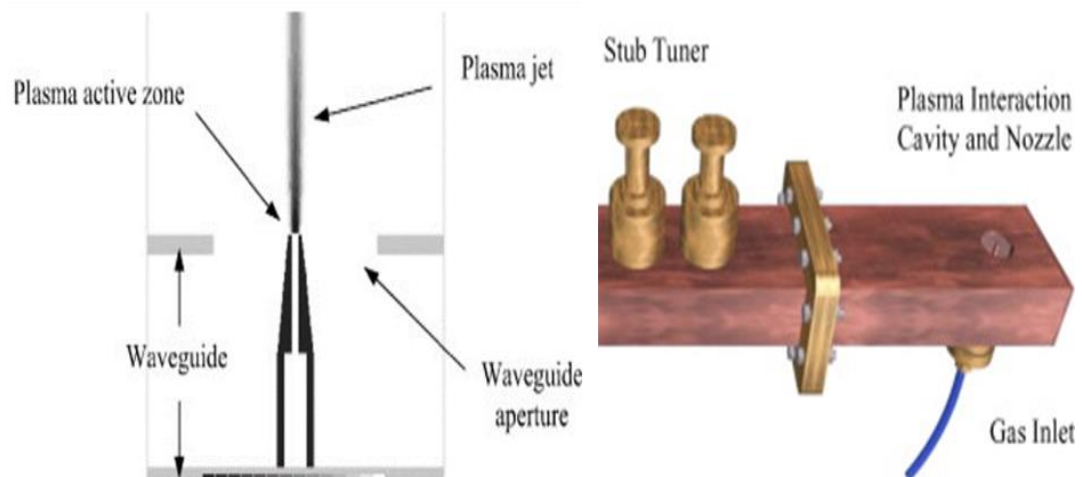


Figure 3-6 Diagram of plasma system parts

Figure 3-6 shows the schematic diagram of the plasma system used. It specifies a simple nozzle design and an impedance matching tuner. Since this microwave plasma

torch is electrodeless, therefore, the problem of electrode vapour contamination that formerly seriously affected the stability and properties of the plasma torch, was avoided, thus, the processing quality is improved. Furthermore, the plasma torch is formed in an open atmosphere at the nozzle tip so there is no direct contact between the nozzle and the plasma. Consequently, the nozzle is relatively cold; hence, electrode erosion problems are insignificant. In addition, this plasma torch functions at atmospheric pressure with a substantial energy change, generating a plasma around a temperature of several thousand degrees kelvin. In contrast with a transferred DC arc, the electrodeless system is more suitable both for use in non-metallic and metallic material treating. In the DC arc, the charge transferred to the material is either positive or negative. Therefore, the functions of the DC arc for processing conducting materials are limited. In the non-transfer arc, a cooling system is commonly essential for the electrodes and an enormous volume of heat energy is wasted to cool the chamber wall. Consequently, the problems of erosion of the electrode and vapour contamination are obvious for the DC arc. The above advantages of the microwave plasma torch system over the conventional system could make it a potential candidate for industrial material processing purposes.

The plasma cavity involves the gas nozzle in the waveguide, directly sitting inside the cavity above an aperture. By employing the aperture and a gas nozzle at a point of maximum electric field, a microwave plasma jet can be produced. The amount of the propagation of the microwave field past the cavity, relies on the diameter of the waveguide aperture.

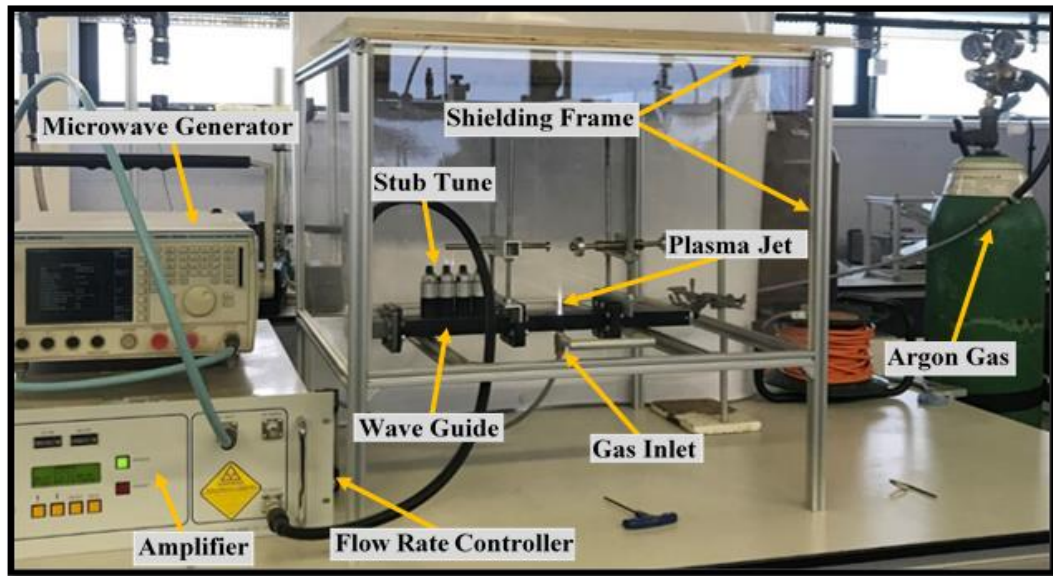


Figure 3-7 Microwave Plasma System

Figure 3-7 shows the plasma system developed in this study. In general, the microwave plasma system involves a signal generator that has been connected to the travelling wave tube (microwave generation source), microwave waveguides and microwave multimode cavity. The travelling wave tube amplifies the generated signals into microwave energy, which can be transferred through the waveguides to the multimode cavity. A frame made of acrylic sheet was also created and placed over the plasma system for the purpose of health and safety.

3.3.2 Specimen Treatment Conditions

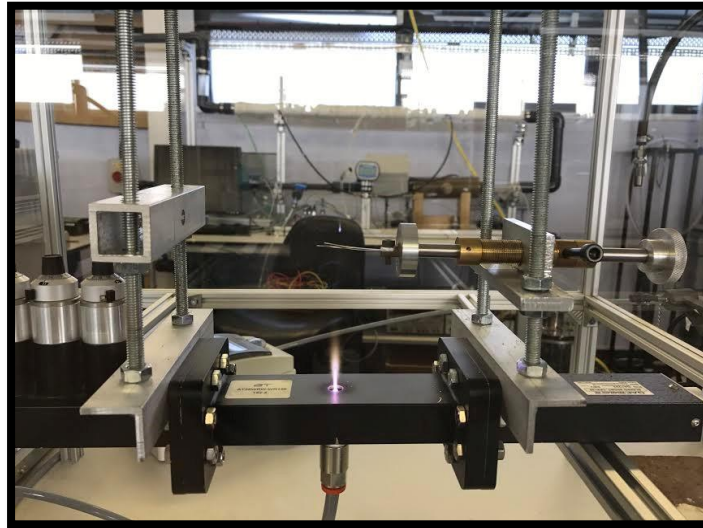


Figure 3-8 Fibre holder frame

Figure 3-8 shows a specially designed experimental rig to hold the single fibres during the first phase of experimental procedure of this study, which was the investigation of the plasma effect on surface characterization of fibres and investigation of the pull-out strength, both of which were used for the purpose of optimizing the plasma treatment. The fibre holder is designed so that the distance of the fibre from the plasma torch can be adjusted. Furthermore, the rig has the capability to move sideways to facilitate various sizes of fibres (25-50 mm) and to rotate so that both sides of fibres can be treated evenly.

The specimen's treatment with plasma was carried out using argon gas. Fibres were treated at the various heights (30, 60 and 100 mm) from the plasma torch. The plasma conditions explored at each distance were the flow rate of the gas and treatment duration. Flow rates of 1, 2 and 3 litre/min were used. Depending on the distance from the plasma jet, the treatment durations were between 40 and 200 seconds. Surface treatment was performed on fibres as they were received from the supplier without further processing with any sort of chemicals or solutions prior to plasma applications.

After the treatment was completed the fibres were kept in aluminium foil to avoid damage and contaminations. The specimens were labelled according to the distance, flow rate and treatment duration. Contact angle measurements were investigated immediately after the treatment process. At the second phase of this study, larger quantities of fibres were required to be treated to use as reinforcement in cementitious $40 \times 40 \times 160$ mm prisms. Therefore, modifications to the previous phase test rig were made.

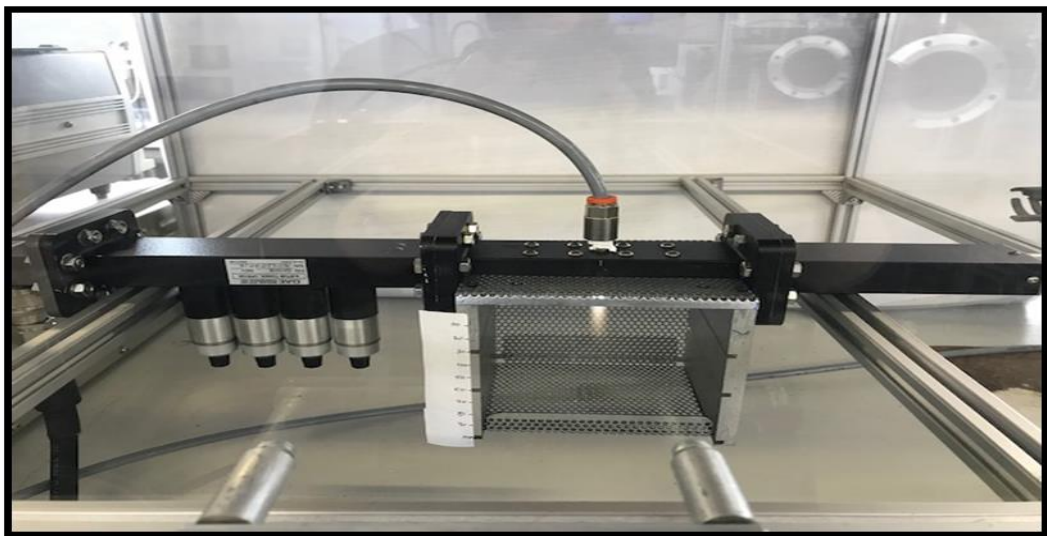


Figure 3-9 Modified fibre holder to facilitate larger amount of fibres to be used in flexural test

As shown in Figure 3-9, the waveguide was rotated by 180° from Figure 3-5 (previous set-up) and a metal cube was made to put the fibres on. Treated fibres at this phase were kept in the aluminium foil immediately afterword to avoid contaminations and possible damage. The fibres were then transferred to the concrete lab to be mixed with cement matrix after the completion of the treatment.

3.4 Specimen Characterisation Techniques

Characterisation of the plasma treated fibres is usually divided into two categories of analysis:

- a. Surface analysis of the fibres; wettability and morphology and
- b. Mechanical analysis; single fibre tensile test, single fibre pull-out test and flexural test.

The single fibre tensile test will reveal any possible damage that occurs to the fibre's tensile performance because of the plasma treatment. Then the pull-out test measures fibre-cement bonding and interface performance in treated specimens compared to control specimens. The flexural performance test will indicate if the plasma treated fibres have an impact on enhancing the flexural performance of the composite. Mechanical data are interrelated with fibre surface analysis to conclude how modifications to the fibre surface have influenced the mechanical performance. The techniques used in the analysis of surface alteration induced by plasma treatments of various fibres can be summarised in the following section (3.4.1).

3.4.1 Surface Characterisation

3.4.1.1 Contact Angle Measurement (CAM)

CAM is a method of determining how wettable the fibre surface is. This could be achieved by measuring the contact angle between the liquid droplet and the surface of the fibre.

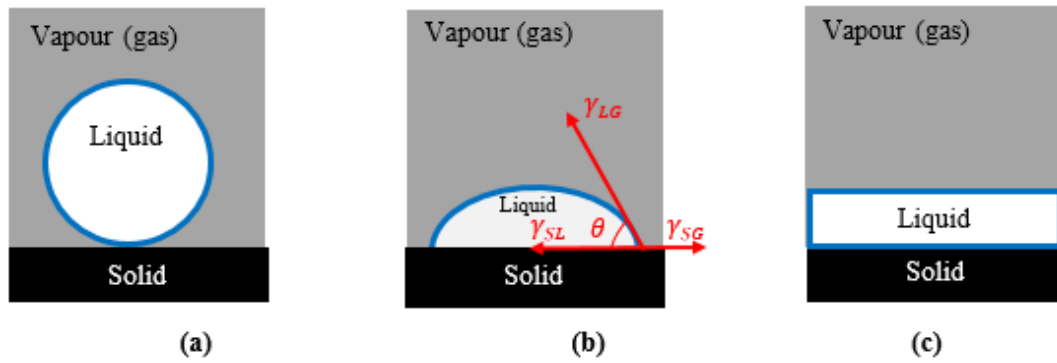


Figure 3-10 Examples of different types of wettability: (a) No wettability, completely hydrophobic, contact angle =180° (b) Partial wettability, partially hydrophobic/philic, contact angle=0-180° and (c) Complete wettability, completely hydrophilic, contact angle

Figure 3-10 illustrates the different types of wettings. Wettability of the fibres by a specific liquid droplet can be determined by measuring the angle between the fibre and the liquid by an edge, which is known as a triple phase boundary. Triple phase boundary is the meeting edge of a fibre, liquid and the air, which creates a fibre-liquid border, a liquid-gas border and a fibre-gas border. The meeting point of these three borders, constructs tangents alongside the liquid-gas border and the solid-liquid border. Contact angle is the angle between these lines, and it is the measurement of wettability of the fibre. The CAM can be interrelated to the surface tension between two phases at each boundary using the Young equation (3.1).

The Young equation
$$\cos \theta = \frac{\gamma_{SG} - \gamma_{SL}}{\gamma_{LG}} \quad 3.1$$

Where:

γ_{SG} is the surface tension between solid and gas phase

γ_{SL} is the surface tension between solid and liquid

γ_{LG} is the surface tension between liquid and gas

θ is the liquid contact angle

This equation takes into consideration that the surface of the fibre is ideal, but in reality, the surface is not. Nevertheless, the measured contact angle is proportional to the Young contact angle. The factor governing the proportionality deviations is dependent on whether the liquid covers the surface area of the fibres completely, or if the liquid rests on the peaks of the surface or on a chemically heterogeneous fibre. Those features are known as roughness as shown in the equations below: Wenzel equation (3.2), for the area(s) of contact, see the Cassie equation (3.3) and the Cassie-Baxter equation (3.4).

$$\text{Wenzel equation} \quad \cos \theta_m = r \cos \theta_y \quad (3.2)$$

$$\text{Cassie equation} \quad \cos \theta_m = X_1 \cos \theta_{y1} + X_2 \cos \theta_2 \quad (3.3)$$

$$\text{Cassie-Baxter equation} \quad \cos \theta_m = X_1 (\cos \theta_y + 1) - 1 \quad (3.4)$$

The term (X), the chemical coverage area on the surface, usually lies between 0 and 1. The subscript y and m measured with the term $\cos \theta$ are for measured (m) and actual (y). The subscript 1 and 2 refers to the two chemicals that construct the surface. The greater the surface energy of the fibre surface, the greater the degree of wetting that takes place (i.e. smaller contact angles).

Especially in case of water, the hydrophilicity or hydrophobicity of a surface is measured using the water contact angle. The midpoint is considered as 90° , with angles to the surface lower than 90° being recognised as hydrophilic and angles to the surface above 90° being recognised as hydrophobic. The larger the angle the more hydrophobic, and the smaller the angle the more hydrophilic the surface. Equally, a surface that is hydrophilic is more likely to have considerable resilient interaction with adhesives or matrix. Therefore, it is desirable that the surface would have a low water contact angle.

In this study contact angle measurements were performed on macro polypropylene and glass fibre. The alterations in the surface energies of the fibres were investigated by means of static CAM. Since the micro fibres such as basalt fibres cannot be provided in the form of thick fibres, the wetting angle is not measured in these fibres.



Figure 3-11 CAM setup

Figure 3-11 shows the setup for the CAM analysis used in this study. In the measurements of wetting angle, drops of pure distilled water with a volume of $5 \mu\text{l}$ were dropped onto the surfaces with a fixed volume automatic pipette. Six individual fibres were investigated and at least 3 drops were placed onto each fibre surface and the wetting angles were measured with the help of computer software called Theta. Theta provides comprehensive analysis of drop shapes. It uses the Young-Laplace equation as a reference method and can fit the entire drop profile. The results are presented in section 4.4.1.

3.4.1.2 Scanning Electron Microscopy (SEM)

SEM is a form of electron microscope that provide images of a specimen by scanning its surface with a high energy focused beam of electrons in a raster scan pattern. Once electrons have bombarded a specimen, it gives off secondary electrons and X-rays. The secondary electron's strength is identified to produce a high-resolution image of the surface. Prior to analysis, it is essential to sputter coat non-conductive material such as polymers with gold or platinum. SEM is a most commonly used technique in surface analysis and characterization and is regularly used in surface topography measurements of materials (Khorasani, Mirzadeh and Kermani, 2005; Falconnet et al, 2006). SEM reveals specific details of about 5 nm in size and can produce very high-resolution images of the specimen surface morphology.

Because of the appropriate slender electron beam, SEM micrographs have an enormous depth of field yielding a specific three-dimensional form suitable for understanding the surface structure of a specimen. Hence, resolution, magnification and depth of field are essential components of SEM.

a. Resolution

In SEM, the electron beam diameter controls the resolution. The smaller the electron beam diameter, the more enhanced resolution results can be obtained. However, the increase of resolution has a restriction due to the defects of condenser and objective lenses such as chromatic aberration and spherical aberration. In addition, the signal will be weak and noisy if the electron beam diameter is too small.

b. Magnification

The magnification of SEM is influenced by the resolution of the screen display. Typically, the minimum size of beam spot is around 0.1mm (100 μ m) for a high-quality cathode tube. Equation (3.5) gives the magnification M .

$$M = 100/d \quad (3.5)$$

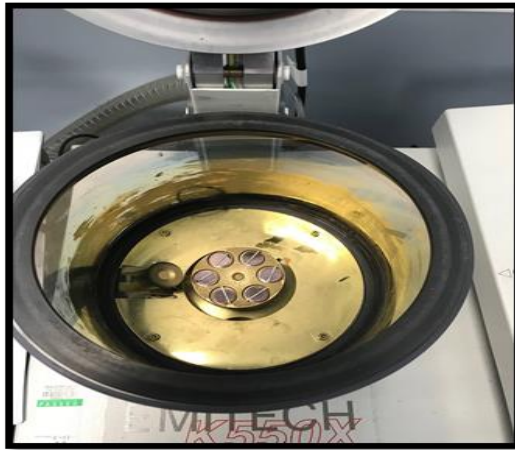
Where d is beam spot diameter (μm).

c. Depth of Field

One of the greatest features of the SEM is the large depth of field. The significant role of the large depth field of the SEM is it can provide a technique of examining roughness or surface fracture at high resolution. Equation (3.6) is used to calculate the depth of field (H)

$$H = 0.2D_w / AM \text{ (mm)} \quad (3.6)$$

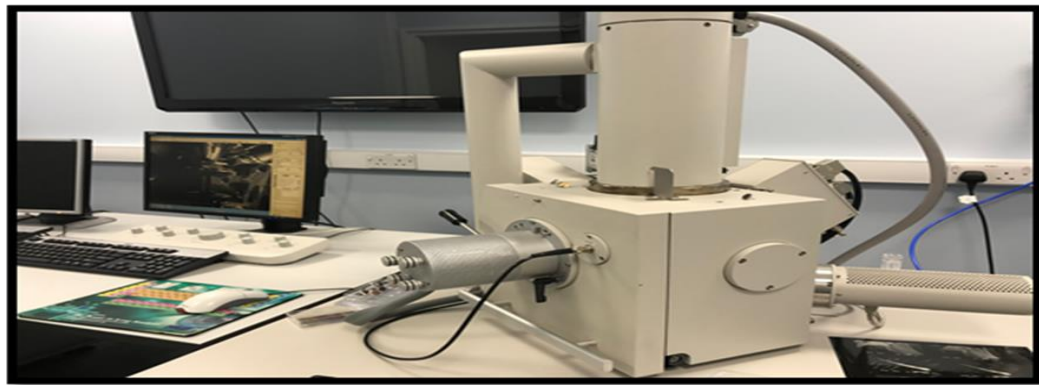
Where, A is the objective aperture diameter, D_w is working distance, M is magnification.



(a)



(b)



(c)

Figure 3-12 Three stages of specimen preparation procedure for the SEM analysis: (a) Specimen coating, (b) Placing the specimen on the SEM stage and (c) Vacuuming process

In this study, scanning electron microscopy (SEM) was used to investigate the surface of fibres before and after they were subjected to plasma treatment, and shown in Figure 3-12. SEM was conducted using an FEI Quanta 200 scanning electron microscope with an accelerating voltage of 5 to 20 kV. The fibres are placed on a carbon tape adhered to an appropriate metal stub. After mounting the specimens on the stub, sputter coating of the specimens with gold was conducted for 3 minutes. Gold dust was dispersed in the thickness with a 10 nm over the surface of the investigated fibres prior to SEM testing, using a sputter coater to provide proper electric conductivity required to produce high quality SEM images. Then the specimens were transferred to

the chamber and the vacuuming process was initiated. SEM images for surface topography analysis of fibres were taken at various suitable magnifications. Figure 3-12 shows the procedures taken for preparing specimens for the SEM analysis. The results are presented in section 4.4.2.

3.4.1.3 Atomic Force Microscopy (AFM)

AFM was initially developed by Binnig, Quate, and Gerber in 1986 by means of a partnership between Stanford University and IBM. AFM is the dominant apparatus to investigate the surface morphology of conductors, semiconductors and insulators (Dvorak, 2003; Vohrer, Hegemann and Oehr, 2003; Poletti et al, 2004). Three-dimensional surface measurements over the scanned surface area and its roughness can be obtained using AFM. In AFM, a cantilever, which has sharp, force sensing tips at its end is positioned parallel to the surface to interact with the surface. The variation in the interaction force between the surface and the cantilever tip produces deflections in the cantilever. A topographic image of the surface can be collected by measuring the deflections.

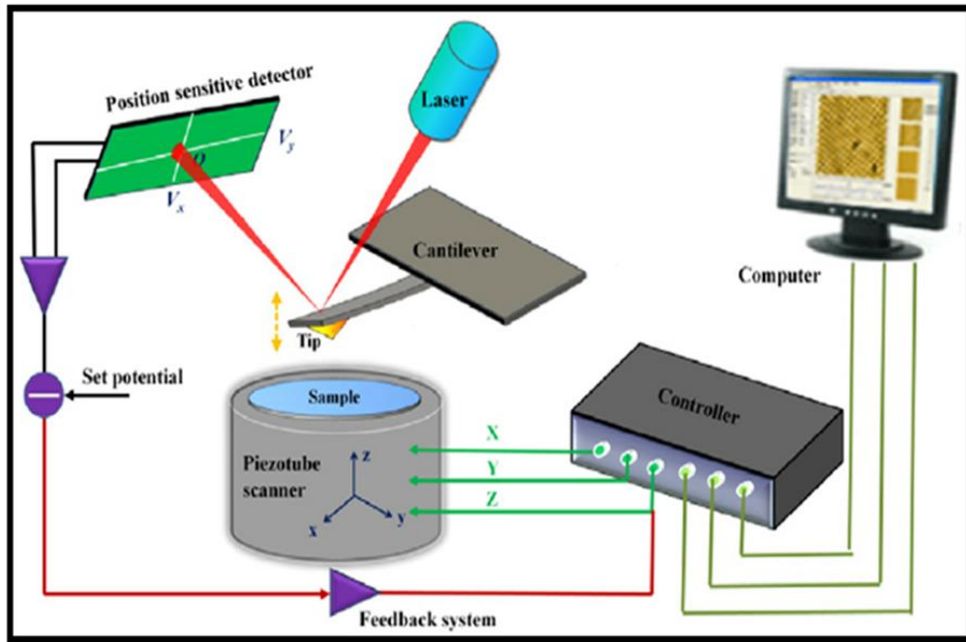


Figure 3-13 Schematic illustration of the operation of AFM (Guo, Xie and Luo, 2014)

Figure 3-13 illustrates the process (Guo, Xie and Luo, 2014). AFM is specially designed to monitor the interactions of forces between the tip and the sample surface. There are two primary methods of interaction between the tip and the surface: attractive and repulsive, which are in the range 10^{-9} - 10^{-6} N. There are three major modes of AFM: contact mode AFM, non-contact mode AFM and tapping mode AFM. The evaluations of these three modes are reported in Table 3-7.

Table 3-7 Evaluation of major modes of AFM

Comparison	Contact Mode	Non-Contact Mode	Tapping Mode
Operator zone	I Zone	II Zone	I/II Zone
Force sensed by tip	Short range repulsive forces	Long Range attractive forces.	Repulsive/attractive forces.
Tip or cantilever position	Tip touches the sample	The tip does not contact the sample surface. The cantilever is oscillated at a frequency slightly above the cantilever's resonance frequency with an amplitude of a few nanometres (<10nm).	The cantilever is oscillated at or near its resonance frequency with an amplitude from 20nm to 100nm.
Feedback loop	Maintain constant cantilever deflection	Maintains a constant oscillation amplitude or frequency.	Maintain its constant oscillation amplitude by maintaining a constant RMS of the oscillation signals.
Advantages	High scan speed Atomic resolution Rough samples can be scanned easily.	No force exerted on the sample surface	Higher lateral resolutions (1~5nm) Lower force and less damage.
Disadvantages	Shear force and normal force can distort images. Damage the soft samples	Lower lateral resolution. Slow scan speed. Usually only works on extremely hydrophobic samples.	Slightly slower scan speed than contact mode.

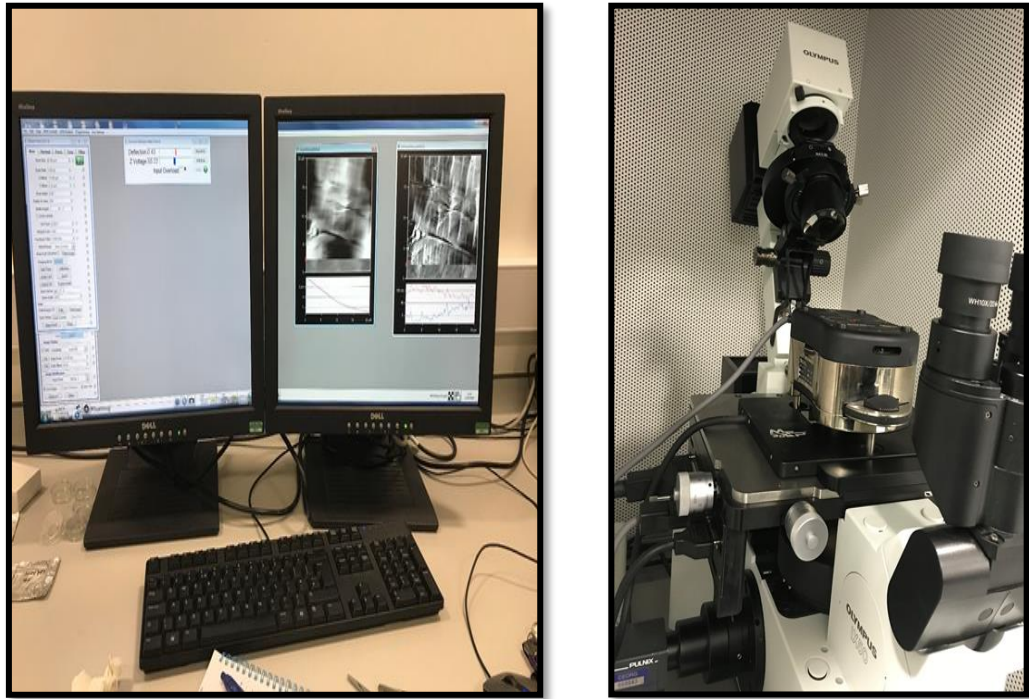


Figure 3-14 AFM used in analysing the surface roughness of the fibres

Figure 3-14 shows the AFM used in this research investigation. AFM was conducted using a Molecular Force Probe-3D (MFP-3D) atomic force microscope (Asylum Research, Santa Barbara, CA) with software written in IGOR pro (Wavemetrics, USA). The MFP-3D is equipped with a 90 μm x-y scanning range, z-piezo range > 16 μm and was coupled to an Olympus IX50 inverted optical (IO) microscope.

The MFP-3D-IO was placed upon a TS-150 active vibration isolation table (HWL Scientific instruments GmbH, Germany), which was located inside an acoustic isolation enclosure (IGAM mbH, Germany) to help eliminate external noise. Images were captured in contact mode using V-shaped, silicon nitride cantilevers (spring constant 0.02 N/m, length 200 μm , OMCL-TR400PSA-1, Olympus).

The fibre specimens were prepared under the same conditions as the sample used in the SEM analysis Section 2.5.1.2. Fibre specimens are glued to a sticky tape surface and scanned on a nanometre vertical scale 200 nm with an area of $5\mu\text{m} \times 5\mu\text{m}$ on the fibre surface. 2-3 randomly selected points on the surface of the fibre were scanned and a three-dimensional image of the surface was obtained. From the produced surface images, surface Nano-roughness (Rms) values of specimens were recorded.

Contact mode AFM controls by scanning a tip, which is connected to the end of a cantilever through the sample surface and monitoring the variation in the deflection of the cantilever with a split photodiode detector. Through sustaining a constant cantilever deflection, the force between the sample and the tip remains constant. Hooke's Law equation (3.3) is used to calculate the force.

Hooke's Law
$$F = -KX \quad (3.7)$$

Where:

F is force (kN)

K spring constant

X is cantilever deflection (mm)

The distance the scanner moves vertically at each (x, y) data point is stored by the computer to construct the topographic image of the sample surface. The results are presented in section 4.4.3.

3.4.2 Mechanical Characterization

3.4.2.3 Tensile Test of Single Fibre

The most fundamental type of mechanical tests for characterizing a material of a fibre is tensile testing of a single fibre, which is fast, simple and fully standardised. The test provides information on tensile strength, tensile modulus and elongation to failure. The tensile tests for all fibres were carried out in accordance with (ISO 11566:1996, 1996) at room temperature. However, some modifications were made in terms of the specimen preparation.

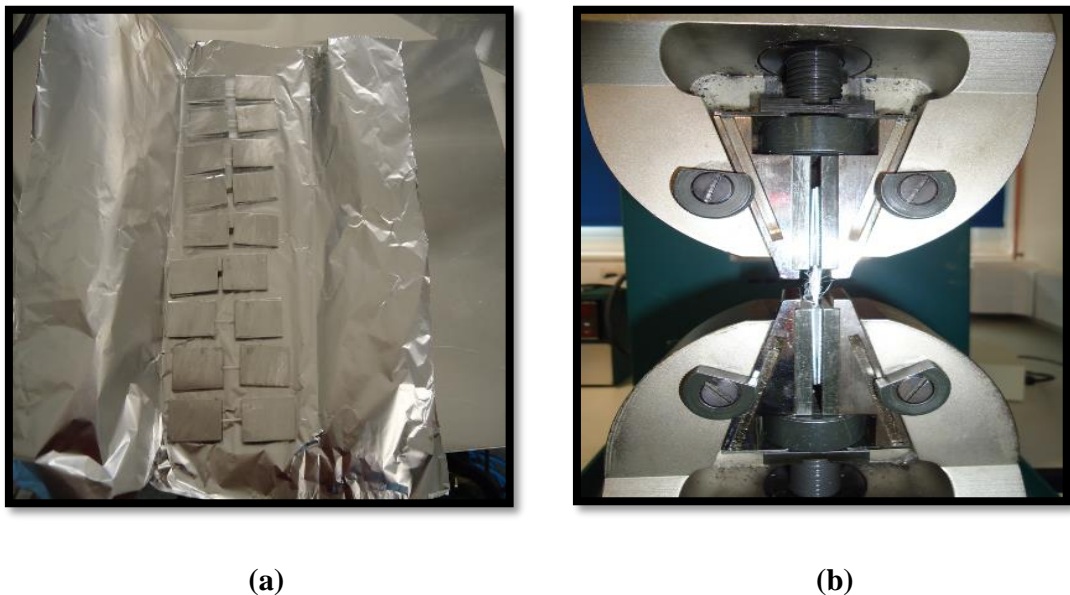


Figure 3-15 Specimen preparation and testing procedure of fibres: (a) fibres glued to the plates, (b) fibre specimen clamped in the machine

Figure 3-15 shows the specimen preparation. Aluminium plates 20×35 mm were cut, sand papered and cleaned with an alcohol solution on both sides. Paper sanding the plates creates the desired finish to provide better grip in the tensile machine's jig head and as a preparation for gluing the fibre in between the two plates. After paper sanding the plates, alcohol solution was used with a cotton cloth to clean the surface and

remove all contaminants on the surface to better prepare the surface for gluing. Epoxy resin (Araldite) glue was then applied to the surface of the plates. Four plates were prepared to glue to the ends of the fibre. A specific length of both ends of each type of single fibres were carefully placed on the two glued plates using tweezers and the other two plates were placed on top of them and slightly pressed. The specimens were covered in an aluminium foil to avoid contamination of the middle portion of the fibres and left for 24 hours in the laboratory condition to ensure that the glue reached its maximum strength. For each type of fibre, 6 specimens were prepared. The fibre's cross section was measured several times along its length using a digital calliper and the average of the diameter was used to estimate the fibre cross sectional area. When the glue had dried, the specimens were clamped with the jig head of the Tinius Olsen tensile machine with the capacity of 25 kN. The rate of the machine was adjusted to 250mm/min to reduce the possibility of the slippage and pull-out of the fibre from the glue. The programme to generate the force-extension graph with a commercial software called Horizon. Maximum load was determined from the graph and the ultimate strength σ of the fibre was calculated by using the following equation (3.8):

$$\sigma = \frac{F_{max}}{A_f} \quad (3.8)$$

Where:

σ is the fibre strength (MPa)

F_{max} is the maximum force to break the fibre (kN)

A_f is the cross sectional area of the fibre (mm)

The experimental results obtained can be found in section 4.5.1.

3.4.2.1 Single Fibre Pull-Out Test

To investigate the effect of plasma treatment, it is essential to study the bond behaviour between the fibre and concrete matrix. Pull-out tests are commonly used in understanding the bond properties of various types of fibres. Pull-out experimental procedures are not usually a straightforward to perform on fibres, since a very high accuracy level is vital for very small loads and displacements. Pull-out procedures were performed in various techniques by different scientists nevertheless to date no technique is recognised being the standard. Different experimental set-ups and loading arrangements can greatly affect the results. To achieve an accurate pull-out result, an appropriate testing technique needs to be developed and tested (Pisanova, 1997). Thus, in the investigation of the effect of plasma treatment on the bond behaviour an experimental set-up was developed. The single fibre pull-out test involves one end of a single fibre embedded into the cementitious matrix at a preferred measurement, the matrix is confined, and the fibre is subjected to a tensile load directly. The applied load to the fibre increases up to a maximum force (F_{max}) being attained at which point the fibre entirely debonds from the surrounding matrix. Once a complete debond has occurred, a reduction in the force is commonly witnessed in the force-extension graph. The fibre at that point begins to pull out from the matrix in contradiction of internal frictional forces (F_{fr}). The applied force to the fibre will steadily increase until the fibre is pulled out of the surrounding matrix. It has been stated in the literature that the fibre can initially debond from the surrounding matrix before F_{max} is attained (pisanova, Zhandarov and Mader, 2001; Mader and Zhandarov, 2005). Initial debond is triggered by an introduction of a crack which spreads over the interface between the matrix and the fibre. The force continues increasing until F_{max} due to the frictional force in the debonded section being involved in the adhesive force from the intact

section of the interface. Consequently, when the F_{max} is reached the crack propagation becomes unstable and the whole inserted length debonds from the matrix and the load drops to frictional force F_{fr} .

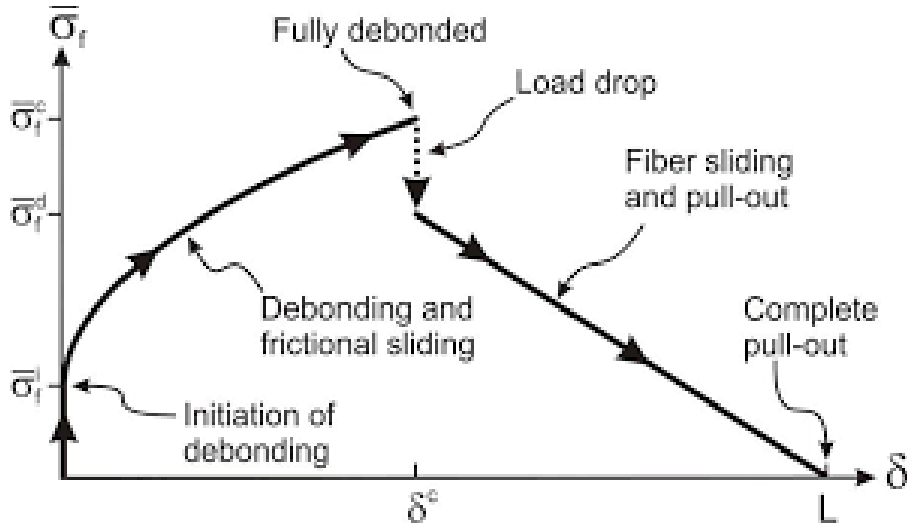


Figure 3-16 Typical single fibre pull-out force- displacement graph (Sørensen and Lilholt, 2016)

This procedure can be observed noticeably in the load–displacement graph shown in Figure 3-16 (Sørensen and Lilholt, 2016).

When the pull-out test is over, the actual interfacial shear strength (τ_{IFSS}) can be estimated from the maximum force and the embedded area of the fibre using equation (3.9) (Craven, Cripps and Viney, 2000; Alvares, Ruscekait and Vazquez, 2003; Yang and Thomason, 2010) (Alvares, Ruscekait and Vazquez, 2003).

$$\tau_{IFSS} = \frac{F_{max}}{\pi D l_e} \quad (3.9)$$

Where D = fibre’s diameter (mm).

l_e = embedded length of the fibre in the matrix (mm).

Equation (3.9) adopts a uniform distribution of shear stress along the interface of the fibre- matrix which is not the actual situation. Hence, the actual interfacial shear strength, established by using the above equation, can be used to compare the bond strength between diverse fibre and matrices.

Numerous models have been established to define the stress distribution along the interface and interfacial failure between the fibre and the matrix (Chua and Piggott, 1985; Piggott, 1993; Nairn, 2000; Rao, Kumar and Narayana, 2013).

These models are typically characterised into two categories; Ultimate shear stress-controlled method and Energy controlled method. The ultimate shear stress-controlled approach is used to determine the local shear stress at the start point at which the fibre firstly debonds from the matrix and stays stable irrespective of crack length. The second method, the energy controlled, is based on fracture mechanics and is used to determine the released interface energy as the fibre debonds from the surrounding matrix.

According to equation (3.9), the interfacial strength is calculated using the diameter of the fibre. However, the fibres used were not circular and using the diameter would probably result in an inaccurate evaluation of interfacial strength. Investigations were carried out by previous researchers to compare the possibility of converting the diameter of the fibre in the equation (3.9) to the perimeter of the non-circular fibres (Manchado et al, 2003; Li, Hu and Yu, 2008; Adusumalli, Weber and Roeder, 2010). Consequently, a modification to equation (3.9) was made by using perimeter (P) instead of diameter (D) to calculate the embedded area. The modified equation is given in equation (3.10)

$$\tau_{IFSS} = \frac{F_{max}}{pl_e} \quad (3.10)$$

Where P = fibre's perimeter (mm).

The experimental technique involves preparation of a specimen and embedding a single fibre in a cementitious matrix, which is then ready for the pull-out test. The specimen preparation process is as follow for all samples.

The fibre reinforced cementitious composite was prepared according to (BS EN 14845-1:2007, 2007). Cement and limestone powder were weighed and positioned in a mixing container. The materials were dry mixed for nearly 1 minute until the dry mix looked to be well mixed. Then, half of the water was added and mixed thoroughly for 2 minutes. The remaining water was mixed with the superplasticizer then added to the mix. The mixing procedure continued for an additional 2 minutes until the mix had transformed into a wet paste homogeneous concrete.



(a)



(b)

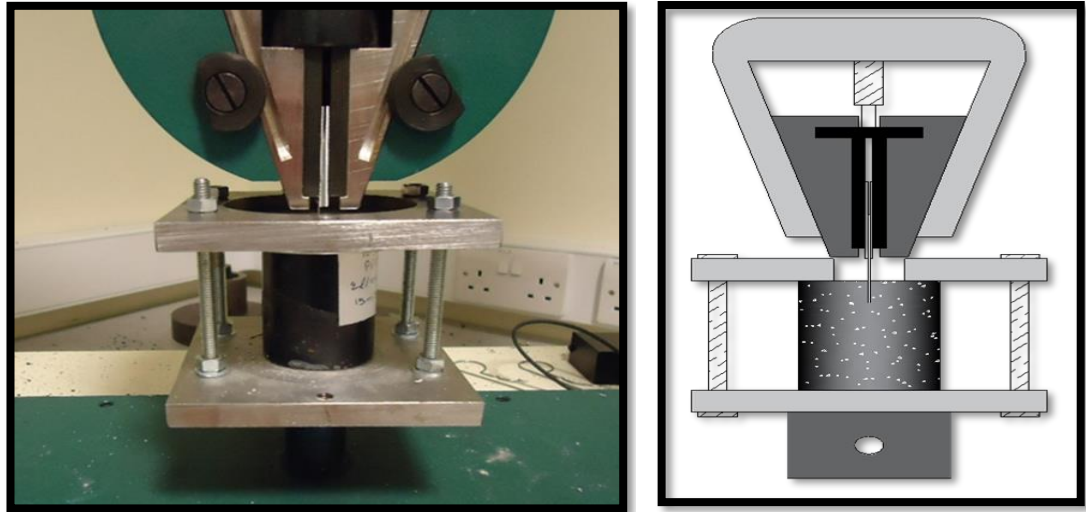


(c)

Figure 3-17 Pull-out specimen preparation: (a) casting, (b) curing and (c) gluing fibres in aluminium plates

Figure 3-17 presents the pull-out specimen preparation process. Disposable plastic tubes 40 mm in diameter and 50 mm high were prepared and placed on an adhesive tape to seal the bottom of the tubes to minimise leaking of the mix. The plastic tubes are filled with the mix in three stages. At every stage, the mix was tamped with a steel rod with a diameter of 5mm for compaction process and to make sure that the trapped air has escaped. Plastic discs were also created with a radial slot to make sure that the fibre was inserted at the centre of the mortar specimens. The specimens were marked according to the date of the mix, the type of fibre, the distance from the plasma jet, the argon flow rate and the treatment duration of the fibre. Specimens were left in the lab for 24 hours. Then the plastic disc was removed, and the top end of the fibres kept wrapped in the foil to prevent any damage during the curing period.

Specimens were later kept in the container for the 27-day curing period. The specimens were not submerged in water completely to avoid any possible damage or property change of the free end of the fibres due to water absorption. The container was covered to keep the moisture and prevent the specimens from drying quickly. After 27 days of the curing process, the specimens were taken out from the water and the free ends of the fibres were glued between two aluminium plates of dimensions 20 × 35 mm to avoid shear stress damage of fibres when it is clamped between the jig head during the tensile test. The specimens were left in the lab for another 24 hours, so the glue reaches its maximum strength. The pull-out test was performed the next day (28 days).



(a)

(b)

Figure 3-18 Pull-out test set-up for single fibre pull-out specimens: (a) pull-out test rig, (b) schematic diagram of pull-out test rig

After curing of the specimens for 28 days and clamping the fibre's free end between the aluminium plates, the pull-out tests were carried out. The pull-out experimental set-up is shown in Figure 3-18. The test rig frame was specially manufactured for securing and restraining the top and bottom of the pull-out specimens while they were mounted on the tensile machine to perform the pull-out test as shown in Figure 3-18(a) and (b). A Tinius Olsen tensile machine of capacity 25 kN was used to demonstrate the pull-out test. The loading rate was kept at 1mm/min for all the specimens. The force-extension graph was produced with the help of Horizon, as shown in Figure 3-18(c). The interfacial strength (τ_{IFSS}) was then calculated using equation (3.10). The length of the embedded section (l_e) of the fibres was kept constant for each type of fibre throughout this study. The l_e was chosen so that the pull-out occurs before the fibre starts to slip from between the aluminium plates. l_e of GF and BF was kept at 10 mm, with 15 mm for the PPF1. The experimental results are presented in section 4.5.2.

3.4.2.2 Flexural Test

The flexural test is an alternative indirect tensile test, which has been used frequently to calculate the tensile strength of concrete where direct tensile tests are unavailable. In this study, flexure tests were performed for fibre volume fraction optimization and for investigating the effect of plasma treatment on flexure performance of FRC. This test is usually implemented on beam samples using two different loading arrangements, three and four-point bending. In this study, three-point bending tests were performed according to (BS EN 12390-5, 2009) and the tests proceeded until failure occurred.

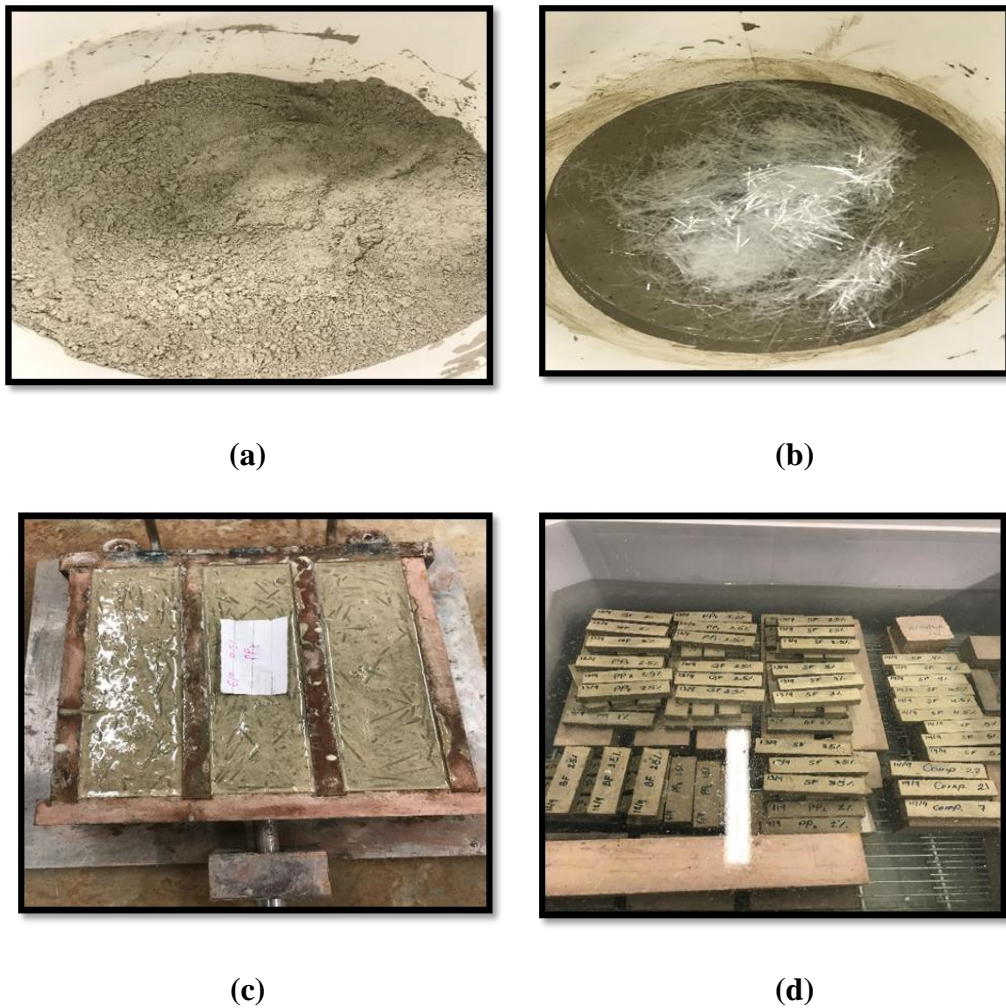


Figure 3-19 Flexural test specimen preparation: (a) dry mix, (b) wet mix with fibre added, (c) moulding, and (d) curing

Figure 3-19 shows the procedure conducted for specimen preparation. Similar guidelines to the pull-out matrix mixing procedure were followed, but instead of casting the concrete and inserting a single fibre in the centre, the fibres were slowly added to the mix and the mixing process was continued for at least 2 minutes longer to guarantee proper distribution of fibres in the mix. Then the FRC mix was cast into moulds manually in a single layer without any tamping. Following casting, specimens were kept at laboratory temperature (approximately 20°C) for the first 24 hours. Once initial setting has occurred at approximately 24 hours, demoulding took place. After the demoulding process, specimens were placed in a curing tank for the next 28 days, after which flexural tests were carried out to obtain a load-displacement graph.



Figure 3-20 Three-point bending test setup

Figure 3-20 presents the set up used in the flexure test. The flexure test was implemented using a three-point bending test on a beam specimen of $40 \times 40 \times 160$ mm in width, depth and length, respectively. The test was performed under a fixed displacement control of 0.2 mm/minute over a clear span of 130 mm using a Tinius Olsen machine with capacity 25 kN. Since the effect of each fibre on the load-

deflection curve of the composite is different, the tail portions of the curves drawn up to 20 mm particularly in the PPF1 fibre series can be observed. The midpoint force-displacement graph was plotted digitally on the computer using Horizon.

Flexural tests were performed for optimizing the volume fraction of each different type of fibre and for investigating the effect of plasma treatment on flexural performance of the composites. In the fibre volume optimization process, three specimens were prepared, and the averages of force-deflection were determined and presented. However, in the case of investigating the impact of plasma treatment, six identical specimens were prepared, and the load-deflection graphs were plotted. From the graph, the first cracking strength and deflection, flexural strength and deflection values at maximum load were determined. The first crack load is taken as the point at which the initial load-deflection curve begins to change from linear to nonlinear. The flexure strength or modulus of rupture were calculated using equation (3.11).

$$\sigma_b = \frac{3P_u l}{2bh^2} \quad (3.11)$$

Where:

σ_b is flexure strength (MPa)

P_u is ultimate load (kN)

l is length of the beam specimen (mm)

b is width of the beam specimen (mm) and

h is height of the beam specimen (mm)

The experimental results are presented in section 4.5.3.

3.5 Summary

In this chapter, the experimental set-up of the MIPT was described. The systems and equipment used in this study were presented and discussed. The fibres in which surface modifications were conducted on are listed along with their sources and properties. The concrete mix design and its constituents are also presented. The various techniques used in surface characterisation such as wetting contact angle measurement, scanning electron microscopy and atomic force microscopy were presented in detail. Mechanical characterisation techniques and processes for plasma treated and untreated fibres were presented. The mechanical techniques consisted of single fibre tensile test to study the effect of plasma treatment on the fibre strength, single fibre pull-out tests to investigate the effect of plasma on fibre/cement interface properties, and three-point bending test for investigating the influence of plasma treated fibres on the performance of fibre cementitious composites. The results are presented in the following chapter (chapter 4).

Chapter 4 **Results and Discussions**

4.1 Introduction

In this chapter, the results from the investigation of surface and mechanical analysis are presented and discussed. First, the CAM used for determining the best plasma condition for PPF1 and GF is presented. Then the surface morphology of the fibres, treated with this plasma, using SEM and AFM are presented. Followed by the tensile performance of treated fibres. Results from single fibre pull-out tests of fibres embedded in a cementitious matrix for 28 days are presented, these data allow the fibre-cement interfacial property data to be determined, which are related to the fibre-cement bonding. The pull-out behaviour of single PPF1, GF and BF at 28 days is presented in conjunction with an evaluation of untreated fibres. Finally, plasma treated prismatic specimens have been prepared and tested in flexure; the effects of the plasma fibre treatment is evaluated, and the results are presented.

4.2 Plasma Temperature Profile

Prior to surface treatment of fibres, the plasma temperature profile was investigated to find the range of temperature for experimental work, to make sure that the right plasma conditions were used. As very low temperature plasma treatment might not make any remarkable difference on the surface of the fibres, meanwhile, very high plasma condition might cause severe damage to the fibres and make them unsuitable as reinforcement in the composites. Three different distances (30, 60 and 100 mm) from the plasma jet were selected. At each distance, three different gas flow rates (1, 2 and 3) l/min were investigated at 10 sec intervals.

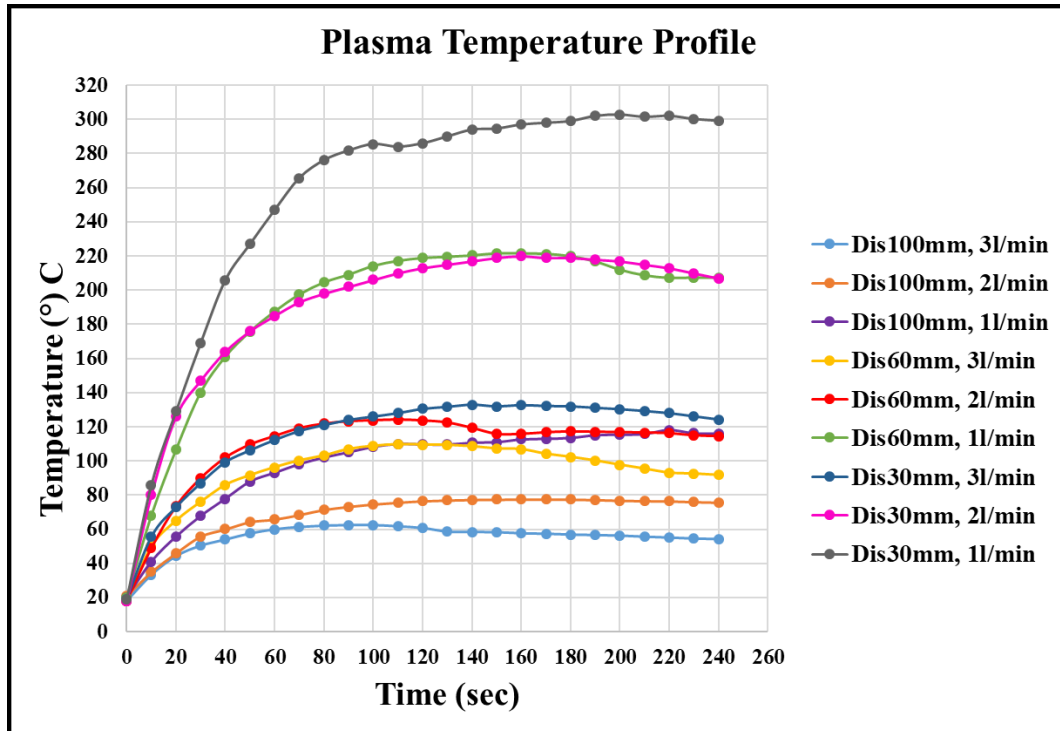


Figure 4-1 Plasma Temperature Profile

From Figure 4-1, it can be observed that the temperature decreases as the gas flow rate increase. This may be attributed to the increase in electron densities when the flow rate is increasing (Moon et al, 2002), resulting in the collision increase between the gas atom and the electron (Bartschat and Kushner, 2016). Thus, the transferred energy from the electrons to the gas particles increases, initiating a rise in the gas temperature by dropping the electron temperature (Humud, Abbas and Rauuf, 2015). It can be observed that over time the plasma temperature is increasing for all flow rates. However, when the temperature reached a particular value, then some stability can be observed, and the temperature remains relatively constant. This instability in the temperature could be attributed to the injecting of cold gas (Fauchais and Vardelle, 2000), or to the influence of the ambient atmosphere cold gas (Russ, Pfender and Strykowski, 1994).

4.3 Surface Characterizations

This section presents the experimental results obtained to evaluate the alteration in the surface properties of fibres before and after plasma treatment. The properties were determined through a combination of experimental measurements of wettability and surface morphology at a micro and nano scale. CAM was employed to characterise the wettability properties of PPF1 and GF over a range of plasma conditions and to optimise the plasma condition. SEM and AFM were employed to measure the effect of plasma treatment on a surface morphology. A description of the test results is given for each fibre type that was investigated.

4.3.1 Contact angle Measurements

In this section, the results of wetting angle measurements of PPF1 and GF using the method described in Section 3.4.1.1 have been examined. The static wetting angle of BF was not measured because the diameter of these fibres is relatively smaller than the diameter of sessile water droplets.

4.3.1.1 Macro Polypropylene Fibre (PPF1)

Despite the wide range of PPF1 applications, technically and industrially, PPF1 is counted as a very hydrophobic material which exhibits a very low surface energy. Thus, an enhancement in wettability is crucial. Surface modification of these fibres to enhance wettability and absorption properties can be achieved using plasma technology (Höcker, 2002).

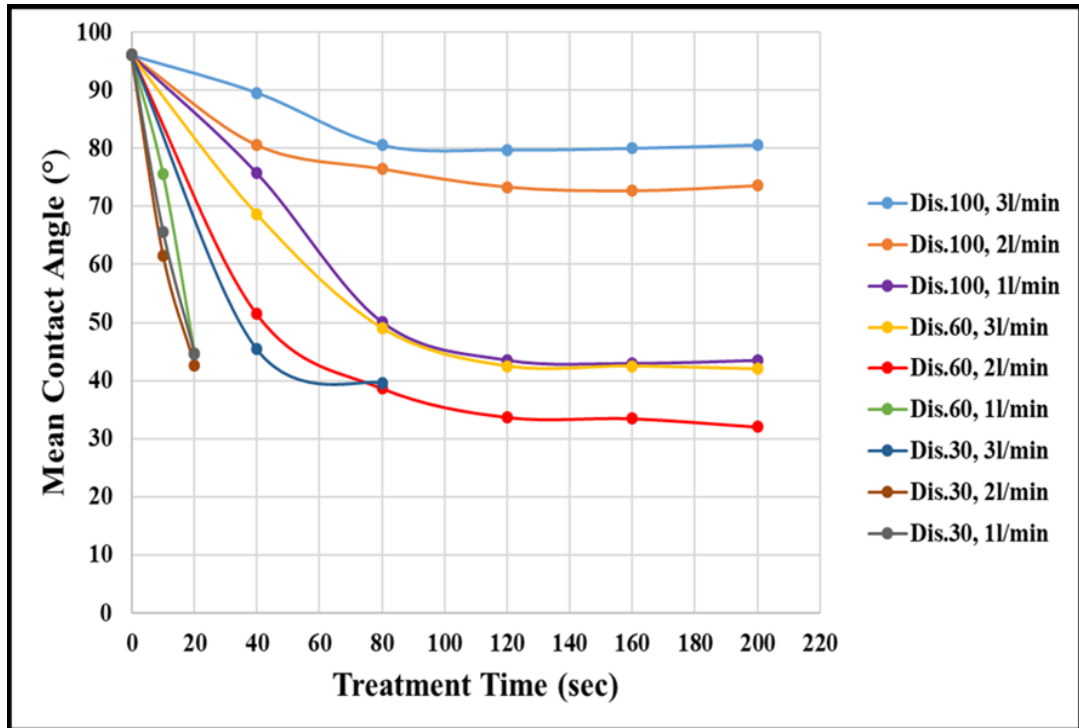


Figure 4-2 Wetting Contact Angle of PPF1 before and After Plasma Treatment

Applications of the 5.8 GHz argon plasma at fibre distances of (30, 60, 100 mm) from the plasma jet and the wetting angle values obtained from the PPF1 surface with regards to treatment duration and an argon flow rate at each distance are presented in Figure 4-2. It can be observed, that the CAM is reduced with an increase in the treatment duration at each flow rate. However, when a maximum plasma temperature was attained at each flow rate, further exposure did not contribute to further reduction in the contact angle. This is because at this stage the free species in the plasma atmosphere have similar density and energy; this means that the state surface saturation was reached (Yang et al, 2016). In addition, despite the differences in the gas flow rate and the distance from the plasma jet, CAM recorded approximately similar values when recorded plasma temperatures were close. For instance, at two different plasma conditions (distance 30 mm, flow rate 3 l/min and treatment duration 80 sec) and (distance 60 mm, flow rate 2 l/min and treatment duration 80 sec) the

plasma temperature recorded was 120° and the wetting angle values were around 40°. From this finding, it can be concluded that the plasma temperature directly influences the wetting angle values for PPF1.

For instance, at a distance of 100 mm from the plasma jet, and with a flow rate of 1, 2 and 3 l/min, the contact angle measurement was reduced. CAM reduction from 96° to 43.5° at flow rate of 1 l/min and for a duration of 120 sec was reported, when a temperature recorded at this condition was 60°C. This reduction in CAM is greater by 25.54% (33.65°C) at distance of 60 mm with gas flow rate 2 l/min and treatment duration 120 sec, however, the plasma temperature recorded at this condition was doubled (120°C).

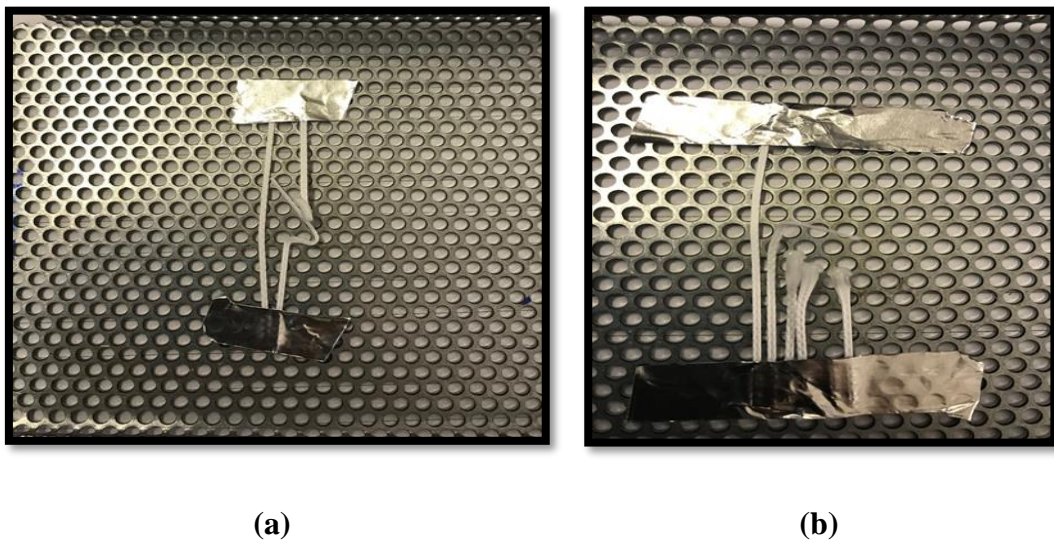


Figure 4-3 PPF1 Failure: (a) Softening of PPF1 at 60 mm, 1 l/min and plasma exposure exceeding 20 sec, (b) Decomposition of PPF1 at 30 mm, 2 l/min, 1 l/min and plasma exposure exceeding 20 sec

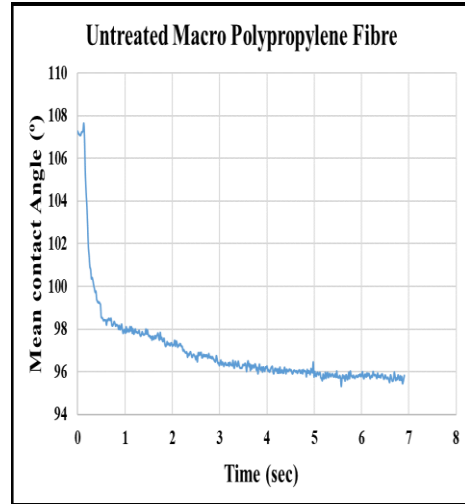
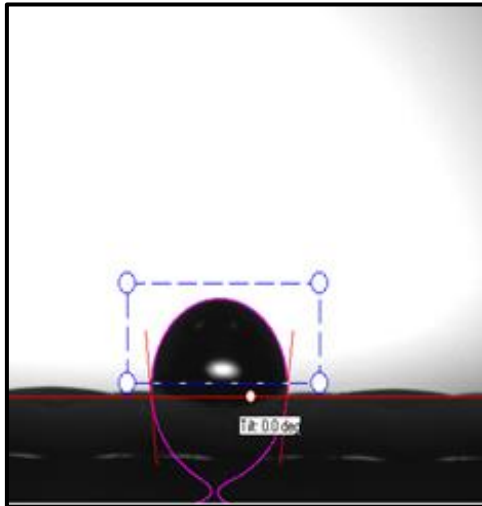
Figure 4-3(a) shows softening of PPF1 when exposed to plasma at distance 60 mm, flow rate 1 l/min and treatment duration exceeding 20 sec. At a distance of 30 mm, CAM recorded 39.65°C with a flow rate of 3 l/min and a treatment duration of 80 sec, and 42.65°C was recorded with a flow rate of 2 l/min and a treatment duration of 20 sec, and was 44.57° recorded with a flow rate of 1 l/min and a treatment duration of

20 sec also. Plasma temperatures recorded at these conditions were 120°C, 130°C and 130°C respectively. Further exposure exceeding 20 sec at this condition caused melting and significant physical changes of PPF1 due to the higher plasma temperature, which exceeded 140°C at this condition compared to the relatively low melting point of PPF1 as shown in Figure 4-3(b).

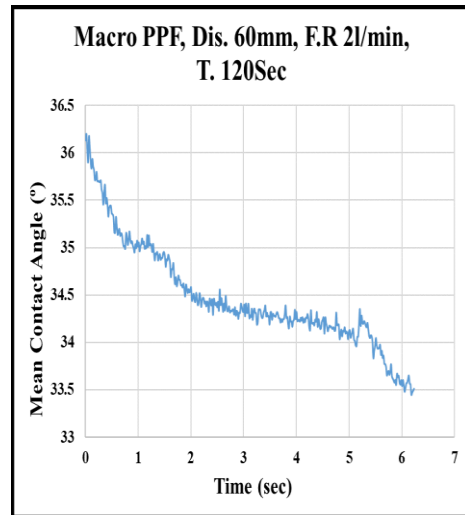
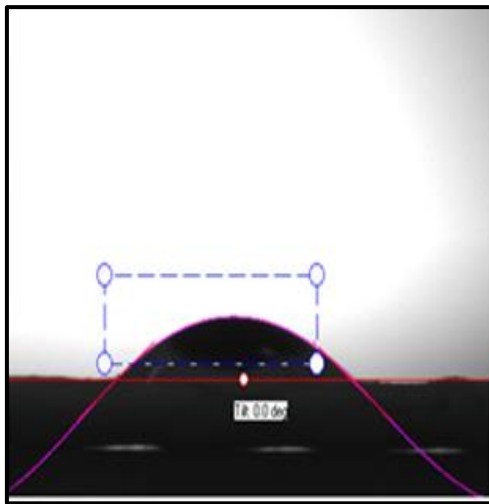
Table 4-1 presents the best plasma conditions selected to investigate the surface morphology, fibre tensile test and single fibre pull-out test of PPF1, as the CAMs were relatively reported the lowest at these conditions. It is clear from the table that at treatment duration 200 sec, the CAM did not further reduce, however, this treatment condition was selected for the purpose of comparison only and to investigate if longer treatment could influence the surface properties or fibre/cement bonding.

Table 4-1 Selected Plasma Conditions for PPF1

Specimen Code	Melting Point (°c)	Distance (mm)	Flow Rate (l/min)	Treatment Time (sec)	Plasma Temperature (°c)	Contact Angle (degree)
PPF1-0	160	-	-	-	-	96
PPF1-60-2	160	60	2	120	123.805	32
PPF1-60-2	160	60	2	200	116.912	32



(a)



(b)

Figure 4-4 Computer Images and Contact Angle-Time Graph of PPF1: (a) Untreated, (b) Treated at Distance 60mm, Flow Rate 2l/min and Treatment Duration of 120 sec

Figure 4-4 presents the images taken from the computer software for untreated and treated PPF1 at a distance of 60mm, a flow rate of 2l/min and a treatment duration of 120 sec along with the contact angle-time graph obtained. The change in wetting angle is clearly visible in the photographs. All these results demonstrate that the surface structure of the plasma induces a significant change on the PPF1 surfaces.

Although, it is difficult to come to a definite conclusion about the physical and / or chemical change by the measurement of wetting angle, some researchers have achieved similar results and offered different explanations. Nevertheless, none of the previous researchers has investigated the link between the plasma temperature and the resulting contact angle. Generally, researchers relied on the chemical analysis of the surface of the plasma treated fibres and the resulting induced functional groups. (Sanaee et al, 2011) stated that the reduction of the wetting angle in argon plasma treated PP fibre could be attributed to the formation of -COOH and -OH groups on the surface of low energy PP with a potential for bonding with water. The development of these groups on the surface of an inert PP can increase the surface energy of the fibre and decrease the simultaneous wetting angle (Morent et al, 2008). Likewise, (Zhang et al, 2017) stated that argon plasma can alter the surface to make it hydrophilic by incorporating cross-linked bonds (C-O, O-C = O, and C = O) created on the surface of the plasma treated fibres. A similar conclusion was made by (Felekoglu, Tosun and Baradan, 2009; Jacobs et al, 2010) that the plasma changes the surface structure of PP by providing cross-linking on the functional surface there.

4.3.1.2 Glass Fibre (GF)

Similar to PPF1, the CAM of GF significantly reduced after the exposure to the 5.8 GHz argon plasma at distance (30, 60 and 100 mm).

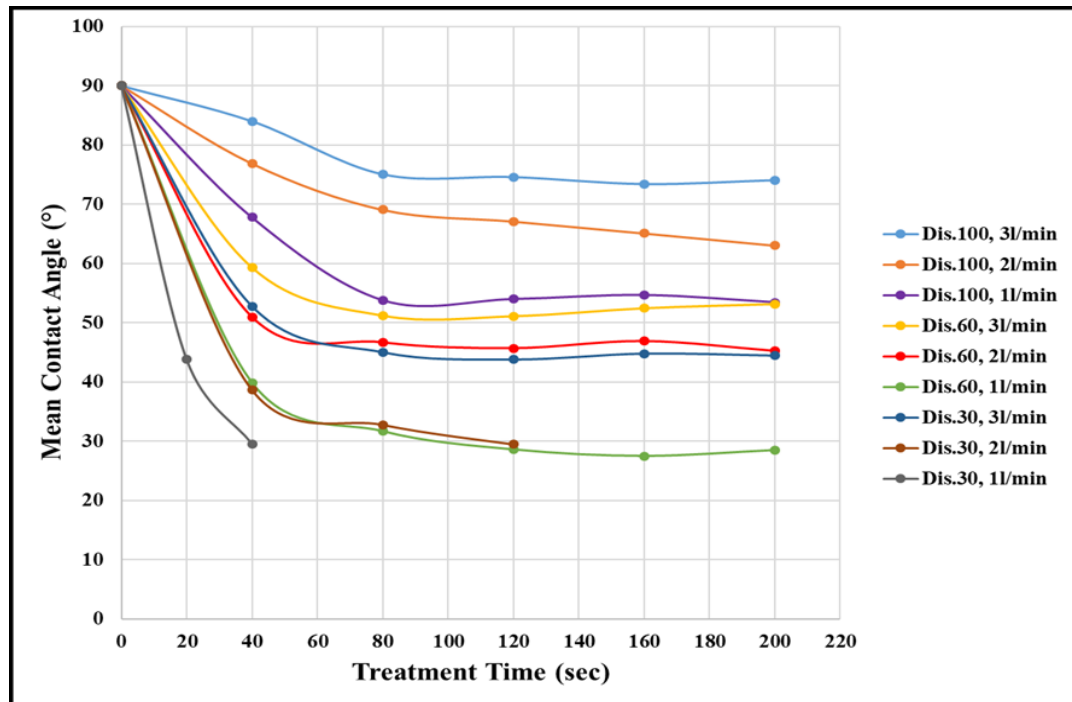


Figure 4-5 Wetting Contact Angle of GF Before and After Plasma Treatment

Figure 4-5 presents the observed wetting angle with regards to treatment duration and argon flow rate at each distance. From the graph, a similar trend to the PPF1 wetting angle can be observed with relation to plasma temperature. As the plasma temperature increases, the reduction in CAM values for GF reduce. For instance, CAM for GF at ambient temperature (untreated) was 90. This value dropped significantly to 51.96 when treated at distance 100 mm at the flow rate of 1 l/min for duration of 120 sec. When the recorded temperature for this condition was 130°C, further reduction in CAM was observed when the plasma temperature increased to 220°C as the distance from the plasma torch reduced to 60 mm until it reached 27.65 at flow rate 1 l/min and treatment duration of 120 sec. On the other hand, at a distance 30 mm the contact angle

reduced to 28.56 at treatment duration of 40 sec when the flow rate was 1 l/min, when plasma temperature was 210°C with 0.92 difference from the previous treatment.



Figure 4-6 Treated at Distance 30 mm, Flow Rate 1 l/min and Treatment Time Exceeding 40 sec

Further exposure at this condition led to the fibre being burned and discoloured, as shown in Figure 4-6. This resulted in the fibre being more brittle during handling. This might be due to chemical decomposition of GF resulting from the chemical bond break due to the high temperature. Table 4-2 presents the best plasma conditions selected to investigate the surface morphology, fibre tensile test and single fibre pull-out test of GF, as the CAMs were indicated the lowest angle at these conditions.

Table 4-2 Selected Plasma Conditions for GF

Specimen Code	Melting Point (°C)	Distance (mm)	Flow Rate (l/min)	Time (sec)	Plasma Temperature (°C)	Contact Angle (degree)
GF-0	860	0	0	0	-	90
GF-30-1	860	30	1	40	205.91	28.56
GF-60-1	860	60	1	120	218.76	27.74
GF-60-1	860	60	1	200	211.93	28.45

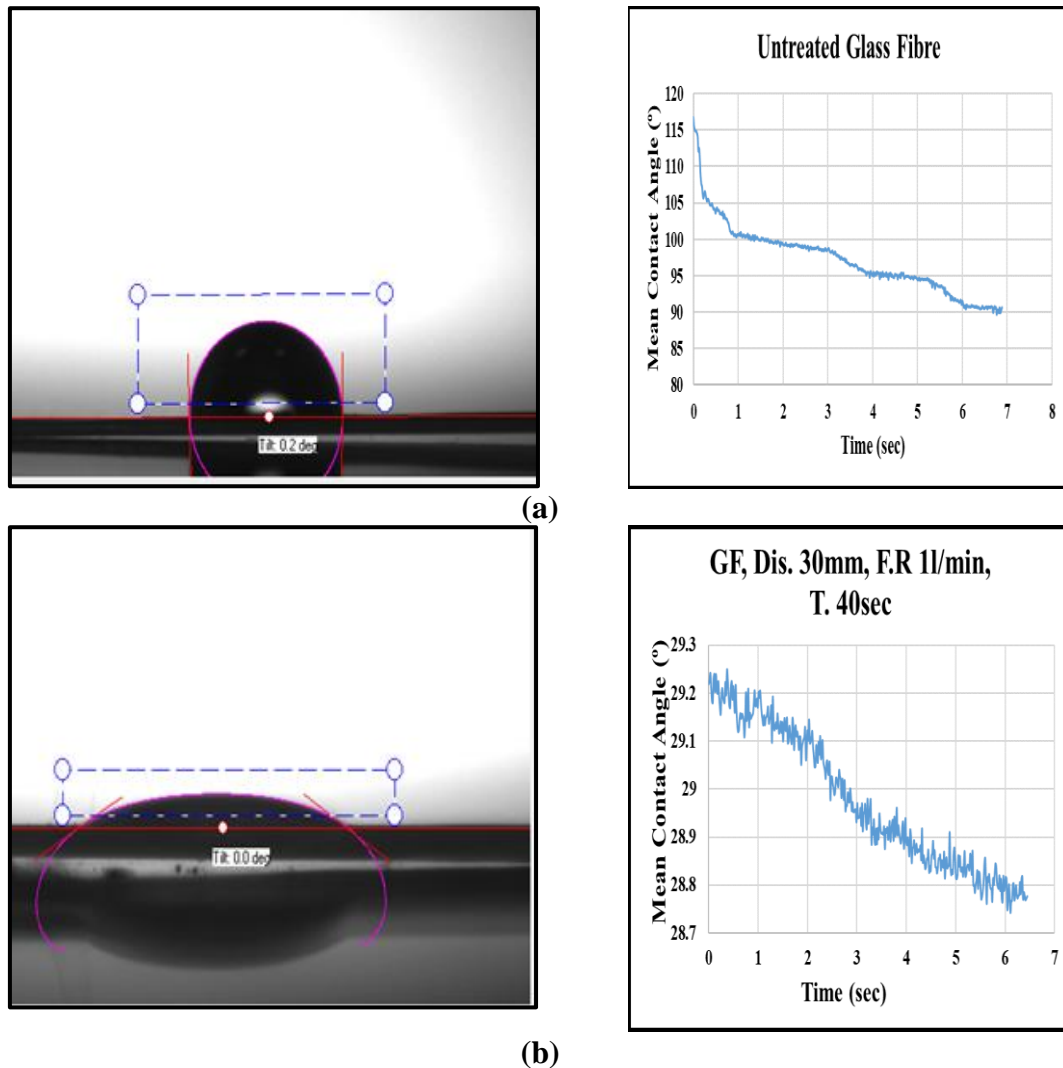


Figure 4-7 Computer Images and Contact Angle-Time Graph of GF: (a) Untreated, (b) Treated at Distance 30mm, Flow Rate 1l/min and Treatment Duration of 40 sec

Figure 4-7 presents the images taken from the computer software for untreated and treated GF at 30 mm, for a flow rate of 1l/min and a treatment duration of 40 sec along with the contact angle-time graph obtained.

The reduction in the wetting contact angle of GF could be attributed to the plasma inducing new functional groups and surface oxidation after treatment, as a result this could enhance a free energy surface and increase the wetting and thus improving the adhesion (Ping LU, 2015). Furthermore, it is verified that plasma treatment can improve the surface roughness of material, which increases wettability (Kostov et al, 2010; Kusano et al, 2010). Moreover, there is a possibility that two processes take

place at same time that lead to the wettability increase in argon plasma treated GF, which are the removal of organic contaminants and the formation of polar groups such as C-O and O-C=O (Homola et al, 2013). Also, the breakdown of O-OH and C-C bonds due to plasma exposure could result in a reduction in wetting angle for GF (Yamamoto et al, 2004).

4.3.2 Scanning Electron Microscopy (SEM)

After the wetting angle measurements, SEM images were taken with suitable magnification for all samples presented in Table 4-1 and Table 4-2 using the SEM device specified in Section 2.5.1.2.

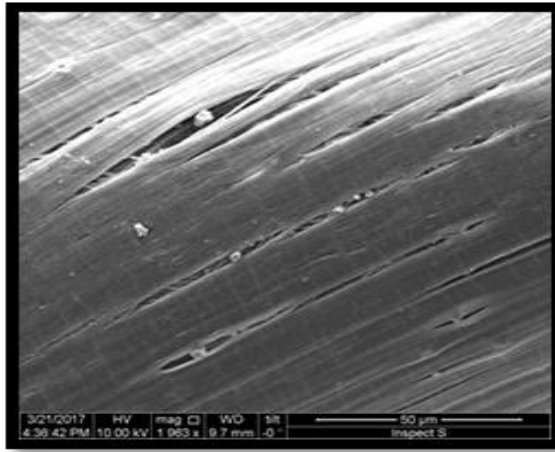
4.3.2.1 Macro Polypropylene Fibre (PPF1)

Plasma treatment also induces physical changes on the PPF1 surface, which can occur with nano and micro size etching or coating. Although, it is difficult to predict the exact altered surface structure of PPF1. If the change occurs in the form of molecular breakdown of the surface, this is called plasma etching. On the other hand, if the effect is formed by splitting and releasing the bonds in the surface, it is defined as plasma polymerization, which describe the formation of functional groups at the surface (Yamamoto and Okubo, 2007). Generally, plasma cleaning, etching and surface morphology changes are more dominant in the gas plasma, whereas, plasma polymerisation occurs when monomers are used (Yamamoto and Okubo, 2007).

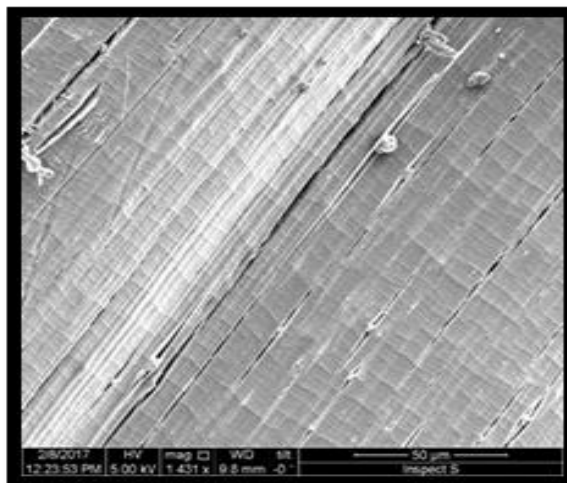
After the CAM were taken, SEM analysis was utilized to observe and verify the changes to the PPF1 and the surface morphology for best plasma condition specimens, which are presented in section 4.3.1.1, Table 4-1.



(a)



(b)



(c)

Figure 4-8 SEM of PPF1: (a) PPF1-0 (b) PPF1-60-2-120 and (c) PPF1 60-2-200

Figure 4-8 presents SEM images of plasma treated and untreated PPF1 specimens. It appears that surface roughness has a significant effect on reducing contact angle measurement for PPF1. Although, small droplets and longitudinal grooves and cracks, resulting from the fibre production process of untreated fibres, are clearly visible in Figure 4-8(a), the observed contact angle measurement reported was a higher value in comparison to the treated fibres. When plasma treatment is implemented at distance 60 mm, gas flow rate 2 l/min and treatment duration of 120 and 200 seconds on the surface, the development of microscopic cracks, droplets and holes on the fibre surface was induced, as shown in Figure 4-8(b) and Figure 4-8(c). The new rougher surface might have contributed to the receding contact angle measurement (96.182%). Therefore, it can be concluded that argon plasma treatment contributed to the alteration in surface morphology of PPF1 through enhancing the surface roughness (Jacobs et al, 2010; Tosun, Felekoğlu and Baradan, 2012; Zhang et al, 2017). The higher the surface roughness of PPF1 the lower contact angle measurement recorded. Thus, the contact angle is directly influenced by surface roughness. A similar conclusion was made by (Wang Xiaodong, Peng Xiaofeng and Buxuan, 2004; Yan et al, 2015; Li et al, 2016). However, some researchers (Lam et al., 2001) reported that the contact angle measurement is more affected by the properties of the liquid such as viscosity.

4.3.2.2 Glass Fibre (GF)

SEM analysis was carried out to observe and validate the alterations in the surface morphology of GF. SEM was conducted on specimens treated with the determined best plasma conditions in section 4.3.1.2, which are presented in Table 4-2. Substantial changes of the GF surface morphology occurred due to exposure to plasma.

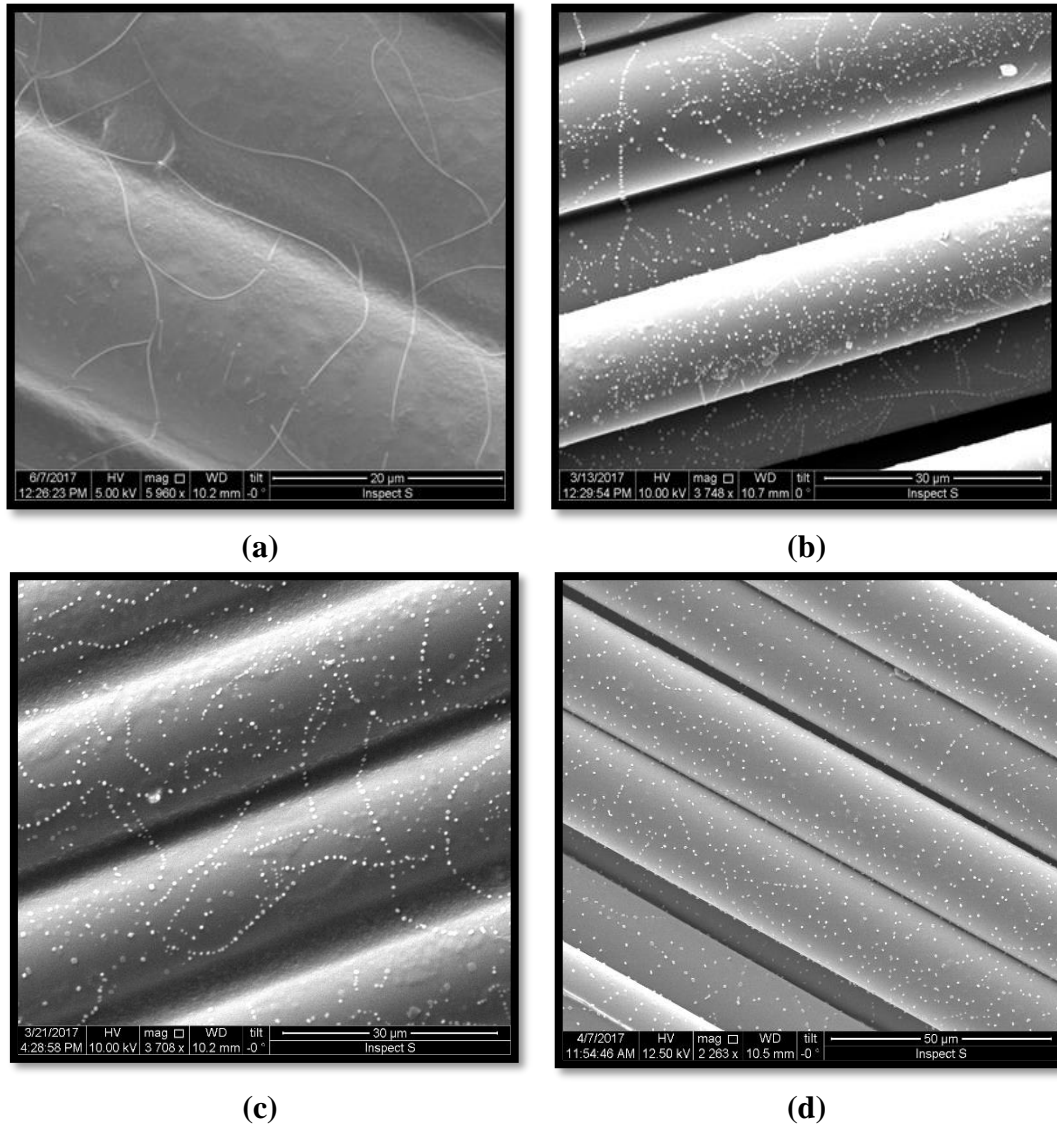


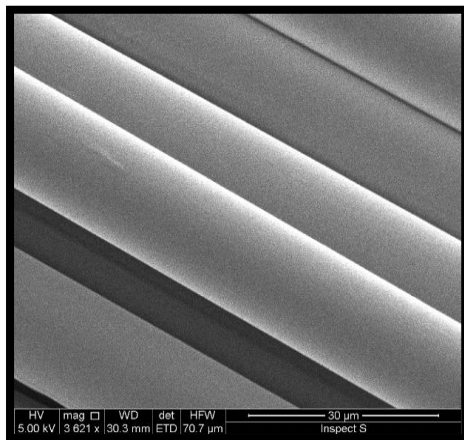
Figure 4-9 Effect of Plasma Treatments on GF Surface Morphology: (a) GF-0 (b) GF-30-1-40, (c) GF-60-1-120 and (d) GF-60-1-200

Figure 4-9 presents the SEM images of GF before and after plasma treatment. In Figure 4-9(a), some thin swirly contaminant has appeared on the surface of untreated GF. It can be observed from Figure 4-9(b), (c) and (d), that due to plasma treatment of GF these weak glass domains have relatively ablated. It can be concluded that there is a possibility that the ablation rate contributed to the reduction in CAM. Moreover, a reduction in CAM could be attributed to the enhanced surface oxidation (Zhang et al, 2013), or an increased polar component of the surface energy of GF during plasma treatment (Kusano et al, 2010). Furthermore, Yang et al. (Yang et al, 2016) suggested

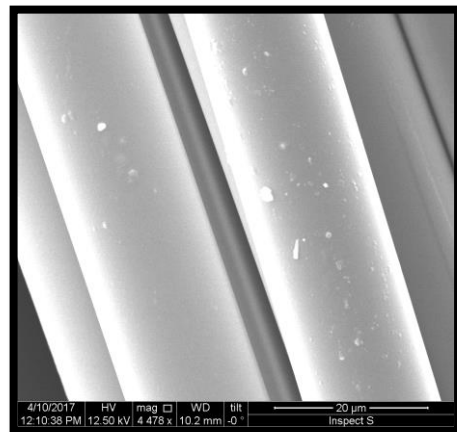
that the increase in CAM of GF after plasma treatment is due to the appearance C=O, COOH and –C-O-C and other new oxygen containing groups on the surface of GF, which resulted in the enhancement of surface energy, which is a molecular force of attraction between fibre and the matrix.

4.3.2.3 Basalt Fibre (BF)

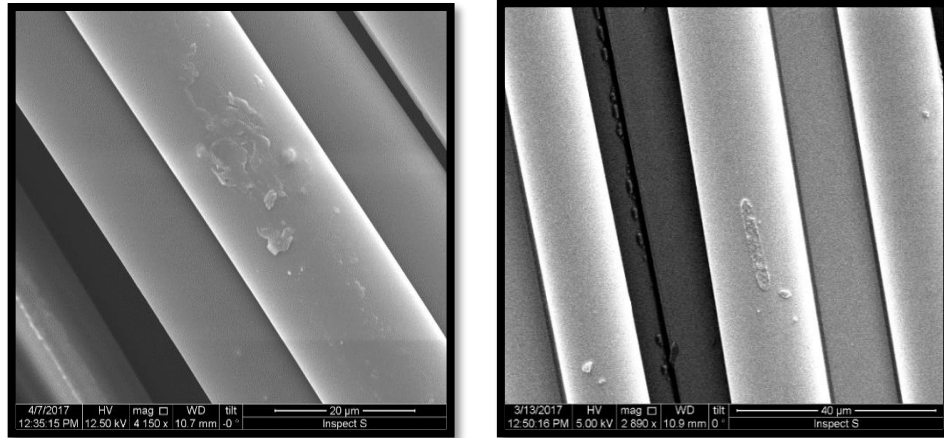
Due to the difficulty of optimizing plasma condition for BF using CAM techniques, similar treatment conditions to the GF were implemented to investigate the effect of plasma treatment on the surface morphology of BF. The treatment conditions were at a distance of 30 mm, a flow rate of 1 l/min and a treatment duration of 40 sec; a distance of 60 mm, a flow rate of 1 l/min and a treatment duration of 120 sec, and a distance of 60 mm, a flow rate of 1 l/min and a treatment duration of 200 sec.



(a)



(b)



(c)

(d)

Figure 4-10 Effect of Plasma Treatments on BF Surface Morphology: (a) BF--0 (b) BF-30-1-40, (c) BF-60-1-120 and (d) BF-60-1-200

Figure 4-10 presents the effect of plasma treatment on the surface morphology of BF. It is obvious from Figure 4-10(a) that the surface of untreated BF is very smooth. In comparisons, dramatic and distinct alterations were observed after the fibres exposure to plasma (Figure 4-10(b), (c) and (d)). BF surfaces were modified from smooth to rough due to plasma induced surface defects, which were predominantly lump and swelling like. This could be attributed to the etching of the BF surface resulting from ion bombardment of the plasma (Wang et al, 2007). Consequently, the surface roughness of BF was increased due to the plasma etching (Moon and Jang, 1999; Kim et al, 2011).



Figure 4-11 BF Treated at Distance 30 mm, Flow Rate 1 l/min and Treatment Time Exceeding 40 sec

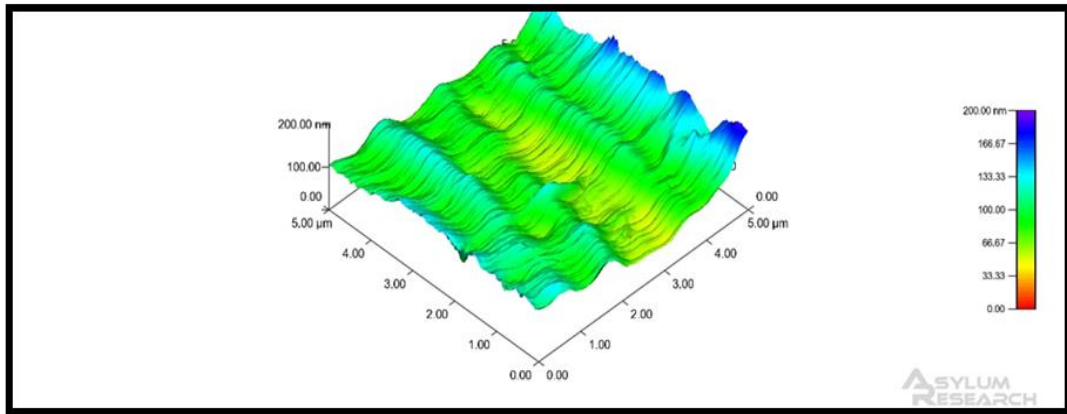
Furthermore, at a distance of 30 mm, when BF was exposed to plasma for a duration exceeding 40 sec, the fibre became very brittle and difficult to handle as shown in Figure 4-11.

4.3.3 Atomic Force Microscopy (AFM) Roughness Analysis

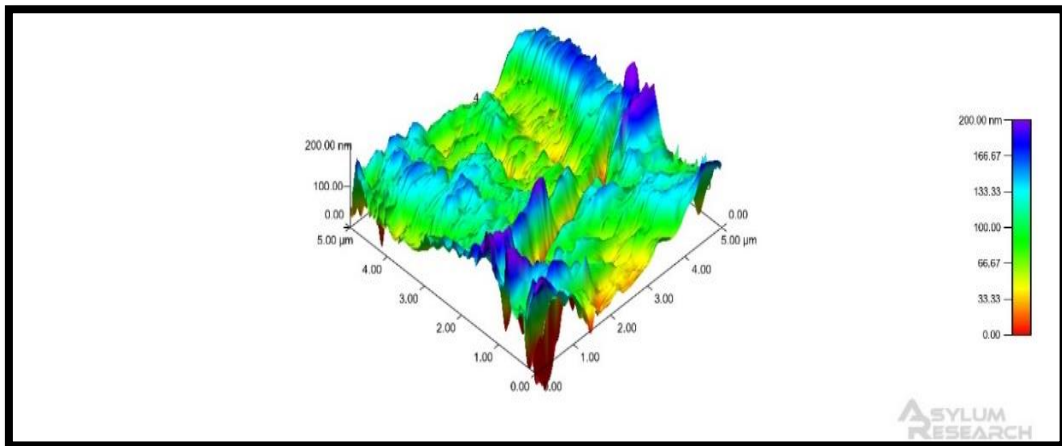
Although, the physical changes occurring in the surface structure can be observed at the micro dimension by SEM, physical changes that occur at the nanometric dimension, which is the main function of the plasma, cannot be detected with this method. For this reason, in the next section, AFM and nanometre scale studies have been made. Nano roughness values (Rms) were obtained from AFM images by the method given in section 2.5.1.3.

4.3.3.1 Macro polypropylene Fibre (PPF1)

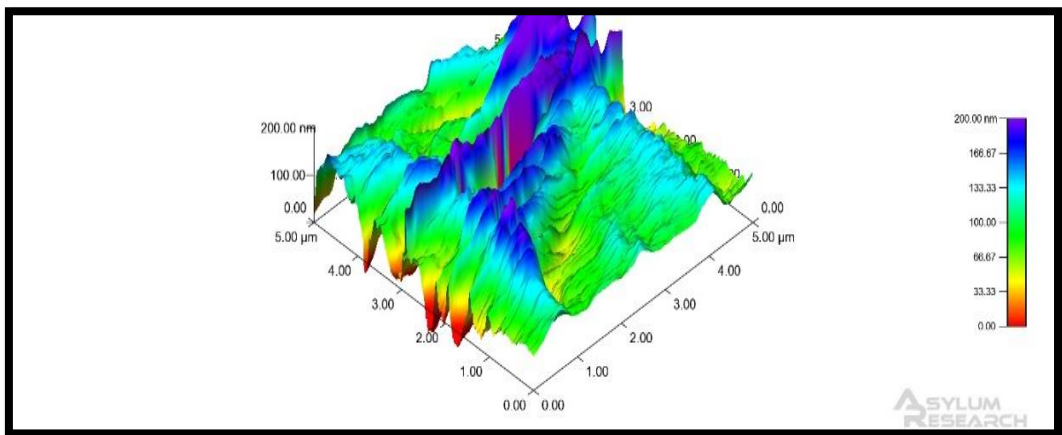
AFM analysis delivered additional evidence for considering the restructuring of the plasma exposed surface of any material.



(a)



(b)



(c)

Figure 4-12 Effect of Plasma Treatment on Nano Roughness of PPF1 Surface: (a) PPF1-0, (b) PPF1-60-2-120 and (c) PPF1-60-2-200

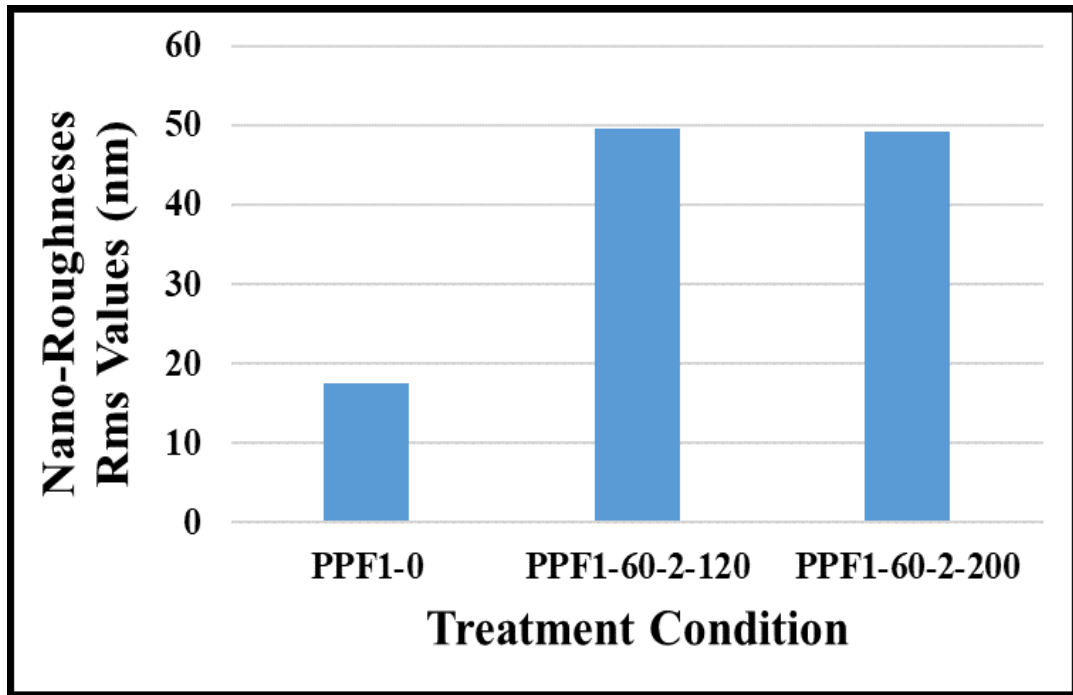


Figure 4-13 Rms Values of PPF1 before and after Plasma Applications

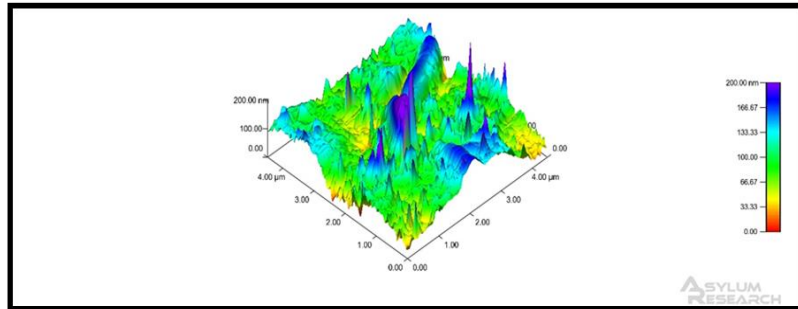
Figure 4-12 and Figure 4-13, shows the topographical properties changes of untreated and plasma treated PPF1 and the Rms values obtained for a surface of ($5 \times 5 \mu\text{m}^2$ scan surface) respectively.

According to the AFM images, the surfaces of untreated PPF1 have very smooth surfaces as shown in Figure 4-12(a), with a Rms values 18.04 nm. However, after exposure to the selected plasma conditions, various sizes of pores, grooves and cracks developed on the entire surface as shown in Figure 4-12(b) and (c). Meanwhile, Rms values increased to around 49 nm in almost all specimens treated with selected plasma conditions. This finding is proof that argon plasma changes the surface topography of PPF1. This alteration in surface topography could be due to alignment of the molecules chain, cross-linking and change in the surface structure after bombardments of PPF1 by plasma species, and high temperature during plasma treatment (Fu, 2012) (Intrater

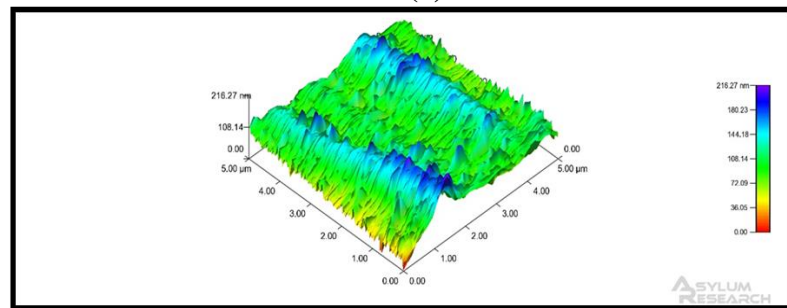
et al, 2006; Švorčík et al, 2006). According to the AFM images and Rms values, it can be concluded that at 60 mm and a flow rate of 2 l/min, plasma exposure exceeding 120 sec, did not contribute to further surface topography change. This behaviour was also observed by SEM analysis of PPF1.

4.3.3.2 Glass Fibre (GF)

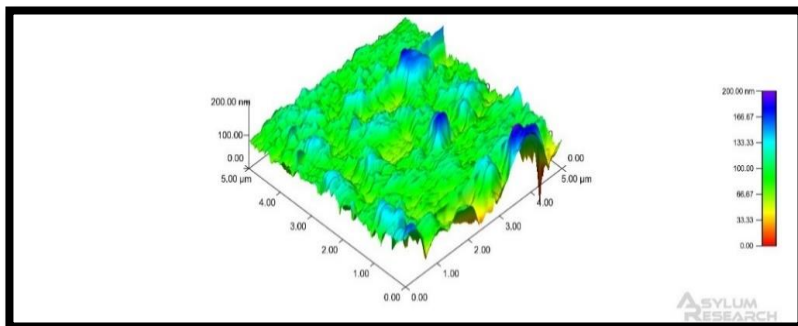
To provide indications for GF surface structure alterations due to plasma exposure, AFM analysis was conducted



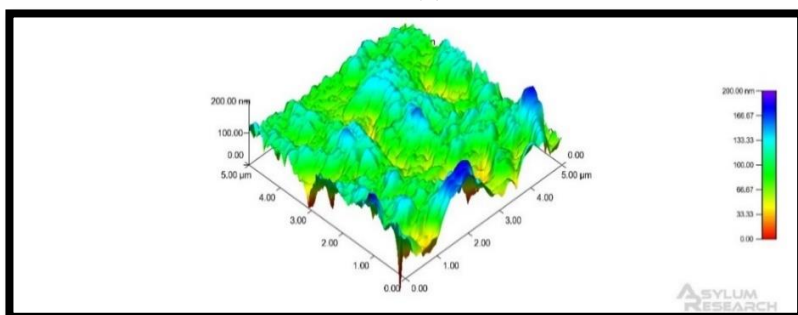
(a)



(b)



(c)



(d)

Figure 4-14 Effect of Plasma Treatment on Nano Roughness of GF Surface: (a) GF-0, (b) GF-30-I-40, (c) GF-60-I-120 and (d) GF-60-I-200

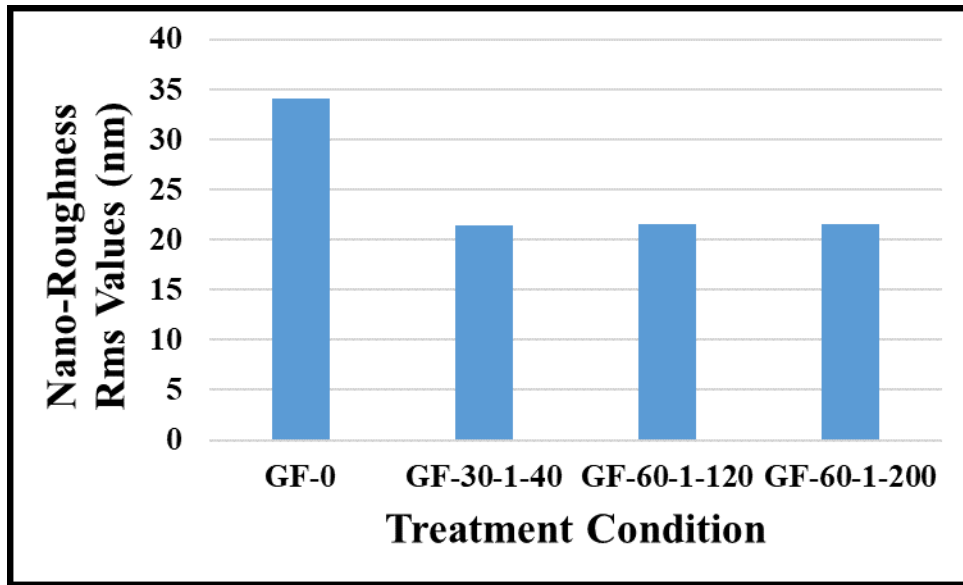
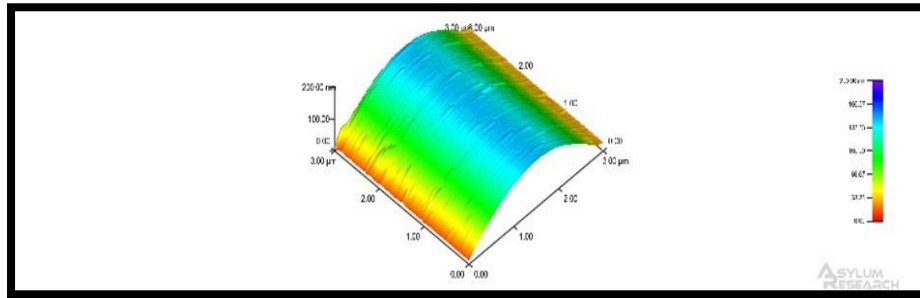


Figure 4-15 Rms Values of GF before and after Plasma Applications

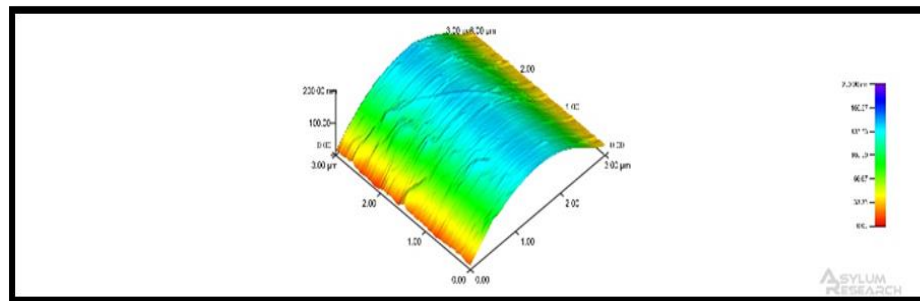
Figure 4-14 and Figure 4-15 present the topographical properties changes of untreated and plasma treated GF and the Rms values obtained for a surface of ($5 \times 5 \mu\text{m}^2$ scan surface) respectively. The initial roughness values of GF are somewhat higher than PPF1 fibres (Rms = 34.23 nm). Which means that GF have a relatively rougher surface compared to PPF1 as shown in Figure 4-14(a). Referencing to AFM images, when the argon plasma is applied to GF, the roughness decreased, as fewer and smaller sized grooves, cracks and surface roughness appeared as shown in Figure 4-14(b), (c) and (d). Moreover, the Rms values for plasma treated GF at distance 30 and 60 mm were around 21.5 nm. This could be concluded as the plasma treatment initially performs some sort of cleaning on the surface of the GF containing macro roughening contaminate, reducing the size of the roughness and homogenizing it, resulting in a decrease in Rms values. This result seems to be contradictory to the results obtained from SEM images presented in section 4.3.2.2, where the removal of the weak surface layers was obvious.

4.3.3.3 Basalt Fibre (BF)

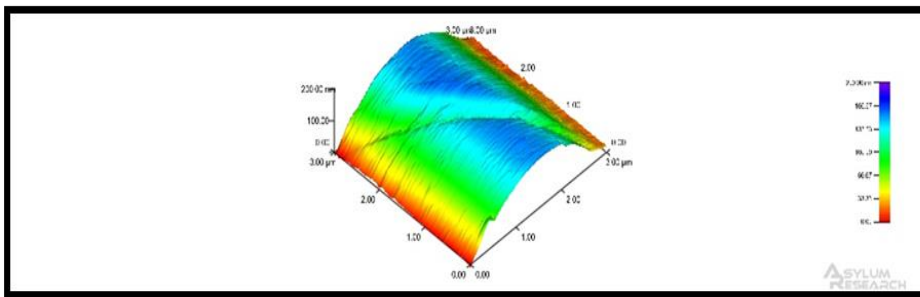
To provide indications for BF surface structure modifications due to plasma exposure, AFM analysis was conducted.



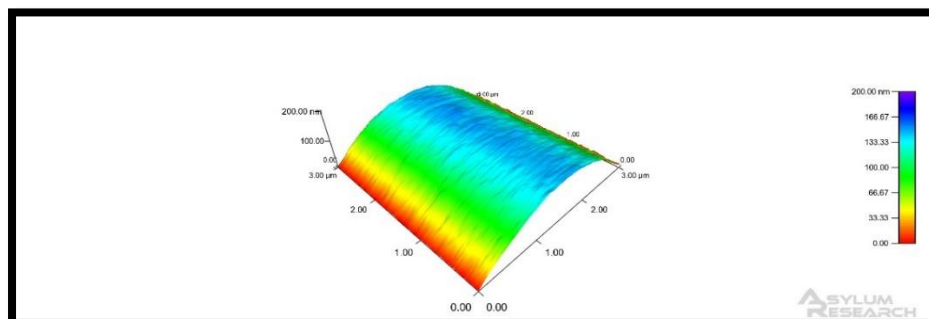
(a)



(b)



(c)



(d)

Figure 4-16 Effect of Plasma Treatment on Nano Roughness of BF Surface: (a) BF-0, (b) BF-30-I-40, (c) BF-60-I-120 and (d) BF-60-I-200

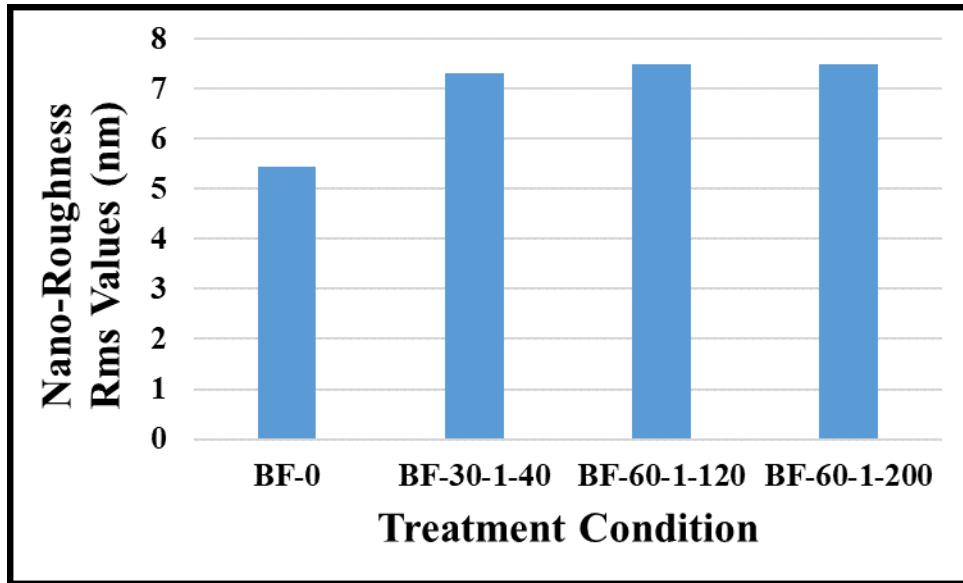


Figure 4-17 Rms Values of BF before and after Plasma Applications

Figure 4-16 and Figure 4-17 present the topographical properties changes of untreated and plasma treated BF and the Rms values obtained for a surface of ($5 \times 5 \mu\text{m}^2$ scan surface) respectively.

Referencing the AFM images, the initial surface roughness values of BF are much lower than PPF1 and GF (Rms = 5.5 nm). This finding proves that BF have a much smoother surface structure. When the argon plasma was applied to BF, the roughness increased, as fewer and smaller sized grooves, cracks and surface roughness appeared Figure 4-16 (b), (c) and (d). Moreover, the Rms values for plasma treated BF at distance 30 and 60 mm were around 7.5 nm. This could be concluded as plasma treatment initially performs some sort of etching on the surface of the BF when the plasma species bombarded the surface, resulting in an increase in Rms values. This result seems to be contradictory to the results obtained from SEM images presented in section 4.3.2.3, where plasma induced surface roughness was observed.

4.3.4 Evaluation Summary

After the plasma application to the fibre surfaces was carried out, CAMs were examined for PPF1 and GF. The lowest contact angle values for each fibre were concluded as the best plasma condition which are presented in Table 4-1 and Table 4-2. Due to the very small diameter of BF, plasma optimizations were unable to be carried out. However, due to the closer melting point of BF to the GF, the same plasma conditions were implemented for BF. SEM analyses, AFM roughness analyses for PPF1, GF and BF are listed in Figure 4-8 to Figure 4-10, and Figure 4-12 to Figure 4-17. The main findings from these investigations are listed below:

- Plasma application significantly increases wettability by reducing static wetting angle values of PPF1 and GF surfaces. Decreased wetting angle with plasma application may show a slight increase when fibres are treated at a shorter distance from plasma jet. When the best plasma condition is reached, further exposure to plasma did not affect the contact angle measurement. The determined best plasma condition was different for each type of fibre.
- Plasma application causes physical changes in PPF1, GF and BF surfaces. These changes can be classified as micro and nano size surface deformations. According to SEM photographs, for the best plasma condition, further exposure did not contribute to significant differences in the surface morphology of the fibres. Plasma treatment increases the roughness in the micro and nano scale for PPF1 and BF. However, AFM analyses have shown that nano-sized roughening does not follow a certain trend with respect to GF, as the SEM images revealed surface decontaminations of these fibres and nano surface roughness from AFM were reduced after plasma applications.

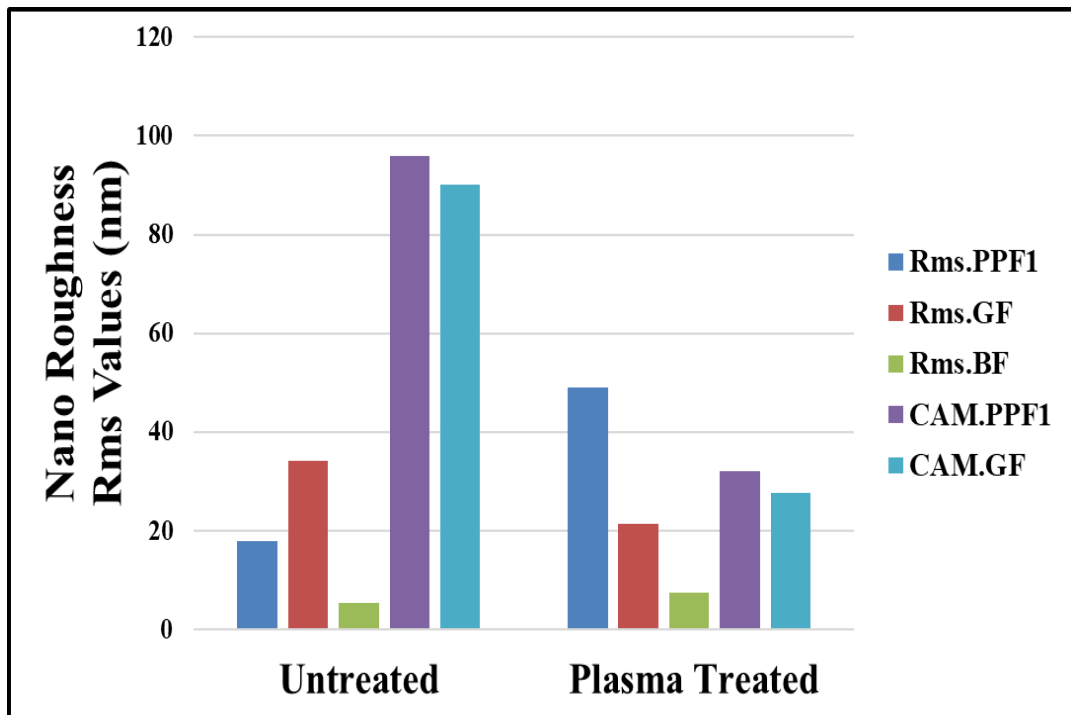


Figure 4-18 Contact Angle and Nano Roughness Comparison of Different Fibres

Figure 4-18 presents a comparison between the CAM and Rms values obtained before and after plasma treatment for PPF1, GF and BF. The CAM values for PPF1 and GF reduced by 66.67% and 69.18% respectively. This could indicate that plasma exposure contributed to fibre surface alterations. Rms values increased by 93.62% and 26.67% for PPF1 and BF respectively. On the other hand, a reduction by 37% was reported for GF. Therefore, unlike CAM, the Rms results did not follow similar trends for PPF1 and GF. This could indicate that plasma exposure provides similar wettability results on the surface of both types of fibres but through different effects. Plasma etching might be predominant for PPF1 and BF, while plasma cleaning occurs for GF. This result is in contrast with the SEM images.

4.5 Mechanical Characterization

4.5.1 Fibre Tensile Test

The most vital mechanical properties of fibres that are used in the production of FRC is the tensile strength. The fibre tensile strength directly influences the post-cracking performance of the FRC. Generally, when the cementitious matrix cracks, the stress distribution moves from the matrix to the fibres. In that circumstance, the higher the fibre tensile strength, the higher the capacity of the composite's residual strength. Therefore, the effect of plasma treatment on the tensile strength of the fibres is a vital aspect.

Tensile strength of single fibres is usually evaluated by monofilament tensile tests. The effect of plasma treatment on the mechanical properties of PPF1, GF and BF was investigated by means of single fibre tensile tests using the method presented in Section 3.4.2.3. The results for each fibre are presented in the following sections.

4.5.1.1 Macro Polypropylene Fibre (PPF1)

To explore the effects of any mechanical damage resulting from plasma treatment of PPF1; single-fibre tensile tests were performed.

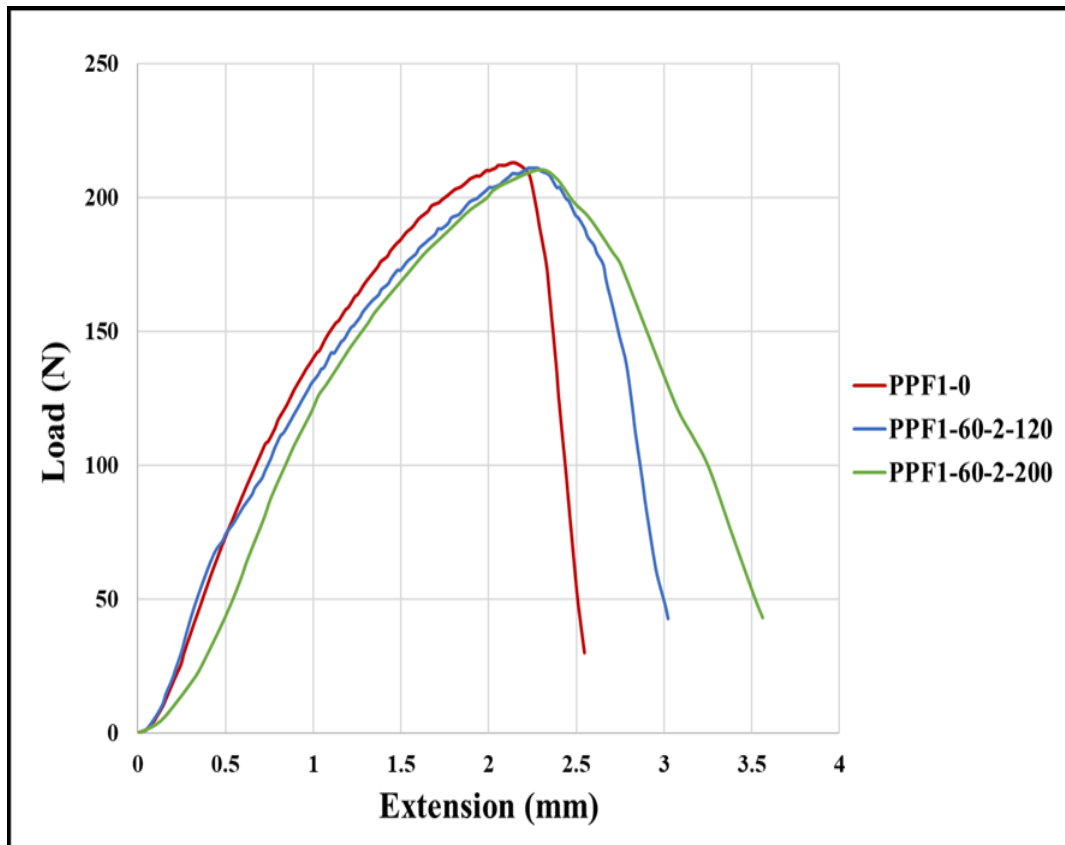


Figure 4-19 PPF1 Load-Extension Graph before and after Plasma Treatments

Figure 4-19 presents the load-extension graphs obtained for the single untreated and treated PPF1. Table 4-3 presents the results of maximum load and tensile strength of the fibres.

Table 4-3 PPF1 Tensile Properties before and after Plasma Treatments

Specimen	Max. Load (N)	Tensile Strength (MPa)
PPF1-0	213	377.66
PPF1-60-2-120	210	372.34
PPF1-60-2-200	210	372.34

From the load-extension graph of a loaded single PPF1, it reaches a complete failure at a maximum load. The corresponding load-extension graph shows that the load increases non-linearly until it reaches the maximum values then decreases dramatically due to the failure of fibres. The load-extension behaviour of the single PPF1 has three distinct regions during loading: elastic region, non-linear failure region and post-peak region. In the elastic region, the PPF1 starts to take the stress, and the load exhibits an increased slope. Before reaching the maximum load (tensile strength), the graph exhibits non-linearity (non-linear failure region). This is probably attributed to random failure of the individual fibres within the bulk of individual PPF1. The last stage, which is a post-peak region, is attributed to a sudden reduction in the load beyond the tensile strength, which is the characteristic of further fibre failure. The load-extension graphs were analysed to measure the maximum tensile load and strength of untreated and treated PPF1.

The tensile strength of untreated PPF1 was found to be 377.66 MPa. When PPF1 exposed to the best plasma conditions at a distance of 60 mm (flow rate 2 l/min, time 120 sec), 60 mm (flow rate 2 l/min, time 200 sec), the tensile strength changed by -10.52%, and -8.82% respectively. This change is relatively minimal and could be attributed to the variation of individual fibre's sizes from the manufacturer or as an effect of plasma treatments. The manufacturing procedure has an abundant impact on the finished properties of the fibre. Extrusion is the commonly used technique for the fibre production. In this technique, temperature is applied to the polymer and then passed over a surface that has multiple holes in it. Followed by the stretching process of the filaments so permanent deformation is introduced onto the fibre surfaces to increase the orientation of the molecular chains (ASTM D2256/ D2256M, 2010). In addition, the cutting process during the fibre production might affect the mechanical

properties of the fibres (ASTM D3822, 2007). Another issue that should be highlighted is that the variable characteristics of the material along its length will affect the mechanical properties of fibres. This may be due to two major aspects: the possibility of having stress concentrations due to the geometrical irregularities and the possibility of weak spots on the fibre's surface across its length (Zohdi and Steigmann, 2002; Zhu et al, 2012).

4.5.1.2 Glass Fibre (GF)

The effect of plasma treatment on the tensile strength of glass fibres was investigated using similar methods to the PPF1.

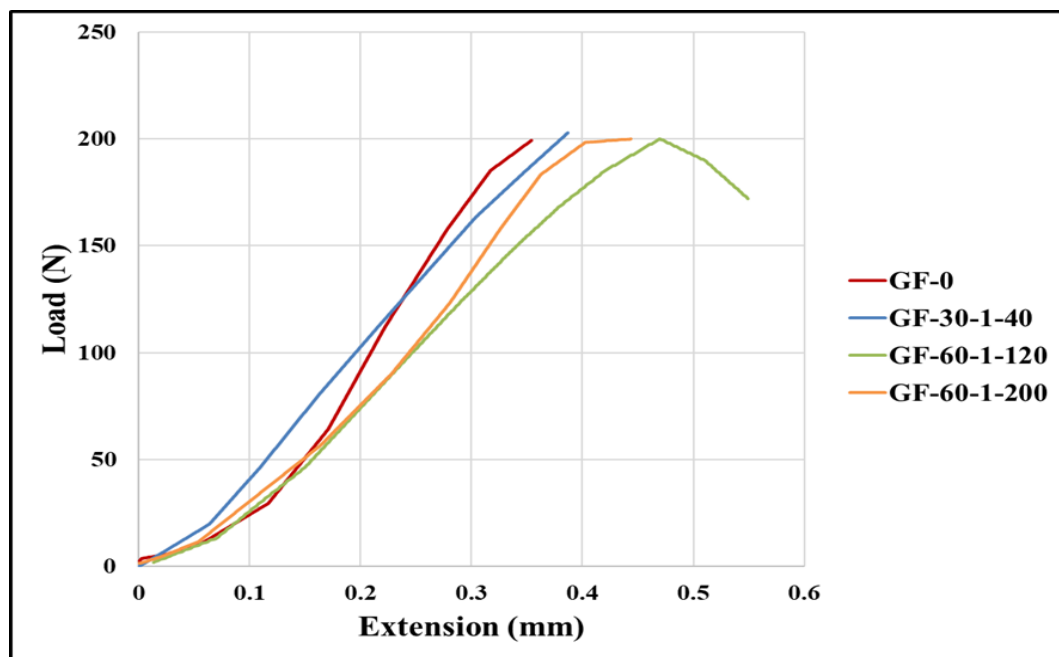


Figure 4-20 GF Load-Extension Graph

Figure 4-20 presents the load-extension relationship of GF before and after plasma treatment. The generated load-extension graph of GF shows non-linear increase in load up to a maximum value which is followed by fibre failure. The load-extension behaviour exhibits three distinct regions during loading: elastic region, non-linear

failure region and post-peak region. In the first region, the GF starts to take the stress until maximum strength is reached, which is characterised by the failure region. The last stage observed in GF, was very short, exhibited in a complete sudden rupture of fibre specimens, and only occurred in few specimens. The load-extension graphs were analysed to measure the maximum tensile load and strength of untreated and treated GF and presented in Table 4-4. The tensile strength of untreated GF was recorded as 761.77 MPa.

Table 4-4 GF Tensile Properties before and after Plasma Treatments

Specimen	Max. Load (N)	Tensile Strength (MPa)
GF-0	199.43	761.77
GF-30-1-40	202.8	774.63
GF-60-1-120	199.5	762.03
GF-60-1-200	200	763.94

After the plasma treatment of GF at distance 30 mm, 60 mm (120 sec) and 60mm (200 sec) the tensile strength changed by +1.674%, +0.034% and +0.28% respectively. This change is minimal and could be attributed to the variation of individual fibre's sizes from the manufacturer or the existence of flaws. Although there is extensive history of GF investigation and development, an essential understanding of the tensile strength properties of GF has not been established (James, Peter and Liu, 2016). As far as the tensile strength of GF is concerned, the effect of flaws must primarily be considered, and it is essential to distinguish between intrinsic and extrinsic flaws and strengths (Otto, 2002). Extrinsic strength is governed by the existence of flaws and their rigorousness. This common expression perhaps states various features, for instance, surface cracks and scratches, devitrified regions or accidental defect formations in the bulk material. On the other hand, intrinsic strength depends mutually on the length and the diameter of tested GF specimens. Although, intrinsic flaws are considered as

structural defects resulting from thermal variation, it is known that the extrinsic flaws determine glass strength, but the effects of the intrinsic flaws on the glass strength are still unclear (Kurkjian et al, 2003).

4.5.1.3 Basalt Fibre (BF)

The effect of plasma treatment on the tensile strength of basalt fibre were investigated using similar methods to the PPF1 and GF.

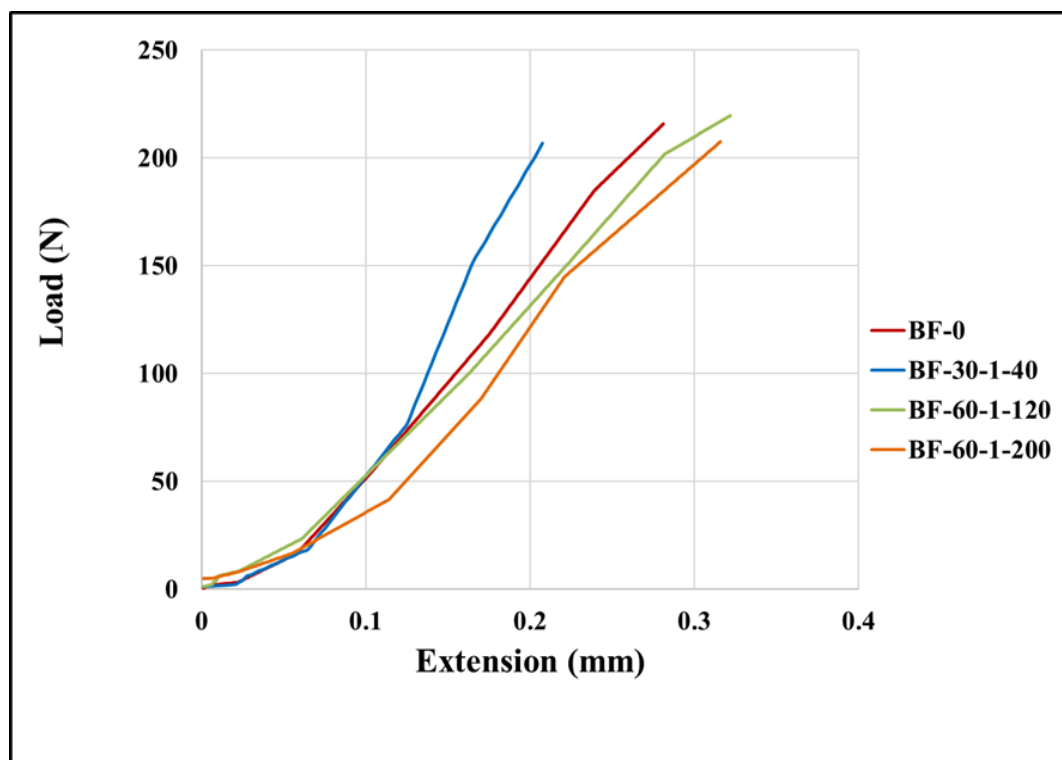


Figure 4-21 BF Load-Extension Graph

Figure 4-21 shows the tensile load-extension relationship of BF before and after exposure to the best plasma conditions. The obtained load-extension graph of BF exhibits a non-linear increase in load up to maximum value is reached followed by fibre failure. The load-extension characteristic shows two distinct regions throughout loading: an elastic region and a non-linear failure region. In the first region, the BF

starts to take the stress until the maximum strength is attained, which is characterised by the final failure region where complete rupture of fibre occurred. The load-extension graphs were analysed to measure the maximum tensile load and strength of untreated and treated GF and presented in Table 4-5. The tensile strength of untreated BF was 675.052 MPa. The plasma conditions for BF were selected to match the best plasma conditions determined for GF. This is due to the relatively close melting point of GF and BF. After plasma treatment at distance 30 mm, 60 mm (120 sec) and 60 mm (200 sec), the changes in tensile strength were -4.26%, +1.62% and -3.92% respectively. This change is relatively small compared to the huge size variation of each individual bulk of fibres.

Table 4-5 BF Tensile Properties before and after Plasma Treatments

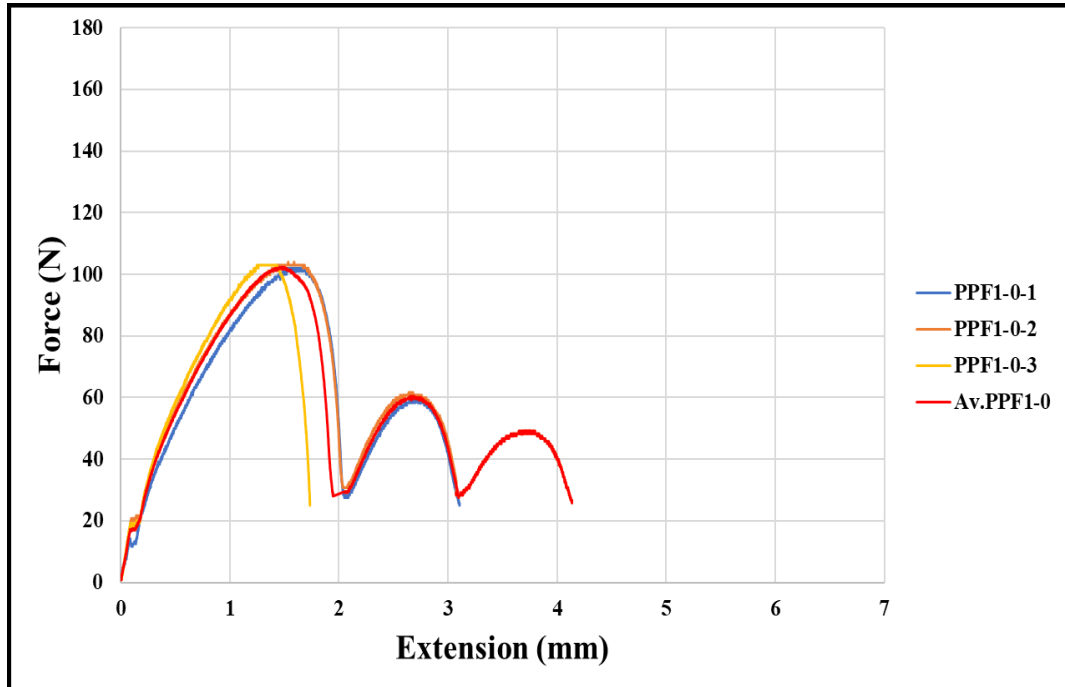
Specimen	Max. Load (N)	Tensile Strength (MPa)
BF-0	216.16	675.052
BF-30-1-40	207	646.875
BF-60-1-120	219.56	686.125
BF-60-1-200	207.7083	649.088

4.5.2 Single Fibre Pull-Out Test

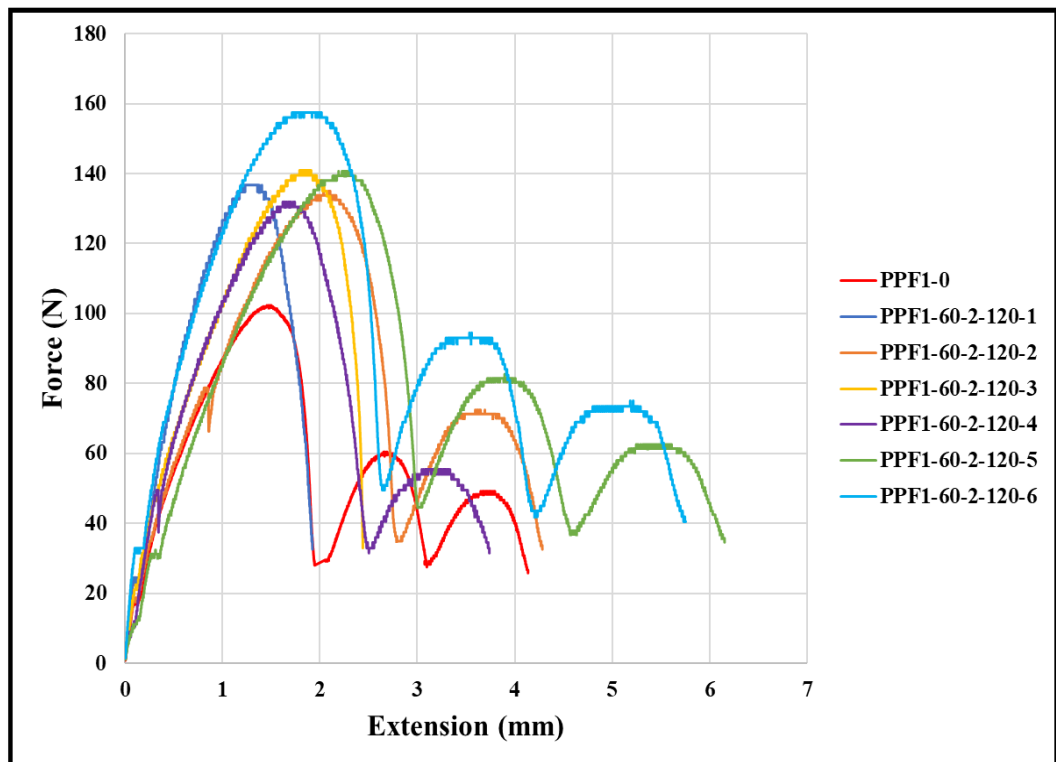
The data from individual pull-out tests were firstly prepared to complete the practical force versus extension. Only three specimens for untreated fibres were prepared, whereas, six identical specimens were prepared for each plasma condition for the purpose of reliability. In each section, the single fibre pull-out behaviour of each different type of fibres is described separately. In this section, the optimum plasma treatment was determined.

4.5.2.1 Macro Polypropylene Fibre (PPF1)

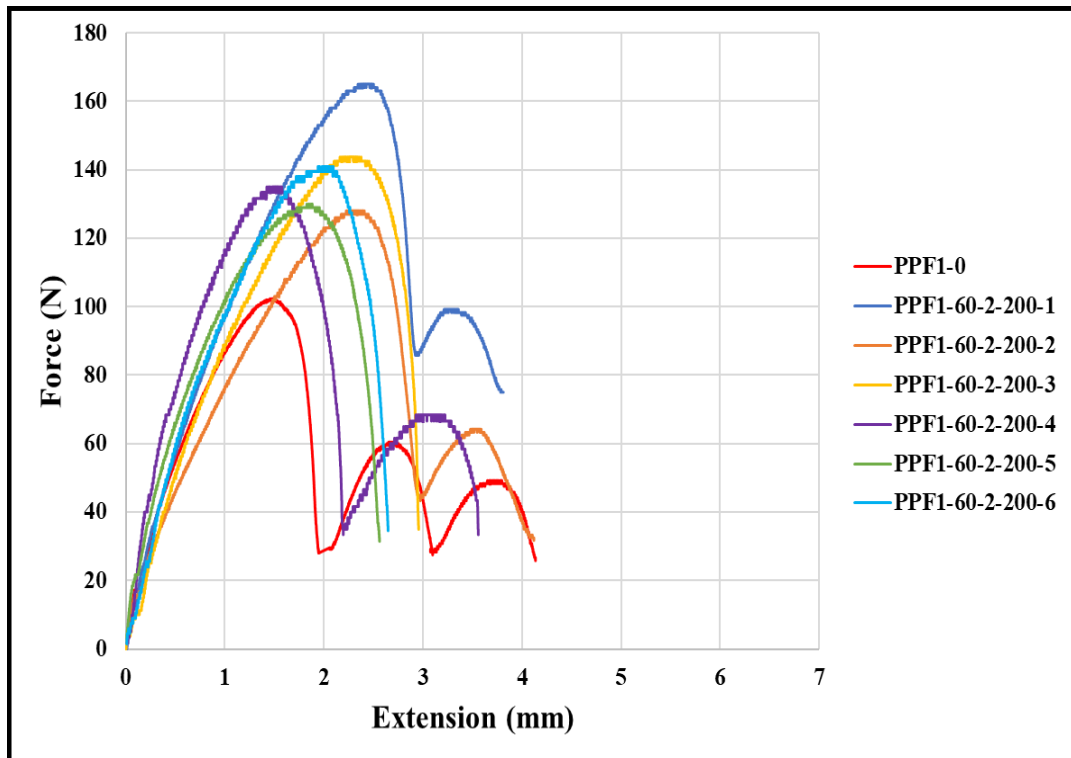
The pull-out test was performed on PPF1 following the methods presented in Section 3.4.2.1.



(a)



(b)



(c)

Figure 4-22 PPF1 Pull-Out Force-Extension Graph: (a) PPF1-0, (b) PPF1-60-2-120 and (c) PPF1-60-2-200

The pull-out graphs of treated and untreated PPF1 have a similar trend as shown in Figure 4-22. In the beginning there is a fibre extension period (linear region), followed by a debonding period between fibre and matrix (non-linear region). This debonding development ends when maximum force is reached. Then, several peaks followed due to the frictional resistance between the fibre and the cement matrix. Furthermore, the energy absorption (area under the force-extension curve) is greater in the case of plasma treated fibres. This indicates that the plasma treated PPF1 demonstrates enhanced bond characteristics. On the other hand, the maximum force for the untreated PPF1 occurs at an extension of less than 1.5 mm, whilst in the case of treated PPF1 this takes place after 2 mm. However, in the case of plasma treated specimens, some

scattering is observed. Three explanations can be assumed for this scatter. Initially, the lack of precise technique to ensure the equal measurement of the embedded length of all specimens. Secondly, despite the use of reasonably high-test speed that reached 1 mm/min, the experiment process, took a few minutes (1.5 – 6.5 min) to be accomplished. Therefore, it can be concluded that during this period of time, the PPF1 was subjected to substantial creep deformation (Vrijdaghs, Prisco and Vandewalle, 2017). This creep is different for identical fibres due to the relatively high variation in fibres selected from the similar batch. Thirdly, the variation in the pull-out results could be due to the variation in ambient temperature, humidity and the flow of air during the experiments which have affected the concentration of plasma species on the fibre surface.

From the pull-out graphs, the average maximum pull-out load and average IFSS are presented in Table 4-6.

Table 4-6 Maximum Force and Interfacial Shear Strength for Untreated and Plasma Treated PPF1

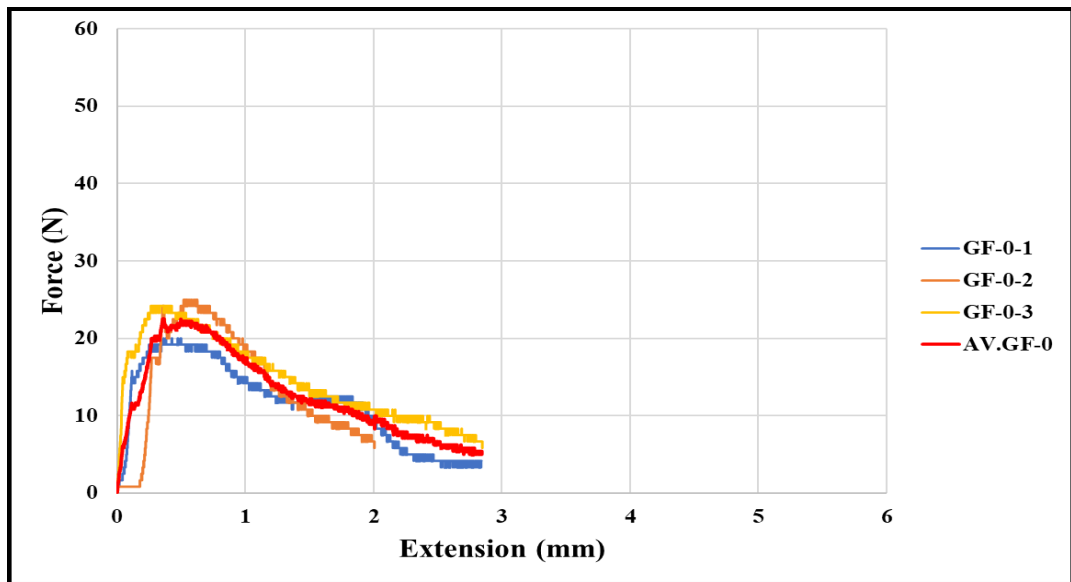
Fibre Code	Treatment Duration (sec)	F_{max} (N)	τ_{IFSS}(MPa)
PPF1-0	N/A	101.6	0.65
PPF1-60-2-120	120	139.7	0.89
PPF1-60-2-200	200	140.53	0.885

A significant increase of the τ_{IFSS} was observed in the treated PPF1. The τ_{IFSS} increased from 0.65 to 0.89 MPa, representing around a 31.17% improvement. The improvement of the interfacial properties was possibly because of the increased surface wettability and increased surface area of the plasma treated PPF1. This can be confirmed in the CAM investigated in section 4.4.1.1 and images taken from the SEM in section 4.4.2.1 which present the small cracking developed on the surface of treated PPF1 that resulted in enhancing the fibre-cement interlocking phenomenon. From the

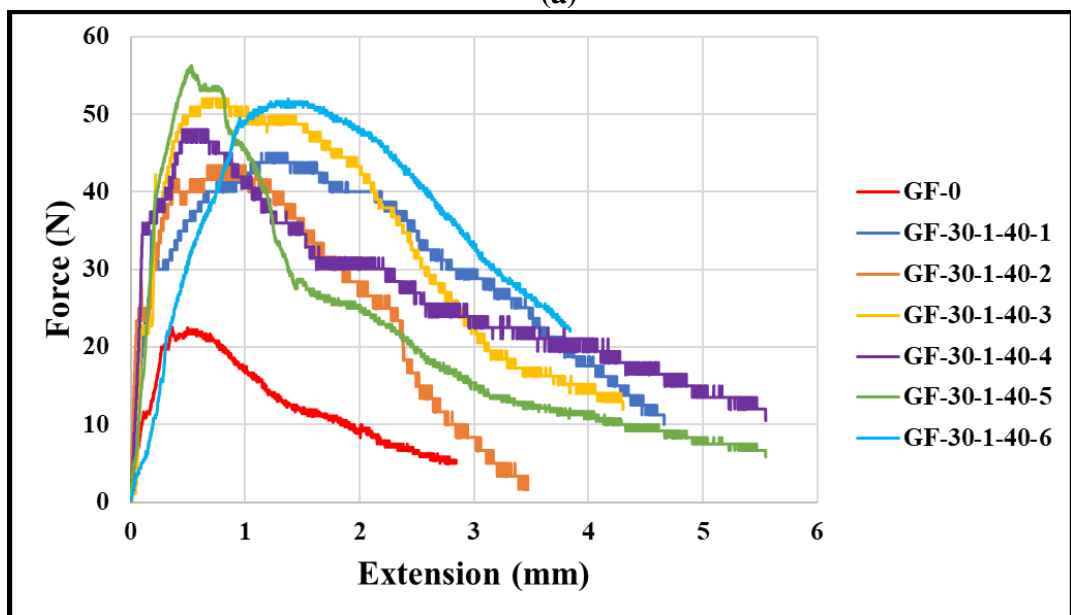
results, it was concluded that the optimum plasma treatment for PPF1 is at the distance of 60 mm, flow rate 2 l/min and the duration of 120 sec (PPF1-60-2-120). Therefore, this plasma condition was used for investigating the bending performance of plasma treated PPF1 in section 4.5.3.2.

4.5.2.2 Glass Fibre (GF)

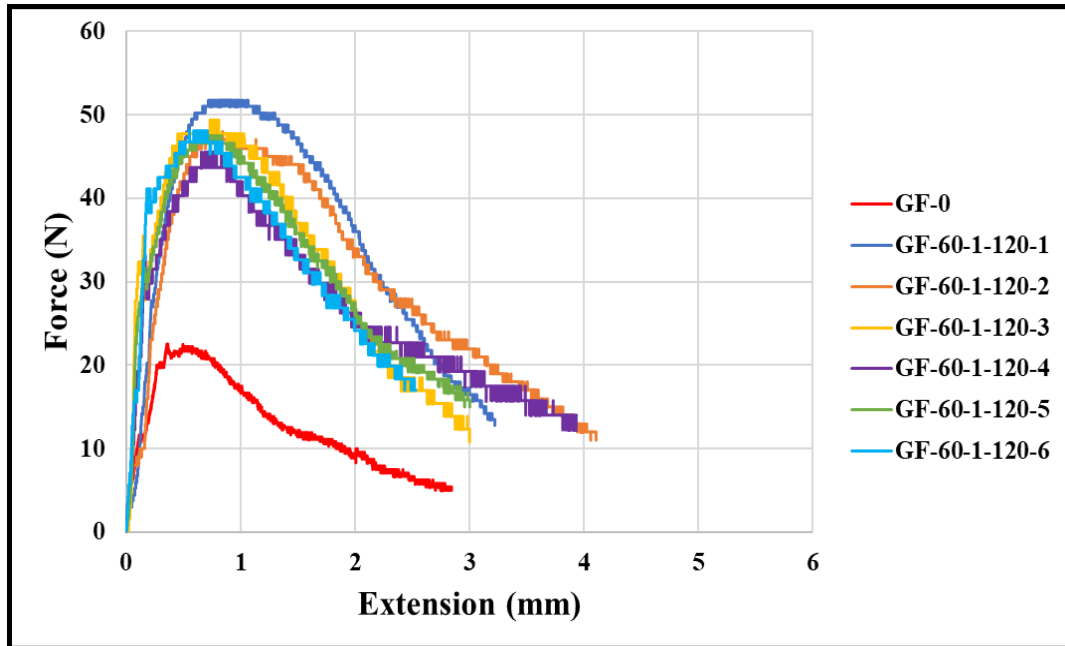
The pull-out test was performed on GF following the method presented in chapter 3 section 3.4.2.1.



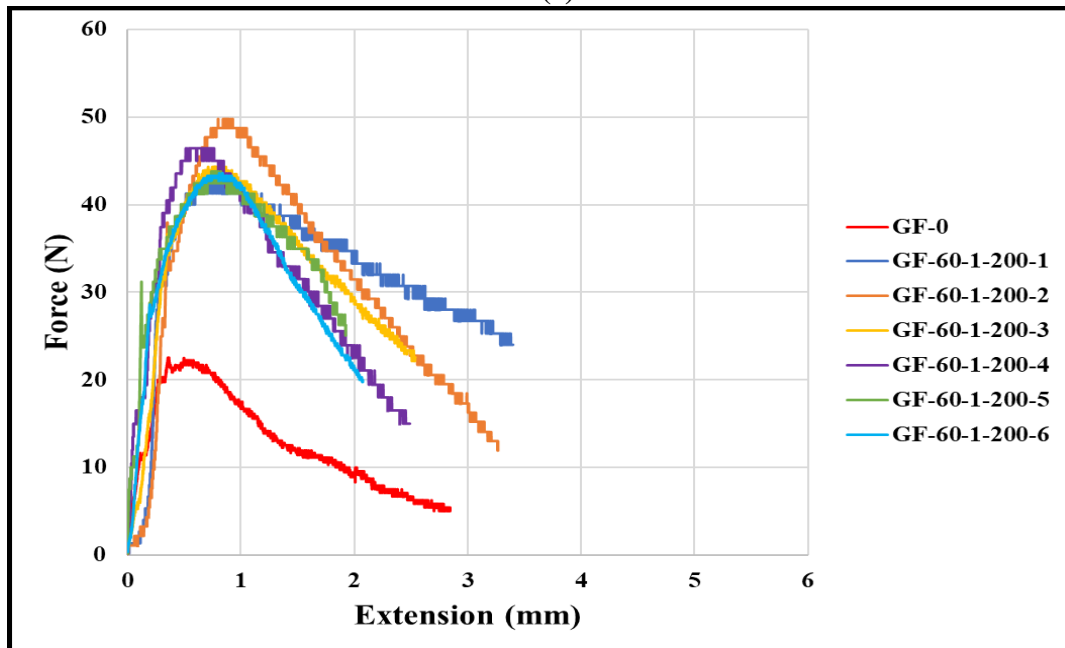
(a)



(b)



(c)



(d)

Figure 4-23 GF Pull-Out Force-Extension Graph: (a) GF-0, (b) GF-30-1-40, (c) GF-60-1-120 and (d) GF-60-1-200

Figure 4-23 presents the pull-out force-extension behaviour of the untreated and plasma treated GF. From the pull-out load-extension graph, three separate zones can be observed. The first zone can be characterized as a debonding zone, when the debonding process occurs along the fibre-cement interface. Complete fibre-cement

debonding occurs when the maximum force is reached. Afterwards, a sudden drop in the force occurred and the second zone is formed. Finally, the friction force between the fibre and the cement matrix promote the resistance to the fibre pull-out. From the pull-out load- extension graphs, the average F_{max} and average τ_{IFSS} are also calculated for untreated and plasma treated GF specimens and presented in Table 4-7.

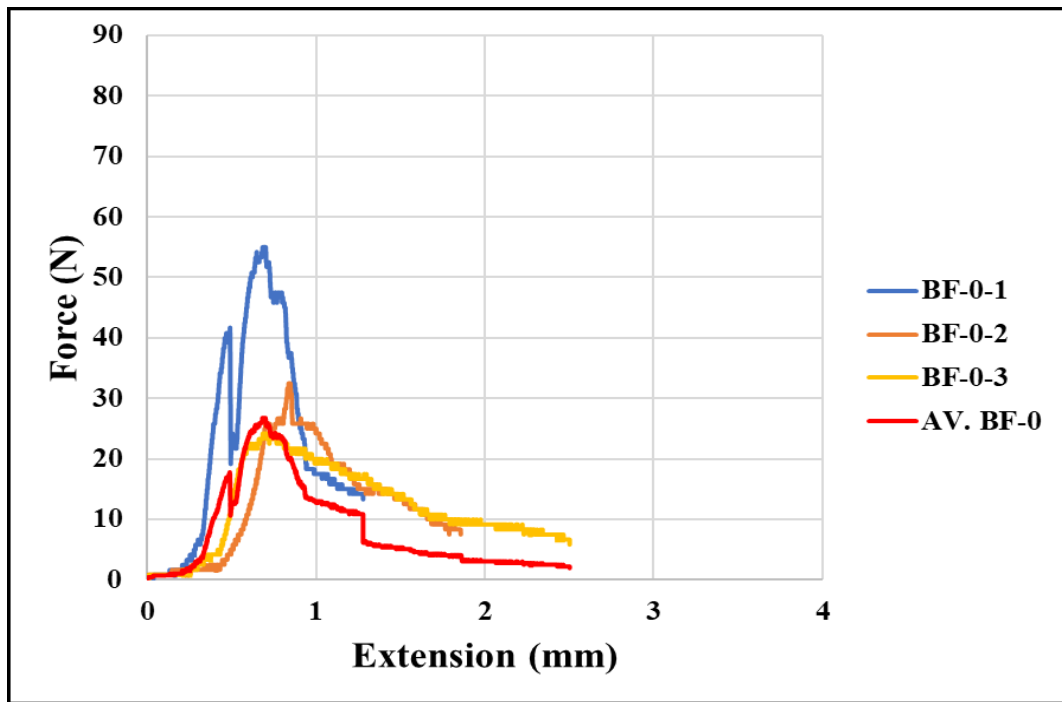
Table 4-7 Maximum Force and Interfacial Shear Strength for Untreated and Plasma Treated GF

Fibre Code	Treatment Duration (sec)	F_{max} (N)	τ_{IFSS} (MPa)
GF-0	N/A	21.7	0.24
GF-30-1-40	40	48.38	0.54
GF-60-1-120	120	47.73	0.53
GF-60-1-200	200	44.7	0.5

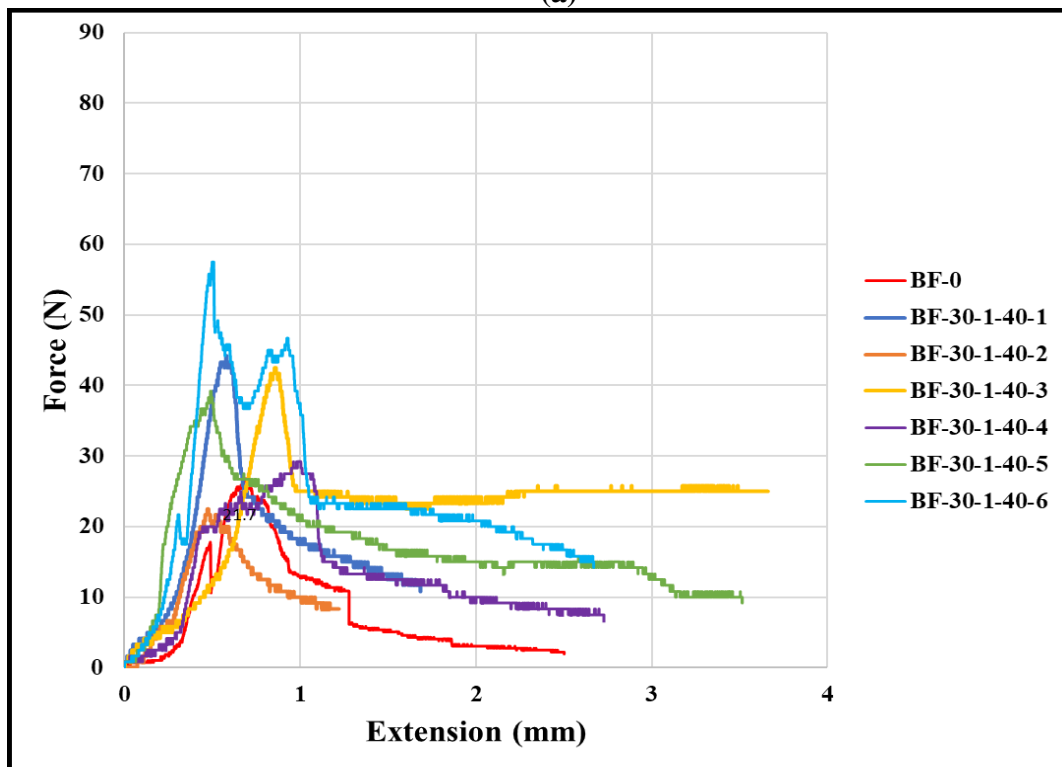
It can be observed that there is a factor exceeding 2 for the F_{max} and τ_{IFSS} between untreated and plasma treated fibres. The τ_{IFSS} figures represent an improvement by 76.92%, 75.32% and 70.27% for GF-30-1-40, GF-60-1-120 and GF-60-1-200 respectively. The improvement of the interfacial properties was possibly because of the increased surface wettability and the removal of the weak boundaries on the surface of GF. This can be confirmed in the CAM investigated in section 4.4.1.2 and images taken from the SEM in section 4.4.2.2 which presents the decontamination of the surface of the GF that resulted in enhancing the fibre-cement adhesion. From the results, it was concluded that the optimum plasma treatment for GF is at a distance of 10 mm, a flow rate of 1 l/min and a duration of 40 sec (GF-30-1-40). Therefore, this plasma condition was used for investigating the bending performance of plasma treated GF in section 4.5.3.3.

4.5.2.3 Basalt Fibre (BF)

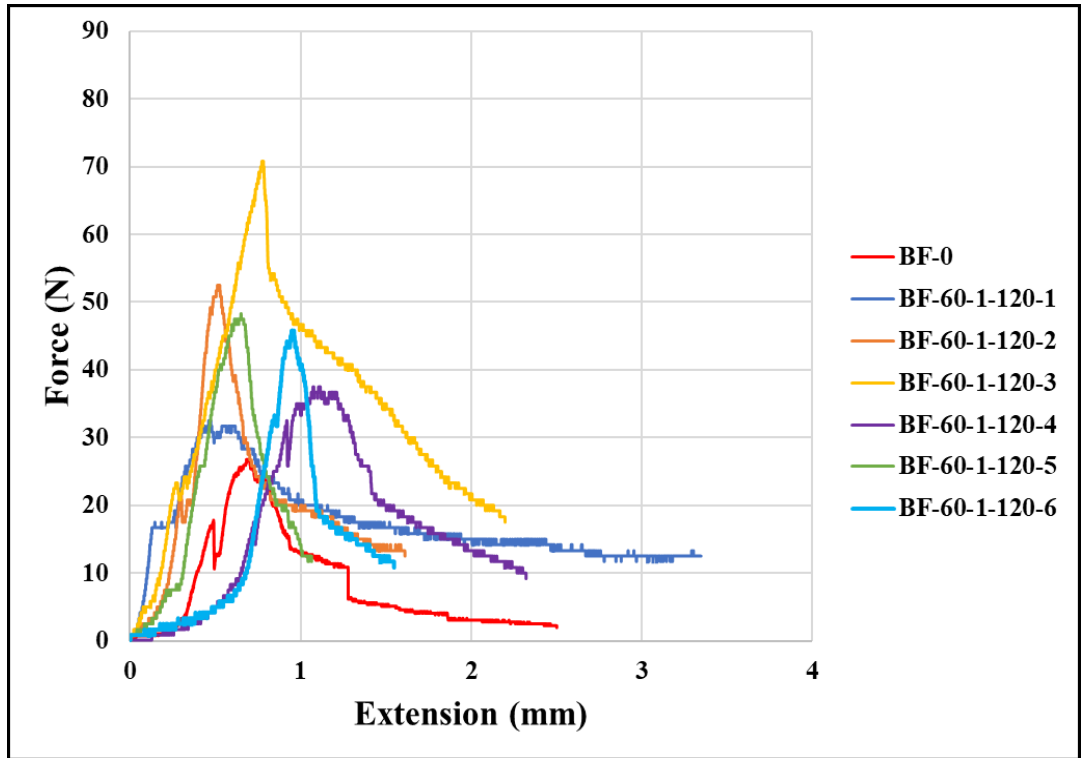
A pull-out test on BF was all conducted using the method presented in Section 3.4.2.1.



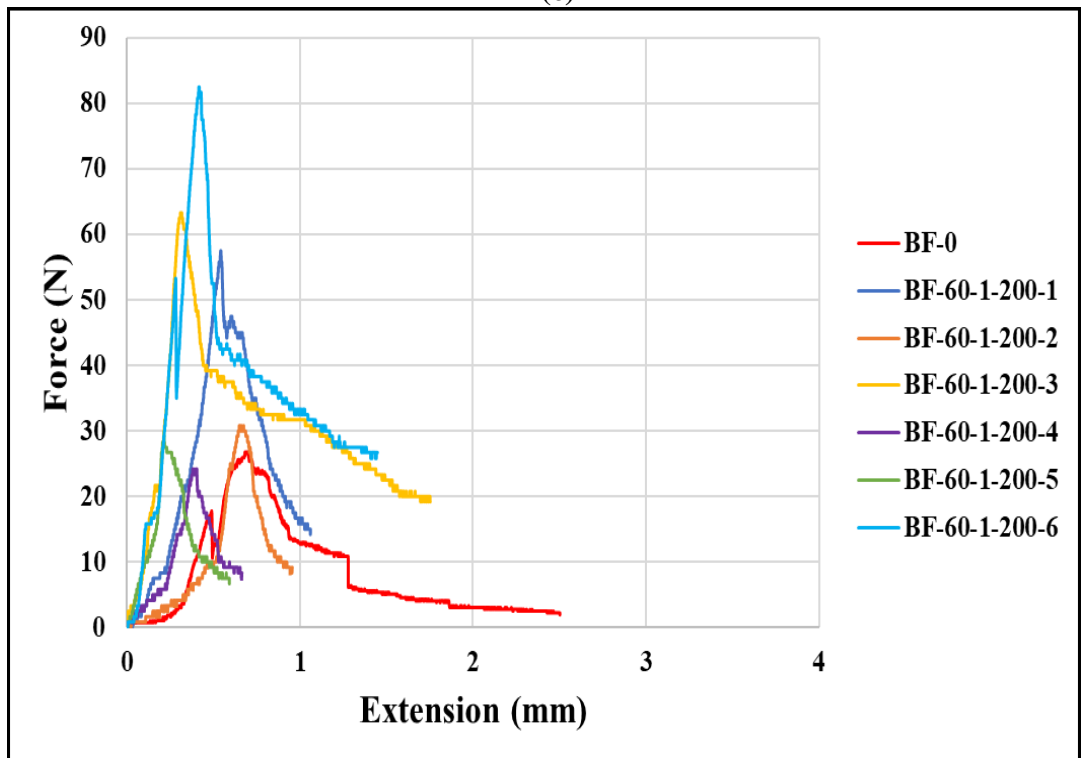
(a)



(b)



(c)



(d)

Figure 4-24 BF Pull-Out Force-Extension Graph: (a) BF-0, (b) BF-30-1-40, (c) BF-60-1-120 and (d) BF-60-1-200

The pull-out response of BF varies considerably in maximum load and energy absorption as shown in Figure 4-24. This scattering of results can be related to the variability in the size of fibre bundle, which caused inaccuracies in the cross-sectional measurement, and the difference in strength of the fibre bundles. From the BF pull-out force-extension graphs it appears that the pull-out behaviour is constituted through a combination of two different mechanisms. The first mechanism involves the debonding of the embedded portion of the fibre completely. Followed by fibre pull-out under the frictional resistance between the fibre and the cement matrix. The higher the F_{max} , the stronger the fibre-cement bond.

From the pull-out load- extension graphs, the average F_{max} and average τ_{IFSS} are also calculated for untreated and plasma treated BF specimens and presented in Table 4-8.

Table 4-8 Maximum Force and Interfacial Shear Strength for Untreated and Plasma Treated BF

Fibre Code	Treatment Duration (sec)	F_{max} (N)	τ_{IFSS} (MPa)
BF-0	N/A	36.94	0.27
BF-30-1-40	40	38.61	0.281
BF-60-1-120	120	46.68	0.34
BF-60-1-200	200	46.54	0.33

The τ_{IFSS} figures represent an improvement by 3.99%, 22.95% and 20% for BF-30-1-40, BF-60-1-120 and BF-60-1-200 respectively. The improvement of the interfacial properties was possibly because of the increased surface area of the plasma treated BF. This can be confirmed in the images taken from the SEM in section 4.4.2.3 which presents the small lumps developed on the surface of the treated BF that resulted in enhancing the fibre-cement interlocking phenomenon. From the results, it was concluded that the optimum plasma treatment for BF occurs at a distance of 60 mm, for a flow rate of 1 l/min and a duration of 120 sec (PPF1-60-1-120). Therefore, this

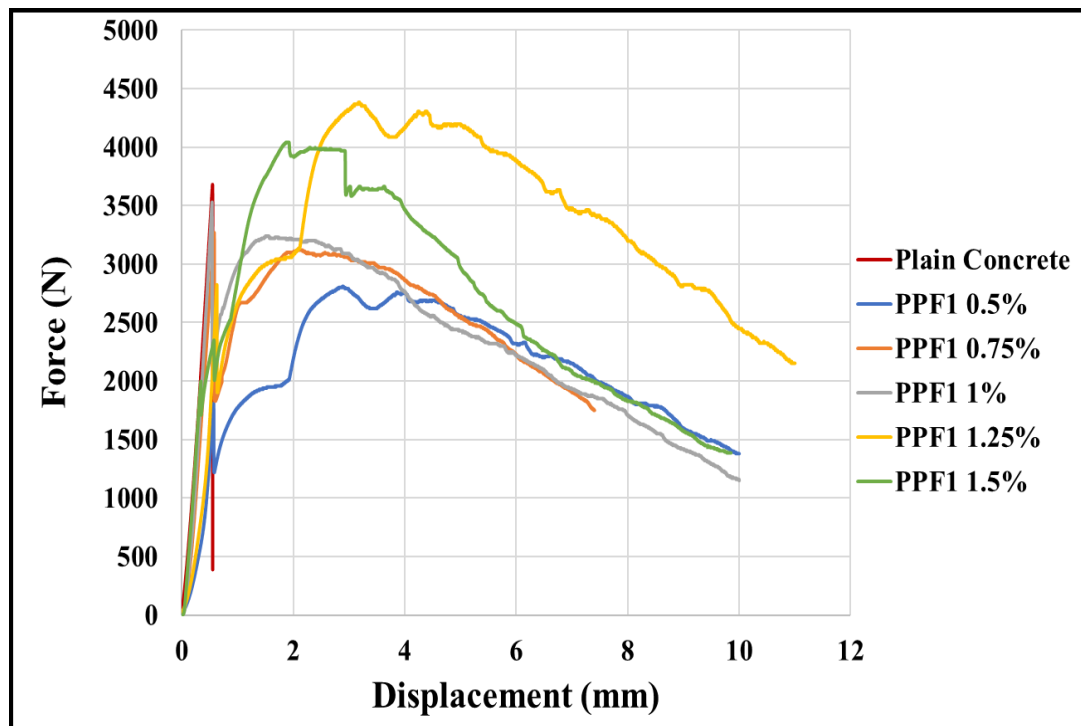
plasma condition was used for investigating the bending performance of plasma treated BF in Section 4.5.3.3.

4.5.3 Flexural Test of Fibrous Composites

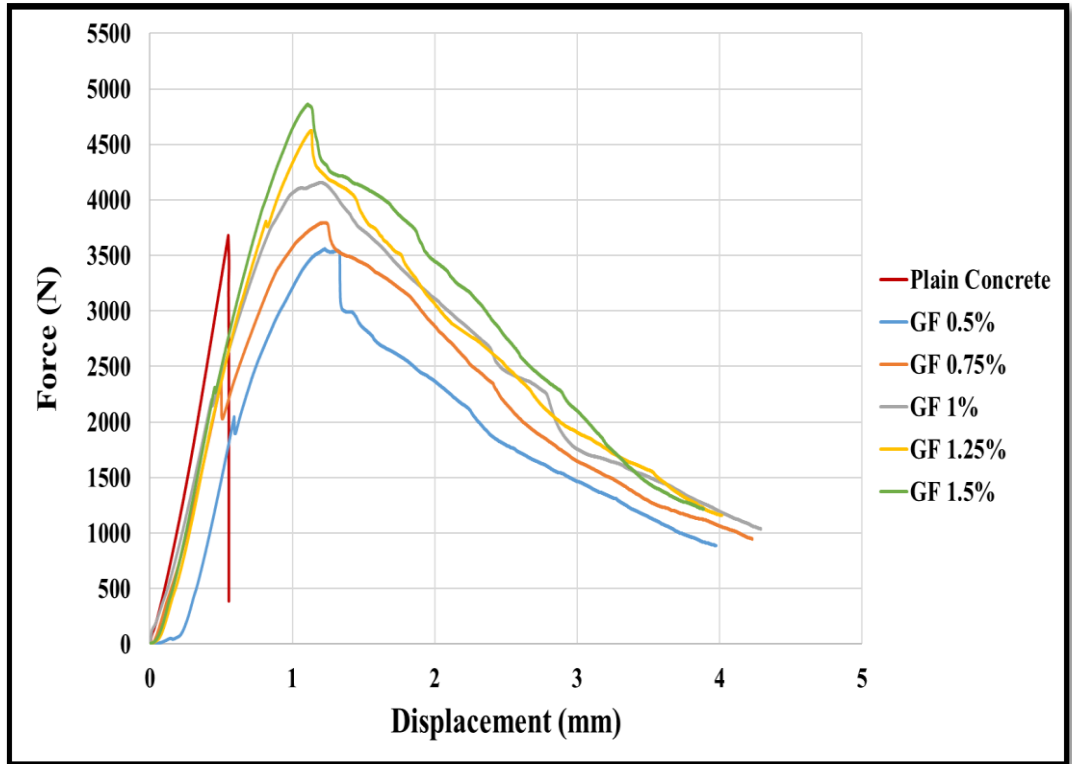
Prior to the investigation of the effect of plasma treatment on the performance of FRCC. The volume ratio of each different type of fibres will be optimised. Then, the bending performances for untreated and treated PPF1, GF and BF will be examined separately. The test results of 28-day specimens and the crack photographs are presented. Furthermore, the characteristic load-deflection curves of the composites are given for each fibre type and plasma treatment condition, the discussions will be carried out using the data from the characteristic load-deflection curve.

4.5.3.1 Fibre volume optimisation

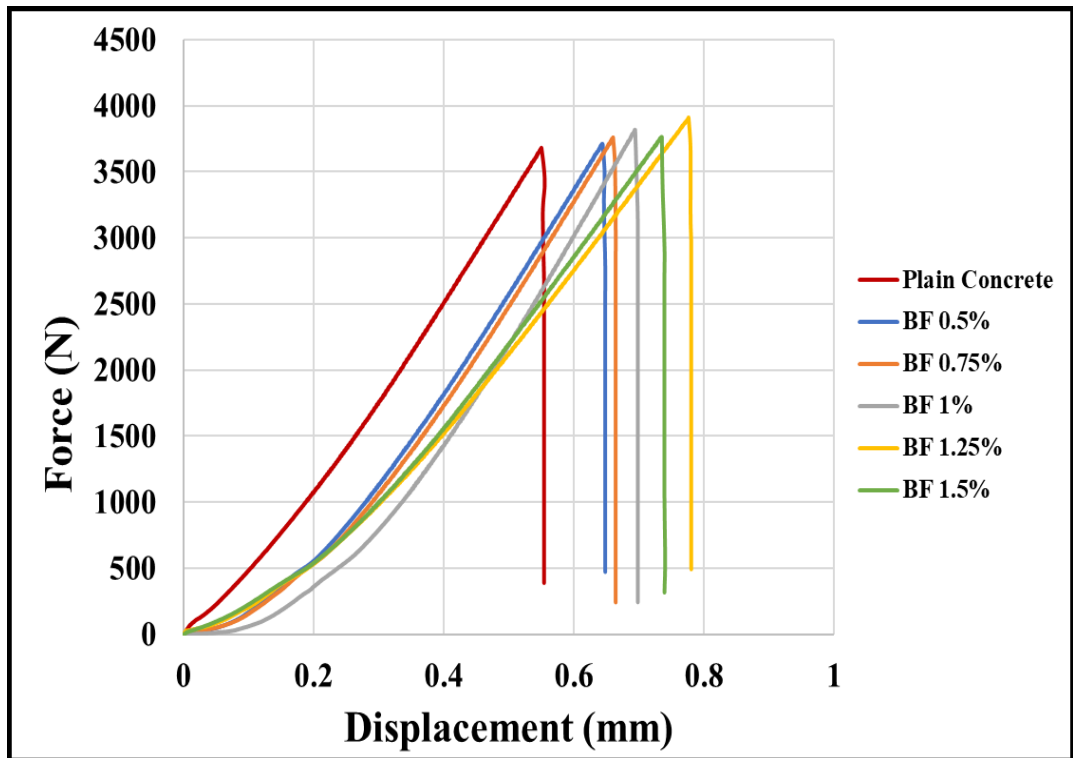
Fibre volume optimisations for all the three types of fibres were performed using the methods presented in Section 3.4.2.2.



(a)



(b)



(c)

Figure 4-25 The Effects of Different Fibre Percentage on the Force-Deflection Curves in: (a) PPF1, (b) GF and (c) BF

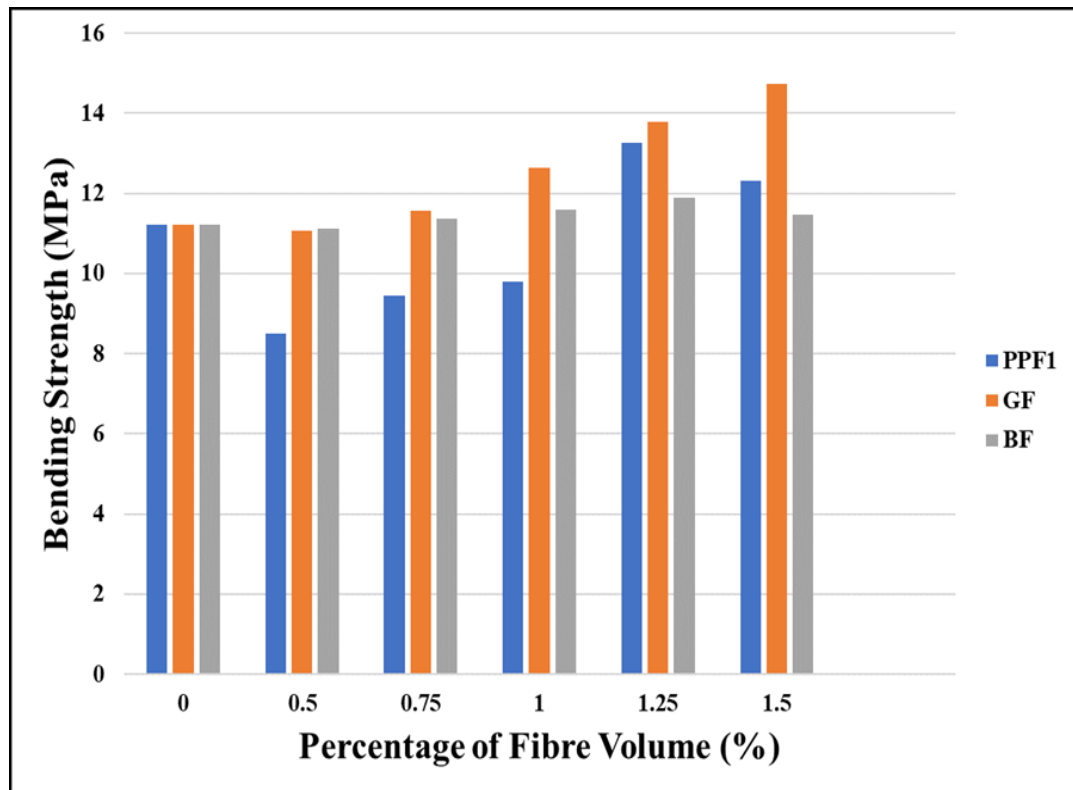


Figure 4-26 Bending Strength of Fibrous Composites: (a) PPF1, (b) GF and (c) BF

The load-deflection curves obtained from samples prepared using three different percentage of fibres are given separately for each fibre type and dosage in Figure 4-25. The 28 days bending strengths of each mixture were calculated using equation (3.11) (page 95) and presented in Figure 4-26. Examination of the obtained load-deflection curves show that each matrix-fibre combination has its own unique structure. When the composites prepared without fibres reach the highest bending load, they lose load carrying capacities after the first crack. Although, in some cases, the bending strength values of fibre-free micro concretes are similar to or even higher than those of some fibrous micro concretes, the ability to absorb energy post cracking are extremely low compared to all the fibrous series.

When the overall performance of the fibrous composites is examined, it has been found that for a fibre dosage exceeding 1%, both the composite bending strength and ability to absorb energy significantly increase.

Comparing the composites prepared with PPF1, GF and BF, relatively different load-deflection curves are obtained. In the PPF1 composite, when low fibre volume fraction 0.5-1 % was used, a sudden load drop is observed mostly after the first crack as in Figure 4-25(a). Depending on the fibre volume, the amount of sudden load drop can vary. The fibres in the cracks, which are exposed at the time of this decline, continue to carry the load by acting as a bridge and arresting the crack, thus the deflection is increased. According to the fibre dosage, if the number of fibres in the cross section of the crack is too large, the fibres in the opened crack can carry higher loads than the first crack load. On the other hand, the composites prepared with GF, did not undergo a sudden drop in load carrying capacity after the first crack. The composites showed significant improvements in term of bending strength and post cracking energy absorption capacity even when the amount of fibres added did not reach 1% as shown in Figure 4-25(b).

BF fibres are unlike PPF1 and GF; they come as a bundle of very thin filaments. When the composites using BF were examined, it was determined that adding the fibre does not have significant effects in terms of the strength and the post crack energy absorption capacity of the composite after the occurrence of the first crack, Figure 4-25(c). Thus, BF fibres did not improve post-cracking properties. The fibres did not bridge the cracks during testing. The failure of BF specimens was in the similar brittle manner of the unreinforced concrete.



Figure 4-27 Failure of Composites Prepared with BF

When the cracked section after failure was examined and shown in Figure 4-27, it was observed that the first crack causes the break off without too much pulling. The addition of BF to the composite did not improve the cracking performance. Although, slight improvement in deflection and bending strength values were observed as the volume fraction of BF exceeded 1%, the post cracking behaviour was not improved compared to composites prepared with PPF1 and GF.

Under the conditions investigated, in general, long and thick diameter fibres (PPF1 and GF) are more numerous than short and thin bundled fibres (BF) with post cracking behaviour.

As a result of the above investigations, the suitable fibre volume fraction for each different type of fibre that will be subjected to plasma treatment has been determined. The fibre dosages were found to be 1.25% by volume for PPF1, 1.5% for GF and 1.25% for BF.

4.5.3.2 28 Days Bending Performance of Plasma Treated PPF1 Composites

The bending behaviour tests of a composite prepared with plasma treated PPF1 were performed using a similar method used for fibre volume optimisation. The method is presented in Section 3.4.2.2.

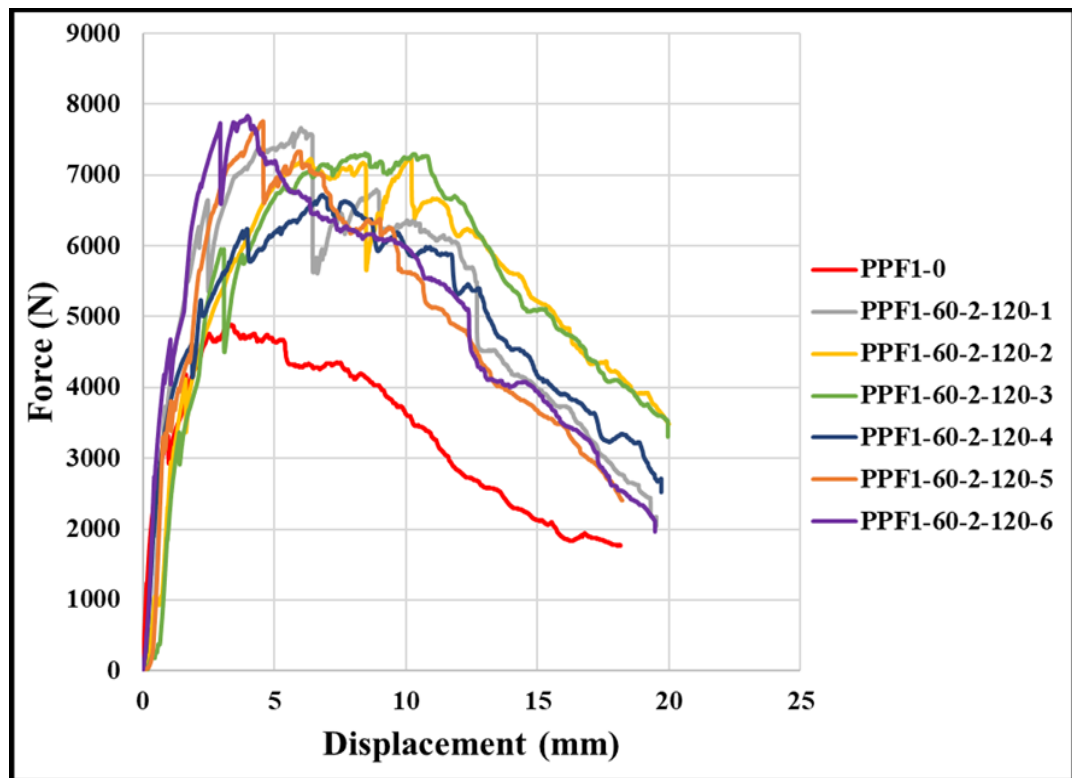


Figure 4-28 The 28 Days Force-Deflection Graphs of PPF1 Treated with Optimum Plasma Condition

The 28-day characteristic load-deflection curves for untreated and optimum plasma treated PPF1 composites are presented in Figure 4-28.

Plasma application caused the upward rise in the load-deflection curves. First crack strengths and flexural strengths increased significantly. Also, flexural strength and deflection at maximum load increased remarkably. These results demonstrate that the adherence between the 28-day matrix and the PPF1 fibres is increased by several

orders of magnitude with plasma application. The increase in the adherence can basically be attributed to two factors:

1. As the water-repellent (hydrophobic) surfaces of PPF1 fibres are made hydrophilic, the fibre and the matrix become closer to each other at the micro scale in the fresh state, so that the porosity in the contact region between fibre and the matrix is reduced. It is also thought that the matrix in this region has a better adherence to the fibres due to an increase in physical adherence. Therefore, it might be that over time hydration develops better on hydrophilic fibre surfaces. Thus, the adherence increase over time will be better than for the untreated PPF1, as the number of voids needed to fill the hydration product at the resulting interface will decrease.

2. The roughness and grooves of the surface of the fibres on the microscale surface can be considered as another physical adherence enhancer when a suitable plasma condition is used.

In Table 4-9, the initial crack deflection, first cracking strength, deflection at maximum load, bending strength, prepared with the help of the data read through the graphs, are presented.

Table 4-9 The 28 Days Flexural Test Results of PPF1 Reinforced Cementitious Specimens

PPF1 28 Days	First cracking strength (MPa)	Deflection at first cracking load (mm)	Flexural strength at max. load (MPa)	Deflection at maximum load (mm)
PPF1-0	9.21	0.928	13.70	3.423
PPF1-60-2-120-1	10.56	0.874	21.30	6.35
PPF1-60-2-120-2	11.51	1.613	20.32	10.152
PPF1-60-2-120-3	9.25	1.363	20.32	10.467
PPF1-60-2-120-4	12.78	1.758	18.77	6.93
PPF1-60-2-120-5	10.71	1.069	21.68	4.583
PPF1-60-2-120-6	12.94	1.01	22.01	4.01

Significant increases in the first crack strengths and bending strength is observed. When the optimum plasma conditions were applied, the average bending strength value for six identical specimens increased from 13.70 MPa to 20.74 MPa.

The behaviour of the untreated PPF1 composites is normally in the form of a sudden load drop after the first crack and then friction of the fibres bridging the load in the crack opening. The first crack opening in a region near the mid-point where the bending moment is greatest is constantly opened and the collapse mechanism is completed. However, in the plasma treated specimens, the load drop level after the first crack decreased and the bridging potentials of the fibres in the opened cracks increased. In some cases, second and third cracks were observed. In this case, the contribution of the fibres in the different cross sections of the new cracks to the load bridging increases both.



(a) PPF1-60-2-120-1



(b) PPF1-60-2-120-2



(c) PPF1-60-2-120-3



(d) PPF1-60-2-120-4



(e) PPF1-60-2-120-5



(f) PPF1-60-2-120-6

Figure 4-29 Multiple Crack Formation in Case of Optimum Plasma Condition of PPF1

Figure 4-29 shows cracks in the fibrous composite treated with a flow rate of 2l/min, at a distance of 60mm and a treatment duration of 120 seconds using argon plasma. Plasma application revealed the possibility of multiple crack formation in 28-day samples. Multiple cracking behaviour can be observed in all the tested specimens.

4.5.3.3 28 Days Bending Performance of Plasma Treated GF Fibre Composites

The bending behaviour test of a composite prepared with plasma treated GF was conducted using the method presented Section 3.4.2.2.

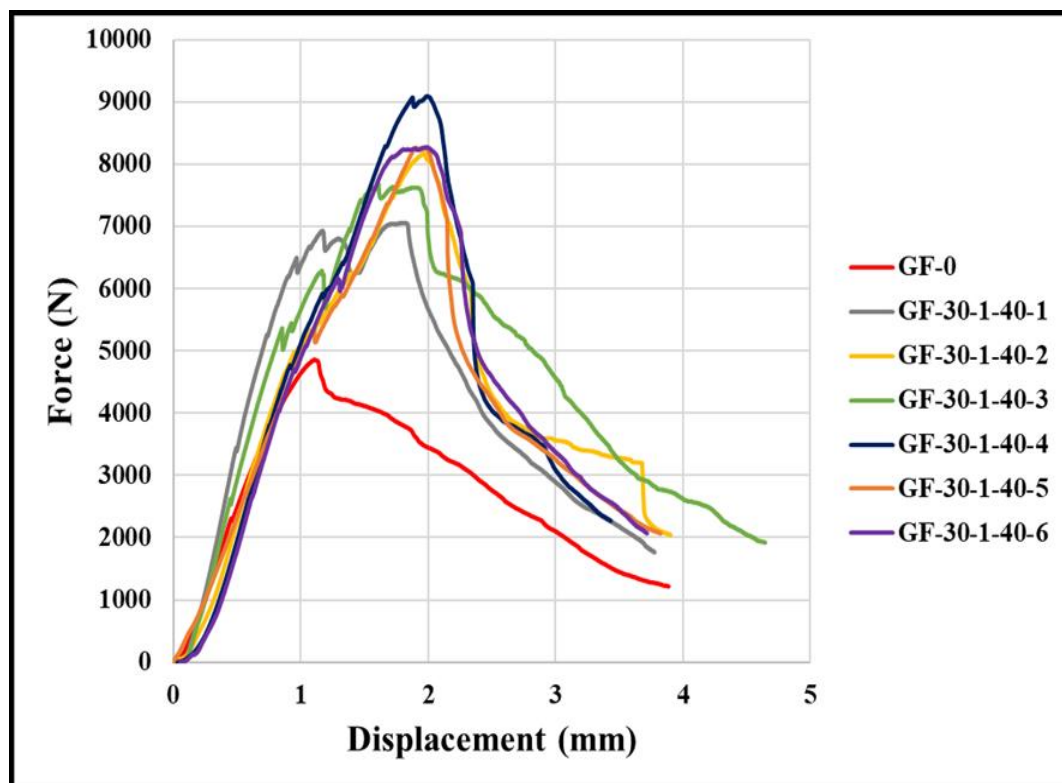


Figure 4-30 The 28 Days Flexural Test Results of GF Reinforced Cementitious Specimens

For the optimum plasma condition, the 28-day characteristic load-deflection curves for GF obtained are presented in Figure 4-30. It can be observed that the plasma shifts the force-deflection graphs upwards. However, from the graphs, it is difficult to notice the first crack for specimens GF-30-1-40-2 and GF-3-1-40-4. In untreated GF and GF-

30-1-40-5 and GF-30-1-40-6 specimens, the load drop values at the first crack were very small. These specimens were made to come to a single crack. However, in specimens GF-30-1-40-1 and GF-30-1-40-3 at the later stages of the testing process, another crack was observed could indicate the changes in the fibre surface structure, and thus the fibre-matrix interface properties, or it could be attributed to the distribution of fibres during the mixing process. In general, it can be said that plasma applications changed the adherence behaviour of the GF fibres with the matrix positively.

In Table 4-10 the mechanical flexural performance values of specimens are compared and presented, it is seen that the average bending strength is increased by plasma application from 13.567 MPa to 22.67 MPa.

Table 4-10 The 28 Days Flexural Test Results of GF Reinforced Cementitious Specimens

PPF 28 Days	First cracking strength (MPa)	Deflection at first cracking load (mm)	Flexural strength at max. load (MPa)	Deflection at maximum load (mm)
GF-0	6.39	0.458	13.567	1.136
GF-30-1-40-1	18.126	0.969	19.845	1.793
GF-30-1-40-2	-	-	22.753	1.986
GF-30-1-40-3	14.816	0.837	21.566	1.613
GF-30-1-40-4	-	-	25.481	1.972
GF-30-1-40-5	14.819	1.083	23.172	1.911
GF-30-1-40-6	17.268	1.295	23.203	1.938



(a) GF-30-1-40-1



(b) GF-30-1-40-2



(c) GF-30-1-40-3



(d) GF-30-1-40-4



(e) GF-30-1-40-5



(f) GF-30-1-40-6

Figure 4-31 The 28 Days Force-Deflection Graphs of GF Treated with Optimum Plasma Condition

Figure 4-31 shows cracks in the fibrous composite treated with flow rate 1 l/min, at distance 30mm and treatment duration of 40 seconds argon plasma. Plasma application revealed that the possibility of multiple crack formation in 28-day samples is lower compared to composites prepared with PPF1.

4.5.3.4 28 Days Bending Performance of Plasma Treated BF Fibre Composites

The bending test of a composite prepared with plasma treated PPF1 was performed using the method presented in Section 3.4.2.2.

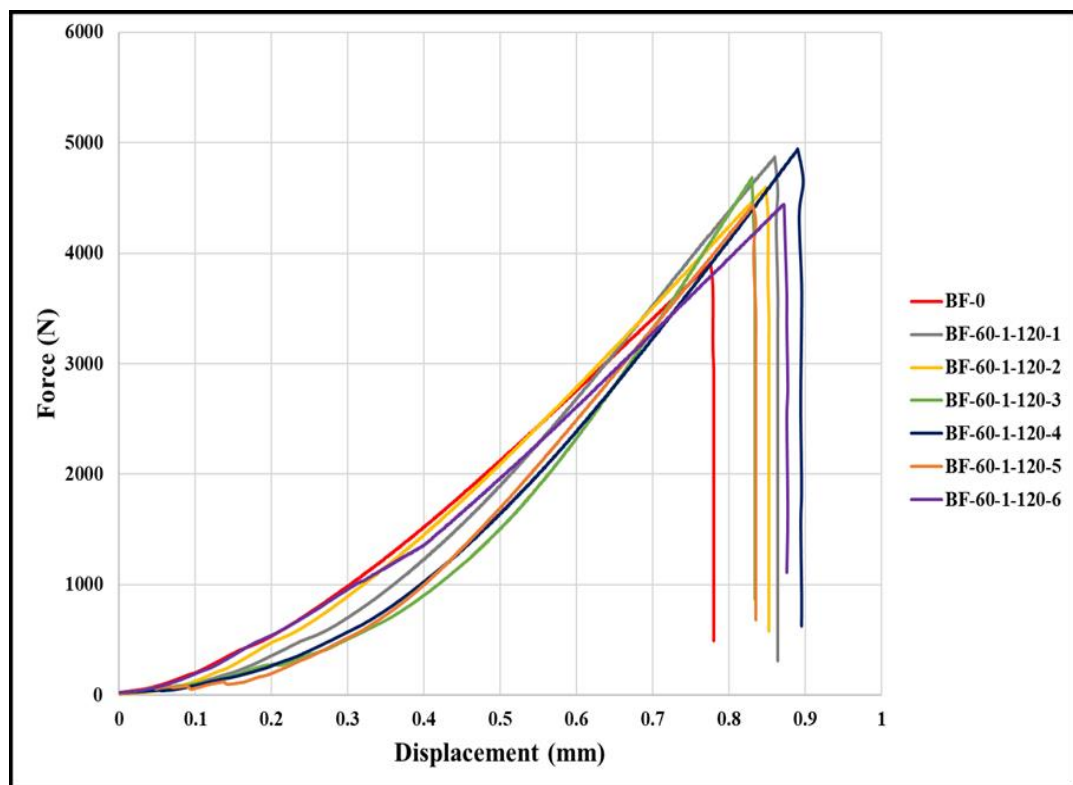


Figure 4-32 The 28 Days Force-Deflection Graphs of BF Treated with Optimum Plasma Condition

The 28-days characteristic load-deflection graph of BF composites is presented in Figure 4-32 for untreated and plasma treated six specimens. The results obtained from these graphs can be related to fibre-matrix adherence as they are obtained when the first crack is forced to form in the middle of the specimen. The increase in the load

and deflection values of the plasma treated specimens can be observed in these graphs but the increase factor is insignificant compared to the PPF1 and GF.

Increased bending strength values of treated specimens was exceeded 13.43 MPa for all specimens as shown in Table 4-11. The flexural strength value increased from 11.49 MPa to 14.16 MPa. This increase could be attributed to the changes in the surface, usually micro sized or nano sized roughness of the BF were revealed by SEM and AFM analysis methods mentioned earlier in section 4.4.2.3 and section 4.4.3.3. In addition, singular crack behaviour was observed in all the treated BF specimens as in the case of the untreated ones.

Table 4-11 The 28 Days Flexural Test Results of BF Reinforced Cementitious Specimens

PPF 28 Days	First cracking strength (MPa)	Deflection at first cracking load (mm)	Flexural strength at max. load (MPa)	Deflection at maximum load (mm)
BF-0	-	-	11.94	0.776
BF-60-1-120-1	-	-	14.814	0.860
BF-60-1-120-2	-	-	13.985	0.847
BF-60-1-120-3	-	-	14.164	0.826
BF-60-1-120-4	-	-	15.066	0.889
BF-60-1-120-5	-	-	13.436	0.827
BF-60-1-120-6	-	-	13.528	0.867

4.5.4 General Evaluation of mechanical Characterization Variations Affected by Plasma Application on PPF1, GF and BF

The single fibre tensile test for treated and untreated fibres confirmed that plasma treatment of fibres does not affect significant change to the mechanical performance of the fibres. Table 4-12 presents the difference between tensile strength of fibres before and after plasma treatment.

Table 4-12 Tensile Strength Difference

Fibre Type	Difference in Tensile Strength (%)
PPF1	-1.446
GF	+1.674
BF	+1.631

The changes in the surface properties of the fibres caused by the plasma application have also improved the single fibre pull-out strength, τ_{IFSS} and composite bending performance considerably. However, it is not possible to generalize the use of a specific plasma condition, despite the study of the three fibre examples, because the changes that the plasma brings to the surface in each type of fibre are different depending on the properties of the materials treated. Therefore, the composite performance due to the plasma effect should be evaluated separately for each fibre type.

Comparing the single fibre pull-out strength and τ_{IFSS} performances of PPF1-60-2-120 and PPF1-60-2-200, it was determined that the effect of longer plasma treatment has an insignificant effect on the bonding performance between the fibre and matrix.

Therefore, the optimum plasma condition was decided to be at a distance of 60 mm, with a flow rate of 1 l/min and a treatment duration of 120 sec.

Like the PPF1, in a comparison made between GF-30-1-40, GF-60-1-120 and GF-60-1-200 on single fibre pull-out test and τ_{IFSS} performances, it was found that longer exposure to plasma does not contribute to the further fibre-cement enhancement. Therefore, the optimum plasma condition was determined to be at a distance of 30 mm, with a flow rate of 1 l/min and a treatment duration of 40 sec.

When 28 days Single fibre pull-out performances of BF were compared, the most effective plasma conditions were at a distance 60 of mm, with a flow rate of 1 l/min and a 120 sec treatment duration. Table 4-13 presents the comparison between the enhancements of pull-out behaviour of different fibres, which reveal that plasma application is more effective in GF than for PPF1 and BF.

Table 4-13 Comparison of plasma effect on the pull-out behaviour of fibres

Fibre Type	Difference in F_{max} (%)	Difference in τ_{IFSS} (%)
PPF1	+31.57	+31.16
GF	+26.67	+76.92
BF	+23.29	+22.95

It was determined that the three different fibrous cement-based composites examined in this project affected the load-deflection behaviours in different ways. The highest performance is obtained from GF in terms of flexural strength values. Whereas, PPF1 exhibited better capacity in post cracking energy absorption behaviour. BF made a small enhancement in the performance of the composite. Table 4-14 presents the

comparison between the bending strength improvement of all fibres before and after plasma treatment.

Table 4-14 Comparison between plasma effect on bending strength values for different fibres

Fibre Type	Fibre Volume (%)	Strength Plain Concrete (MPa)	Strength Fibrous Concrete (MPa)	Difference (%)
PPF1	1.25	11.209	13.257	+16.74
GF	1.5	11.209	14.742	+27.22
BF	1.25	11.209	11.884	+5.84

Plasma effect on bending strength varied for each fibre type. Table 4-15 presents the bending strength improvement for all fibres.

Table 4-15 Comparison of bending strength improvement for different fibres

Fibre Type	Difference in Bending Strength (%)
PPF1	+40.88
GF	+49.32
BF	+17.01

4.5.4.1 Evaluation of Bending Performances of PPF1 Fibre Composites

Composites using PPF1 showed multiple crack behaviour under all optimum plasma conditions. When multiple crack behaviour was examined, it was determined that the plasma effect mostly increased both the number of cracks and that the crack spread over a wider area in the sample. It has been determined that there is a strong relationship between multiple crack behaviour and post cracking behaviour, since each

new crack opening increases the number of load-bridging fibres of the composites. The alteration approaching of the brittle structure of the cementitious composite to the considerable ductile behaviour will affect the performance of the building elements, which are to be manufactured in the composite, in a positive way.

When the values obtained from optimum the plasma conditions were examined, bending strength improvement up to 40.88% was observed in the PPF1 composite. The extraordinary performance increase is due to the multiple crack behaviour observed in these specimens. In the case of the same age untreated PPF1, the multiple cracking phenomenon was not apparent. This result proves that the plasma effect increases the fibre-matrix adherence. In the characterization of the fibres' surface roughness, it has been found that plasma causes changes in the surface as shown previously in Figure 4-12. The Rms values are increased by the plasma effect and the surface is roughened at the nano scale. The fluid consistency of the matrix in its fresh state may have improved the physical adherence by filling this roughness and cracks in the most appropriate way.

4.5.4.2 Evaluation of Bending Performances of GF Fibre Composites

GF fibres have produced very high-performance composites in terms of both strength and post cracking properties. The tensile strength of these fibres reached 650 MPa which could be the reason for the increase in composite performance. However, it is intended that the composites prepared with these fibres should achieve a higher bending strength values by plasma application, since their surfaces are contaminated and hydrophobic.

From the bending test for GF, it was found that the bending strength is significantly greater (49.32%) compared to the untreated GF specimens. The application of plasma

conditions has often resulted in surface ablations of GF and the formation of a new decontaminated surface free from weak layers. This resulted in enhancing the bond between the GF and the cement matrix. Although there is no increase in roughness, the increase in bending strength can be explained by the decontamination of GF proved by the AFM analysis made, which showed that the Rms value of GF reduced after plasma application. Therefore, a better new bond between the plasma treated GF and the cement matrix, which resulted in the increases in fibre-matrix adherence, and this led to the improvement in the GF composite bending performance.

4.5.4.3 Evaluation of Bending Performances of BF Fibre Composites

Given the absence of observable fibres in the cracked cross-section of BF specimens, the poor post-crack behaviour was not surprising even after plasma treatments. Even after the exposure of the fibres to plasma treatment, BF was not observable by eye in the cracked section, and therefore, some degree of deformation and degradation in the fibres in the alkali cement matrix was assumed. Regardless, the plasma treatment increased the maximum load and deflection at maximum load, and thus, provided some benefit.

4.5.5 Summary

In this research study, contact angle measurements were conducted on PPF1 and GF for plasma condition optimisation. However, CAM using a sessile drop technique could not be applied to thinner micro sized fibres such as BF. From the CAM results, a significant reduction in wettability angles was observed, and the best plasma condition was determined for all the different fibre types. The plasma effect on the surface morphology and roughness was evaluated and it was found that the effect varies according to the material treated. Surface etching was predominant in PPF1 and BF, however, surface decontamination in the case of GF. Single fibre tensile tests were conducted to examine any negative impact of plasma treatment on the mechanical performance of the individual fibres. It was found that the effect of plasma treatment on the tensile strength of the fibres is minimal and that the change could be attributed to the huge variation of the fibres. Pull-out tests were also performed to investigate the plasma effect on the fibre/cement bonding characteristics. Despite the different effects of the plasma treatment on the surface morphology and the nano roughness of the fibres, all the treated fibres showed an improvement in the bonding performance with the matrix. Moreover, from the pull-out tests, the optimum plasma condition for each type of fibre was established. Finally, the bending performance of the untreated and plasma treated composites were compared. It was found that the plasma treatments have a positive impact on the performance of the composites. The improvement values vary according to the material treated.

Chapter 5 Conclusions and Recommendations

5.1 Introduction

The core purpose and contribution of this study was to develop and design a novel microwave induced plasma torch for the continuous surface modification of fibres to produce fibre reinforced cementitious composites. The purpose of surface modifications of fibres was to improve the surface energy and morphology, and thus, enhance adhesion with the matrix. This will contribute to the improvement of fibrous composite products used in the building material producing industry. It was found that the developed plasma system contributed to the enhancement of the surface properties of the fibres and makes it possible to produce composite elements with high mechanical properties and improved post cracking energy absorption capacities. The improved crack arresting properties of the material brings the possibility of its being used in concrete structures exposed to harsh environments where the degradations of concrete members due to the corrosion of steel reinforcement is the main problem. This has been attained by undertaking comprehensive experimental works on various types of corrosion resistant fibres such as (macro polypropylene, glass and basalt fibre) and various plasma conditions (different distances from the plasma jet, different flow rates and different treatment durations).

The experimental investigation was conducted in two phases. In the first phase, the plasma condition was optimised using contact angle measurement for polypropylene and glass fibre. Surface morphology in micro and nano scales were performed for fibres treated with the optimum plasma conditions using scanning electron microscopy and atomic force microscopy. Fibre/cement bonding were investigated by the mean of single fibre pull-out test. Cylindrical concrete specimens were prepared with single

plasma treated fibres inserted in the centre to be compared with the controlled untreated fibres to predict the impact of plasma treatment on the bonding performance with the cementitious matrix. The second phase of the experimental study focused mainly on the structural behaviour of prismatic specimens of fibre reinforced composites prepared with treated fibres and compared with the untreated control specimens. In this study, important findings on the surface characteristics, pull-out behaviour and flexural performance of plasma treated fibres and plasma treated cementitious composites were obtained. The findings reported here can be applied in the production of high-performance fibre reinforced concrete.

5.2 Conclusions

This study allowed to note that the plasma treatment system can be operated for enhancing the surface properties of fibres, thus, the performance of the composite.

In this section, all the findings described are presented. For simplicity, the conclusions have been separated into three sections, each concentrating on the results stated in Chapters 4.

5.2.1 Surface Characterisation

5.2.1.1 Contact Angle Measurement (CAM)

In all the different types of fibres, plasma exposure caused a reduction in contact angle measurement. The recorded reduction in CAM was + 66.67%, and +69.18% for PP1 and GF respectively.

The material properties of the treated fibre have an influence on the optimum plasma condition. The optimum plasma condition for each fibre was in contrast with the plasma temperature and the melting point of the fibre. Generally, the lower the melting point of the fibre, the lower the optimum plasma temperature.

5.2.1.2 Surface Morphology (SEM) and (AFM)

Plasma treatment alters the surface morphology of each fibre in different ways. In the case of PPF1 and BF, plasma etching was predominant as plasma treatment roughened the smooth surfaces. Longitudinal cracks and grooves developed on the surface of PPF1 and a few bumps and lumps appeared on the BF. Therefore, nano roughness values were increased. In the case of GF, the effect of plasma treatment mainly contributed to the ablation and removal of weak surface boundaries. Due to surface decontamination of GF, the nano roughness values were reduced. Nano roughness values were +92.36%, -45.68% and +30.76% for PPF1, GF and BF respectively.

5.2.2 Mechanical Characterisation

5.2.2.1 Single Fibre Tensile Test

Plasma treatment does not affect the bulk properties of the materials, as it affects only a thin layer of the surface predominantly, in the scale of nanometers. Test results indicated that the effect of plasma application is relatively minimal for all three tested fibres. Tensile strength changes were -18.52%, +1.674% and -4.26% for PPF1, GF and BF respectively. It was concluded that these small changes in the mechanical performance could be attributed to the variations of fibre size of a similar batch.

5.2.2.2 Single Fibre Pull-Out Test

The fibre-cement τ_{IFSS} , for all the fibre types were enhanced. In the case of PPF1 and BF, this could be attributed to the enhancement of fibre-cement interlocking, due to the etching and increased surface after plasma exposure. On the other hand, in the GF the improvement of τ_{IFSS} , was due to the removal of weak boundaries and decontamination of the fibre surface. The τ_{IFSS} , improved by 31.16% , 72.92% and 22.95% for PPF1, GF and Bf respectively.

5.2.2.3 Flexural Test

By considering the current state of the surface properties of the fibres, it is possible to increase both the multi-crack potential and the bending strength when modified for the purpose according to the fibre type. Therefore, the plasma treatment of PPF1, GF and BF enhanced the performance of the composites. This change provided the potential for multiple crack formation in all series of PPF1 fibres and cracks caused the expansion of the fracture spread in the specimen. It also allowed the PPF1 to increase the load level carried by the first crack after peeling, to a considerable extent, allowing for improvement in the post cracking behaviour. The same modification method has been applied to GF. Very few of the GF specimens underwent multiple cracking behaviour. However, plasma treatment did not affect the post cracking behaviour of BF composites. The addition of BF improved the first-crack strength of composites subjected to flexural loading but did not contribute to the post-cracking behaviour enhancement. The bending strength improvements were 40.88%, 49.32% and 11.49% for PP1, GF and BF respectively.

5.2.3 General Conclusion

There is a potential in using the developed plasma system in enhancing the mechanical properties of fibre reinforced cementitious composites. It is possible to enhance the surface characterisation of low surface energy fibres in more cost-effective ways compared to conventional low-pressure plasma treatments. The improved fibre-cement interfacial properties, bending strength and extraordinary crack arresting will make it possible for this novel system to be used as a treatment technique in producing construction materials for concrete structures.

5.3 Recommendations for Future Work

Due to the timespan and facility limitations of this research, it was not possible to consider some vital areas. These are recommended below for future research:

1. Further investigation on how to improve the plasma system so that the plasma temperature remains constant over a long period of treatment. This is a crucial process particularly when plasma treatment is applied to continuous fibres.
2. In plasma condition optimisation of micro fibres such as BF, a proper CAM technique should be considered for such a small sized fibre. This will allow us to precisely predict the optimum plasma condition that could deliver positive alteration to the surface of these fibres. Thus, the reliability of plasma applications to these fibres will be confirmed.
3. Chemical analysis of the surface of the fibres before and after plasma exposure is a vital process to verify the surface modifications and any possible functional groups induced by plasma application that could cause the reduction of CAM. This would offer an additional and detailed analysis and conclusion of the absolute contributions of each mechanism on wettability and interfacial bonding.
4. Further experimental studies on other types of fibres such as natural fibres and micro polypropylene fibres are required for future applications of plasma treatments to produce fibre reinforced concrete especially when the fibre/cement adhesion is of great concern. Furthermore, the long-term effect of plasma treatment on surface characteristics of fibres is crucial to verify the validity of plasma application.

5. Analyse the surface characteristic of fibres at various post-treatment intervals to identify the time-frame in which the composite can be produced using treated fibres.
6. Further experimental investigations of concrete strengthened with plasma treated fibres is required to verify the impact of plasma treatments of fibres on the mechanical and structural behaviour of the composite. Furthermore, investigating the long-term mechanical and structural performance of plasma treated fibre reinforced composites is vital to verify the applicability of the plasma technique on the production of fibre reinforced cementitious composites.
7. Investigating various concrete mixes produced using various additives is also of great importance to highlight the applicability of plasma treatment on a great range of commercially available cementitious mixtures and its compatibility with various additives.
8. Further modifications to the plasma treatment test rig are important so that continuous fibres could be treated on both sides in a shorter time and pultruded to be chopped to desired sizes later. In addition, this could speed up the treatment process duration when a relatively large amount of fibres is required to be treated for an application.
9. Further studies on plasma conditions should be considered. Different gases might bring different surface characterisation, thus, different impact on the performance of the composites.

References

- Ababneh, A., Al-Rousan, R., Alhassan, M. and Alqadami, M. (2017) Influence of Synthetic Fibers on the Shear Behavior of Lightweight Concrete Beams. *Advances in Structural Engineering*, 20 (1), 1671-1683.
- Abe, D.K., Ngo, M.T., Levush, B., Antonsen Jr, T.M., Danly, B.G. and Chernin, D. (2000) Modeling Single- and Multi-Carrier Performance of a Helix TWTA with the 1-D Parametric Code, CHRISTINE. *IEEE MTT-S International Microwave Symposium Digest*, 3, 1727-1730.
- Abrishambaf, A., Pimentel, M. and Nunes, S. (2017) Influence of Fibre Orientation on the Tensile Behaviour of Ultra-High Performance Fibre Reinforced Cementitious Composites. *Cement and Concrete Research*, 97, 28-40.
- ACI 544 1R-96 (2002) State-of-the-Art Report on Fibre Reinforced Concrete 70 (11), 729-744.
- Adasooriya, N., Samarakoon, S. and Gudmestad, O. (2017) *Corrosion Propagation Phase and Bond Strength Degradation of Reinforced Concrete Structures: State of the Art*.
- Adusumalli, R.B., Weber, H.K. and Roeder, T. (2010) Evaluation of Experimental Parameters in the Microbond Test with Regard to Lyocell Fibers. *Journal of Reinforced Plastics and Composites*, 29 (15), 2356-2367.
- Al-Shamma'a, A.I., Wylie, S.R., Lucas, J. and Pau, C.F. (2001) Design and Construction of a 2.45 GHz Waveguide-Based Microwave Plasma Jet at Atmospheric Pressure for Material Processing. *Journal of Physics D: Applied Physics*, 34 (18), 2734-2741.
- Alani, A.M. and Beckett, D. (2013) Mechanical Properties of a Large Scale Synthetic Fibre Reinforced Concrete Ground Slab. *Construction and Building Materials*, 41, 335-344.
- Alvares, V.A., Ruscekait, R.A. and Vazquez, A. (2003) Mechanical Properties and Water Absorption Behaviour of Composites made from a Biodegradable Matrix and alkaline-Treated Sisal Fibres. *Composite Materials*, 37 (17), PP. 1575-1590.
- Amin, A., Foster, S.J., Gilbert, R.I. and Kaufmann, W. (2017) Material Characterisation of Macro Synthetic Fibre Reinforced Concrete. *Cement and Concrete Composites*, 84, 124-133.

Anandan, S., Vallarasu Manoharan, S. and Sengottian, T. (2014) Corrosion Effects on the Strength Properties of Steel Fibre Reinforced Concrete Containing Slag and Corrosion Inhibitor. *International Journal of Corrosion*, 2014.

Anandaraj, S., Rooby, J., Awoyera, P.O. and Gobinath, R. (2018) Structural Distress in Glass Fibre-Reinforced Concrete under Loading and Exposure to Aggressive Environments. *Construction and Building Materials*, 197 (10), 862-870.

ASTM D2256/ D2256M (2010) *Standard Test Method for Tensile Properties of Yarns by the Single-Strand Method*.

ASTM D3822 (2007) *Standard Test Method for Tensile Properties of Single Textile Fibers*.

Babafemi, A.J. and Boshoff, W.P. (2015) Tensile Creep of Macro-Synthetic Fibre Reinforced Concrete (MSFRC) under Uni-Axial Tensile Loading. *Cement and Concrete Composites*, 55, 62-69.

Balouch, S.U., Forth, J.P. and Granju, J.L. (2010) Surface Corrosion of Steel Fibre Reinforced Concrete. *Cement and Concrete Research*, 40 (3), 410-414.

Banthia, N. (2005) Flexural Responce of Hybrid Fibre Reinforced Cementitious Composites. *ACI Material Journal*, 102 (6), pp. 382-389.

Baron, J. (1987) Technical and Economical Aspects of the Use of Limestone Filler Additions in Cement. *World cement*, 100-104.

Bartschat, K. and Kushner, M.J. (2016) Electron Collisions with Atoms, Ions, Molecules, and Surfaces: Fundamental Science Empowering Advances in Technology. *Proceedings of the National Academy of Sciences*, 113 (26), 7026-7034.

Bentur, A. (2000) Role of Interfaces in Controlling Durability of Fiber-Reinforced Cements. *Journal of Materials in Civil Engineering*, 12 (1), 2-7.

Bentur, A., Mindess, S. and Vondran, G. (1989) Bonding in Polypropylene Fibre Reinforced Concretes. *International Journal of Cement Composites and Lightweight Concrete*, 11 (3), 153-158.

Bentur, A., Peled, A. and Yankelevsky, D. (1997) Enhanced Bonding of Low Modulus Polymer Fibers-Cement Matrix by Means of Crimped Geometry. *Cement and Concrete Research*, 27 (7), 1099-1111.

Borcia, G., Anderson, C.A. and Brown, N.M.D. (2006) Surface Treatment of Natural and Synthetic Textiles Using a Dielectric Barrier Discharge. *Surface and Coatings Technology*, 201 (6), 3074-3081.

Borhan, T.M. (2012) Properties of Glass Concrete Reinforced with Short Basalt Fibre. *Materials and Design*, 42, 265-271.

Boulos, M.I., Fauchais, P. and Pfender, E. (2013) Thermal Plasmas: Fundamentals and Applications. In: (ed.) 1 ed.: Springer Science & Business Media. pp. 1-41.

Brandan, B., Tosun, K. and Felekoglu, B. (2008) *Applicability of Cold Plasma Techniques in the Production of High Performance polymer Fibre Reinforced Cement Mortar Composites.TUBITAK Research project (MAG 107M170).*

Brandt, A.M. (2008) Fibre Reinforced Cement-Based (FRC) Composites after ver 40 Years of Development in Building and Civil Engineering. *Composite Structures*, 86 (3), 3-9.

Branston, J., Das, S., Kenno, S.Y. and Taylor, C. (2016) Mechanical Behaviour of Basalt Fibre Reinforced Concrete. *Construction and Building Materials*, 124, 878-886.

BS EN 12390-5 (2009) *Testing Hardened Concrete. Flexural Strength of Test Specimens.*

BS EN 14845-1:2007 (2007) *Test Methods for Fibres in Concrete. Reference Concretes.*

Buratti, N., Mazzotti, C. and Savoia, M. (2011) Post-cracking Behaviour of Steel and Macro-Synthetic Fibre-Reinforced Concretes. *Construction and Building Materials*, 25 (5), 2713-2722.

Burgoyne, C. (2001) Non-Metallic Reinforcement for Concrete. *Concrete*, 35 (6), 14.

Chan, Y.-W. (1994) *Fiber/Cement Bond Property Modification in Relation to Interfacial Microstructure.* Doctoral Dissertation thesis, University of Michigan.

Chan, Y.-W. and LI, V.C. (1997) Age Effect on the Characteristics of Fibre/Cement Interfacial Properties. *Journal of Materials Science*, 32 (19), 5287-5292.

Chen, P., Wang, J., Wang, B., Li, W., Zhang, C., Li, H. and Sun, B. (2008) Improvement of Interfacial Adhesion for Adhesion for Plasma Treated Aramid Fibre

Reinforced Poly(Phthalazinone Ether Sulfone Ketone) Composite and Fibre Surface Ageing Effect. *Surface and Interface Analysis*, 41, 38-43.

Chua, P.s. and Piggott, M.R. (1985) The Glass fibre-polymer Interface : II work of fracture and shear stresses. *Composites Part A: Applied Science and Manufacturing*, 22, PP. 107-119.

Craven, J.P., Cripps, R. and Viney, C. (2000) Evaluating the Silk/Epoxy Interface by Means of the Microbond Test. *Composites Part A: Applied Science and Manufacturing*, 31 (7), PP. 653-660.

Deák, T. and Czigány, T. (2009) Chemical Composition and Mechanical Properties of Basalt and Glass Fibers: A Comparison. *Textile Research Journal*, 79 (7), 645-651.

Denes, F., Feldman, D., Hua, Z.Q., Zheng, Z. and Young, R.A. (1999) Cementitious-Matrix Composites from SiCl₄-Plasma-Activated Polypropylene Fibres. *Adhe Science and Technology*, 10 (1), 61-77.

Denes, F.S. and Manolache, S. (2004) Macromolecular Plasma-Chemistry: an Emerging Field of Polymer Science. *Progress in Polymer Science*, 29 (8), 815-885.

Dvorak, J.A. (2003) The Application of Atomic Force Microscopy to the Study of Living Vertebrate Cells in Culture. *Methods*, 29 (1), 86-96.

Eliasson, B. and Kogelschatz, U. (1991) Nonequilibrium Volume Plasma Chemical Processing. *IEEE transactions on plasma science*, 19 (6), 1063-1077.

Erdogmus, E. (2015) Use of Fiber-Reinforced Cements in Masonry Construction and Structural Rehabilitation. *Fibers*, 3 (1), 41-63.

Falconnet, D., Csucs, G., Michelle Grandin, H. and Textor, M. (2006) Surface Engineering Approaches to Micropattern Surfaces for Cell-based Assays. *Biomaterials*, 27 (16), 3044-3063.

Farhat, F.A., Nicolaidis, D., Kanellopoulos, A. and Karihaloo, B.L. (2007) High Performance Fibre-Reinforced Cementitious Composite (CARDIFRC) – Performance and Application to Retrofitting. *Engineering Fracture Mechanics*, 74 (1), 151-167.

Farris, S., Pozzoli, S., Biagioni, P., Duó, L., Mancinelli, S. and Piergiovanni, L. (2010) The Fundamentals of Flame Treatment for the Surface Activation of Polyolefin Polymers – A review. *Polymer*, 51 (16), 3591-3605.

- Fauchais, P. and Vardelle, A. (2000) Pending Problems in Thermal Plasmas and Actual Development. *Plasma Physics and Controlled Fusion*, 42 (12B), 365-383.
- Favia, P., Creatore, M., Palumbo, F., Colaprico, V., d'Agostino, R. and (2001) Process Control for Plasma Processing of Polymers. *Surface and Coatings Technology*, 142-144, 1-6.
- Feldman, D., Denes, F., Zeng, Z., Denes, A.R. and banu, D. (2000) Polypropylene Fibre-Matrix Bonds in Cementitious Composites. *Adhesion Science and Technology*, 14 (13), 1705-1721.
- Felekoglu, B., Tosun-Felekoglu, K., Ranade, R., Zhang, Q. and Li, V.C. (2014) Influence of Matrix Flowability, Fiber Mixing Procedure, and Curing Conditions on the Mechanical Performance of HTPP-ECC. *Composites Part B: Engineering*, 60, 359-370.
- Felekoglu, B., Tosun, K. and Baradan, B. (2009) A comparative Study on the Flexural Performance of Plasma Treated Polypropylene Fibre Reinforced Cementitious Composites. *Journal of Materials Processing Technology*, 209 (11), 5133-5144.
- Feng, G., Wang, X., Zhang, D., Cao, H., Qian, K. and Xiao, X. (2017) A comparative Study on Mechanical Properties of Surface Modified Polypropylene (PP) Fabric Reinforced Concrete Composites. *Construction and Building Materials*, 157, 372-381.
- Ferrara, L. (2019) High Performance Fibre Reinforced Cementitious Composites: Six Memos for the XXI Century Societal and Economical Challenges of Civil Engineering. *Case Studies in Construction Materials*, 10 (2), e00219.
- Ferrara, L., Krelani, V., Moretti, F., Roig Flores, M. and Serna Ros, P. (2017) Effects of Autogenous Healing on the Recovery of Mechanical Performance of High Performance Fibre Reinforced Cementitious Composites (HPFRCCs): Part 1. *Cement and Concrete Composites*, 83, 76-100.
- Foti, D. (2011) Preliminary Analysis of Concrete Reinforced with Waste Bottles PET Fibers. *Construction and Building Materials*, 25 (4), 1906-1915.
- Fu, X. (2012) *Active Screen Plasma Surface Modification of Polymeric Materials for Biomedical Application*. Doctoral Dissertation thesis, University of Birmingham.
- Gabouze, N. (2002) Electrochemical Properties of Plasma-Modified Si Surfaces. *Surface Science*, 507, 695-699.

Gao, S.L., Mäder, E. and Plonka, R. (2004) Coatings for Glass Fibers in a Cementitious Matrix. *Acta Materialia*, 52 (16), 4745-4755.

Gao, Z., Peng, S., Sun, J., Yao, L. and Qiu, Y. (2009) Influence of Processing Parameters on Atmospheric Pressure Plasma Etching of Polyamide 6 Films. *Applied Surface Science*, 255 (17), 7683-7688.

Garbassi, F., Morra, M. and Occhiello, E. (1998) Polymer Surfaces: from Physics to Technology. *American Institute of Chemical Engineers*, 42 (9), 2699-2700.

Gijsbertus, J. and Terlingen, A. (1993) *Introduction of Functional Groups at Polymer Surfaces by Glow Discharge Techniques*.

Gilmour, A. (2011) Travelling Wave Tube. In: (ed.) *Klystrons, Traveling Wave Tubes, Magnetrons, Crossed-Field Amplifiers, and Gyrotrons*. 1st ed.: Artech house. pp. 317-340.

Goddard, J.M. and Hotchkiss, J.H. (2007) Polymer Surface Modification for the Attachment of Bioactive Compounds. *Progress in Polymer Science*, 32 (7), 698-725.

Goldman, M. and Sigmond, R. (1982) Corona and Insulation. *IEEE Transactions on Electrical Insulation* (2), 90-105.

Granju, J.-L. and Ullah Balouch, S. (2005) Corrosion of Steel Fibre Reinforced Concrete From the Cracks. *Cement and Concrete Research*, 35 (3), 572-577.

Guerrini, G.L. (2000) Applications of High-Performance Fiber-Reinforced Cement-Based Composites. *Applied Composite Materials*, 7 (2), 195-207.

Guo, D., Xie, G. and Luo, J. (2014) Mechanical Properties of Nanoparticles: Basics and Applications. *Journal of Physics D: Applied Physics*, 47 (1), 13-25.

Han, J.W., Lee, S.K., Jeon, J.H., Yu, C., Oh, R.O. and Park, C.G. (2015) Strength and Durability Characteristics of Latex-Modified Jute/Macro-Synthetic Hybrid Fibre-Reinforced Concrete. *Materials Research Innovations*, 19 (sup5), S5-894-S895-897.

Hannant, D.J., Zonsveld, J.J. and Hughes, D.C. (1978) Polypropylene Film in Cement Based Materials. *Composite*, 8 (2), 8-83.

Hawai-Chung, W. and Victor, C.L. (1999) Fiber/Cement Interface Tailoring with Plasma Treatment *Cement and Concrete Composites*, 21 (3), 205-212.

Henriksen, T., Lo, S. and Knaack, U. (2016) A New Method to Advance Complex Geometry Thin-Walled Glass Fibre Reinforced Concrete Elements. *Journal of Building Engineering*, 6, 243-251.

High, C., Seliem, H.M., El-Safty, A. and Rizkalla, S.H. (2015) Use Of Basalt Fibers For Concrete Structures. *Construction and Building Materials*, 96, pp. 37-46.

Höcker, H. (2002) Plasma Technology for Textile Fibres. *Pure and applied chemistry*, 74 (3), 423-427.

Homola, T., Matoušek, J., Kormunda, M., Wu, L.Y.L. and Černák, M. (2013) Plasma Treatment of Glass Surfaces Using Diffuse Coplanar Surface Barrier Discharge in Ambient Air. *Plasma Chemistry and Plasma Processing*, 33 (5), 881-894.

Hong, Y.C. and Uhm, H.S. (2001) Electrodeless Microwave Plasma-Torch at Atmospheric Pressure. *IEEE Conference Record - Abstracts. PPPS-2001 Pulsed Power Plasma Science 2001. 28th IEEE International Conference on Plasma Science and 13th IEEE International Pulsed Power Conference (Cat. No.01CH37, 17-22 June 2001 of Conference.*

Hozbor, M. (1993) Plasma Processes Boost Bondability of rubber and metal. *Adhesives Age*, 62 (36), 5-32.

Huang, F., Wei, Q., Wang, X. and Xu, W. (2006) Dynamic Contact Angles and Morphology of PP Fibres Treated with Plasma. *Polymer Testing*, 25 (1), 22-27.

Humud, H.R., Abbas, Q.A. and Rauuf, A.F. (2015) Effect of Gas Flow Rate on The Electron Temperature, Electron Density and Gas temperature for Atmospheric Microwave Plasma Jet. *International Journal of Current Engineering and Technology*, 5 (3), 2277-4106.

Hwang, J.P., Jung, M.S., Kim, M. and Ann, K.Y. (2015) Corrosion Risk of Steel Fibre in Concrete. *Construction and Building Materials*, 101 (P1), 239-245.

Intrater, R., Hoffman, A., Lempert, G., Gouzman, I. and Grossman, E. (2006) Effect of Imaging Techniques on the Observed Surface Morphology of Oxygen Plasma Etched Polyethylene Fibres. *Polymer Degradation and Stability*, 91 (9), 1948-1953.

ISO 11566:1996 (1996) *Carbon Fibre-Determination of the Tensile Properties of Single-Filament Specimens.*

Jacobs, T., Morent, R., De Geyter, N., Desmet, T., Dubruel, P. and Leys, C. (2010) Effect of Humid air Exposure Between Successive Helium Plasma Treatments on PET Foils. *Surface and Coatings Technology*, 205 (7), 2256-2261.

James, T., Peter, J. and Liu, Y. (2016) Glass Fibre Strength—A Review with Relation to Composite Recycling. *Fibers*, 4 (2), 18.

Jeroen Jonkers, Marco Van de Sande, Antonio Sola, Antonio Gamero and Mullen, J.v.D. (2002) On the Differences Between Ionizing Helium and Argon Plasmas at Atmospheric Pressure. *Plasma Sources Science and Technology*, 12 (1), 30-38.

Kan, C.W. and Yuen, C.W.M. (2013) Effect of Atmospheric Pressure Plasma Treatment on Wettability and Dryability of Synthetic Textile Fibres. *Surface and Coatings Technology*, 228, S607-S610.

Kang, S.-B., Tan, K.H., Zhou, X.-H. and Yang, B. (2017) Influence of Reinforcement Ratio on Tension Stiffening of Reinforced Engineered Cementitious Composites. *Engineering Structures*, 141, 251-262.

Karihaloo, B.L. and Wang, J. (2000) Mechanics of Fibre-Reinforced Cementitious Composites. *Computers & Structures*, 76 (1), 19-34.

Khorasani, M.T., Mirzadeh, H. and Kermani, Z. (2005) Wettability of Porous Polydimethylsiloxane Surface: Morphology Study. *Applied Surface Science*, 242 (3-4), 339-345.

Kim, K.N., Lee, S.M., Mishra, A. and Yeom, G.Y. (2016) Atmospheric Pressure Plasmas for Surface Modification of Flexible and Printed Electronic Devices: A Review. *Thin Solid Films*, 598, 315-334.

Kim, M.T., Kim, M.H., Rhee, K.Y. and Park, S.J. (2011) Study on an Oxygen Plasma Treatment of a Basalt Fiber and its Effect on the Interlaminar Fracture Property of Basalt/Epoxy Woven Composites. *Composites Part B: Engineering*, 42 (3), 499-504.

Koch, G., Varney, J., Thompson, N., Moghissi, O., Gould, M. and Payer, J. (2016) International Measures of Prevention, Application, and Economics of Corrosion Technologies Study. *NACE International IMPACT Report*.

Kostov, K.G., dos Santos, A.L.R., Honda, R.Y., Nascente, P.A.P., Kayama, M.E., Algatti, M.A. and Mota, R.P. (2010) Treatment of PET and PU Polymers by Atmospheric Pressure Plasma Generated in Dielectric Barrier Discharge in Air. *Surface and Coatings Technology*, 204 (18), 3064-3068.

Kuk, K.J. and Kaushik, P. (2011) Surface Modifications in WPC with Pre-Treatment Methods. In: (ed.) *Recent Advances in the Processing of Wood-Plastic Composites*. Springer Science and Business Media. pp. 23-57.

Kurkjian, C.R., Gupta, P.K., Brow, R.K. and Lower, N. (2003) The Intrinsic Strength and Fatigue of Oxide Glasses. *Journal of Non-Crystalline Solids*, 316 (1), 114-124.

Kusano, Y., Mortensen, H., Stenum, B., Kingshott, P., Andersen, T.L., Brøndsted, P., Bilde-Sørensen, J.B., Sørensen, B.F. and Bindselev, H. (2007) Atmospheric Pressure Plasma Treatment of Glass Fibre Composite for Adhesion Improvement. *Plasma Processes and Polymers*, 4 (S1), S455-S459.

Kusano, Y., Singh, S.V., Bardenshtein, A., Krebs, N. and Rozlosnik, N. (2010) Plasma Surface Modification of Glass-Fibre-Reinforced Polyester Enhanced by Ultrasonic Irradiation. *Journal of Adhesion Science & Technology*, 24 (11/12), 1831-1839.

Lai, J., Sunderland, B., Xue, J., Yan, S., Zhao, W., Folkard, M., Michael, B.D. and Wang, Y. (2006) Study on Hydrophilicity of Polymer Surfaces Improved by Plasma Treatment. *Applied Surface Science*, 252 (10), 3375-3379.

Lee, H., Ohsawa, I. and Takahashi, J. (2015) Effect of Plasma Surface Treatment of Recycled Carbon Fiber on Carbon Fiber-Reinforced Plastics (CFRP) Interfacial Properties. *Applied Surface Science*, 328 (C), 241-246.

Lee, S.D., Sarmadi, M., Denes, F. and Shohet, J.L. (1997) Surface Modification of Polypropylene Under Argon and Oxygen-RF-Plasma Conditions. *Plasmas and Polymers*, 2 (3), 177-197.

Leis, F. and Broekaert, J.A.C. (1984) A High Power Microwave Induced Plasma for the Analysis of Solutions. *Spectrochimica Acta Part B: Atomic Spectroscopy*, 39 (9), 1459-1463.

Li, R., Ye, L. and Mai, Y.-W. (1997) Application of Plasma Technologies in Fibre-Reinforced Polymer Composites: A Review of Recent Developments. *Composites Part A: Applied Science and Manufacturing*, 28 (1), 73-86.

Li, S., Han, K., Rong, H., Li, X. and Yu, M. (2014) Surface Modification of Aramid Fibers via Ammonia- Plasma Treatment. *J. Appl. Polym. Sci.*, 131 (10).

Li, V.C. (2001) Large Volume, High-Performance Applications of Fibers in Civil Engineering. *Journal of Applied Polymer Science*, 83 (3), 660-686.

Li, V.C. and Stang, H. (1997) Interface Property Characterization and Strengthening Mechanisms in Fibre Reinforced Cement Based Composites. *Advanced Cement Based Materials*, 6 (1), 1-20.

- Li, V.C., Wang, Y. and Backer, S. (1987) Effect of Fiber-Matrix Bond Strength on the Crack Resistance of Synthetic Fiber Reinforced Cementitious Composites. *MRS Online Proceedings Library Archive*, 114.
- Li, V.C., Wang, Y. and Backer, S. (1990) Effect of Inclining Angle, Bundling and Surface Treatment on Synthetic Fibre Pull-Out From a Cement Matrix. *Composites*, 21 (2), 132-140.
- Li, V.C., Wu, H.C. and Chan, Y.W. (1996) Effect of Plasma Treatment of Polyethylene Fibers on Interface and Cementitious Composite Properties. *Journal of the American Ceramic Society*, 79 (3), 700-704.
- Li, X.L., Luo, M. and Wang, J. (2014) Experimental Research on Flexural Toughness of Green High Performance Fibre Reinforced Cementitious Composites. *Materials Research Innovations*, 18 (sup2), S2-43-S42-47.
- Li, Y., Hu, C. and Yu, Y. (2008) Interfacial Studies of Sisal Fiber Reinforced High Density Polyethylene (HDPE) Composites. *Composites Part A: Applied Science and Manufacturing*, 39 (4), 570-578.
- Li, Y., Manolache, S., Qiu, Y. and Sarmadi, M. (2016) Effect of Atmospheric Pressure Plasma Treatment Condition on Adhesion of Ramie Fibers to Polypropylene for Composite. *Applied Surface Science*, 364, 294-301.
- Lipatov, Y.V., Gutnikov, S.I., Manylov, M.S., Zhukovskaya, E.S. and Lazoryak, B.I. (2015) High Alkali-Resistant Basalt Fiber For Reinforcing Concrete. *Materials & Design*, 73, pp. 60-66.
- Lippert, T. (2005) Interaction of Photons with Polymers: From Surface Modification to Ablation. *Plasma Processes and Polymers*, 2 (7), 525-546.
- Liston, E.M., Martinu, L. and Wertheimer, M.R. (1993) Plasma Surface Modification of Polymers for Improved Adhesion: A Critical Review. *Journal of Adhesion Science and Technology*, 7 (10), 1091-1127.
- Liu, D., Song, J., Anderson, D.P., Chang, P.R. and Hua, Y. (2012) Bamboo Fiber and its Reinforced Composites: Structure and Properties. *Cellulose*, 19 (5), 1449-1480.
- Lopresto, V., Leone, C. and De Iorio, I. (2011) Mechanical Characterisation of Basalt Fibre Reinforced Plastic. *Composites Part B: Engineering*, 42 (4), 717-723.
- Lovata, N.L. and Fahmy, M.F. (1987) Interfacial Bond Study of a Chemically Treated Polypropylene Fibre-Reinforced Concrete. *Construction and Building Materials*, 1 (2), 83-87.

Lura, P. and Terrasi, G.P. (2014) Reduction of Fire Spalling in High-Performance Concrete by Means of Superabsorbent Polymers and Polypropylene Fibers: Small Scale Fire Tests of Carbon Fiber Reinforced Plastic-Prestressed Self-Compacting Concrete. *Cement and Concrete Composites*, 49, 36-42.

Mader, E. and Zhandarov, S. (2005) Characterization of Fiber/Matrix Interface Strength: Applicability of Different Tests, Approaches and Parameters. *Composites Science and Technology*, 65 (1), PP. 149-160.

Mahendra, M. (2017) Single and Double Stub Matching Techniques *Advanced Research in Engineering & Management*, 3 (4), 55-69.

Manchado, M.A.L., Arroyo, M., Biagiotti, J. and Kenny, J.M. (2003) Enhancement of Mechanical Properties and Interfacial Adhesion of PP/EPDM/Flax Fiber Composites Using Maleic Anhydride as a Compatibilizer. *Applied Polymer*, 90 (8), 2170-2178.

Marcos-Meson, V., Michel, A., Solgaard, A., Fischer, G., Edvardsen, C. and Skovhus, T.L. (2018) Corrosion Resistance of Steel Fibre Reinforced Concrete - A Literature Review. *Cement and Concrete Research*, 103, 1-20.

Massicotte, B. and Bischoff, P.H. (2000) Fibre Reinforced Concrete: A Structural Perspective. *Proceedings of the Fifth International RILEM Symposium-BEFIB*, 193-202.

Massines, F., Messaoudi, R. and Mayoux, C. (1998) Comparison Between Air Filamentary and Helium Glow Dielectric Barrier Discharges for the Polypropylene Surface Treatment. *Plasmas and Polymers*, 3 (1), 43-59.

Matthews, F.L. and Rawlings, R.D. (1999) Reinforcements and the Reinforcement–Matrix Interface. In: (ed.) *Composite Materials: Engineering and Science*. 1st ed.: Woodhead Publishing Limited. pp. 29-77.

Meng, L.J.Y.Y.Y. and Yan, Z. (2007) Experimental Research on the Mechanical Behaviour of Chopped Basalt Fibre Reinforced Concrete. *Industrial Construction*, 6 (002).

Meng, W., Valipour, M. and Khayat, K.H. (2017) Optimization and Performance of Cost-Effective Ultra-High Performance Concrete. *Materials and Structures*, 50 (1), 29.

Mobasher, B. and Cheng Yu, L. (1996) Effect of Interfacial Properties on the Crack Propagation in Cementitious Composites. *Advanced Cement Based Materials*, 4 (3), 93-105.

Moon, G.D., Oh, S., Jung, S.H. and Choi, Y.C. (2017) Effects of the Fineness of Limestone Powder and Cement on the Hydration and Strength Development of PLC Concrete. *Construction and Building Materials*, 135, 129-136.

Moon, S.I. and Jang, J. (1999) The Effect of the Oxygen-Plasma Treatment of UHMWPE Fiber on the Transverse Properties of UHMWPE-Fiber/Vinylester Composites. *Composites Science and Technology*, 59 (4), 487-493.

Moon, S.Y., Choe, W., S. Uhm, H., Hwang, Y.-s. and J. Choi, J. (2002) *Characteristics of an Atmospheric Microwave-Induced Plasma Generated in Ambient Air by an Argon Discharge Excited in an Open-Ended Dielectric Discharge tube.*

Morent, R. (2011) Plasma Surface Modification of Biodegradable Polymers: A Review. *Plasma Processes and Polymers*, 8 (3), 171-190.

Morent, R., De Geyter, N., Verschuren, J., De Clerck, K., Kiekens, P. and Leys, C. (2008) Non-Thermal Plasma Treatment of Textiles. *Surface and Coatings Technology*, 202 (14), 3427-3449.

Naaman, A. (1985) Fibre Reinforcement for Concrete. *Concrete International Journal*, 21-25.

Naaman, A. and Reinhardt, H. (1995) Characterization of High Performance Fiber Reinforced Cement Composites—HPFRCC. *High performance fiber reinforced cement composites* of Conference.

Naaman, A.E. (2003) Engineered Steel Fibers with Optimal Properties for Reinforcement of Cement

Composites. *Advanced Concrete Technology*, 1 (3), 241-252.

Naaman, A.E. (2008) High Performance Fiber Reinforced Cement Composites. In: (ed.) *High-performance construction materials: Science and applications*. World Scientific. pp. 91-153.

Nairn, J.A. (2000) Analytical Fracture Mechanics Analysis of the Pull Out Test Including the Effects of Friction and Thermal Stresses. *Advanced Composite Letter*, 9 (6), 59-70.

Nordström, E. (2005) *Durability of Sprayed Concrete: Steel Fibre Corrosion in Cracks*. Doctoral Dissertation thesis, Luleå tekniska universitet.

Oladele L. and A., A. (2009) Development of Fibre Reinforced Cementitious Composite for Ceiling Application *Journal of Minerals & Materials Characterization & Engineering*, 8 (8), 583-590.

Oláh, A., Hempenius, M.A., Zou, S. and Vancso, G.J. (2006) Adhesion Studies of Latex Film Surfaces on the Meso- and Nanoscale. *Applied Surface Science*, 252 (10), 3714-3728.

Otto, W. (2002) Relationship of Tensile Strength of Glass Fibers to Diameter. *American Ceramic Society*, 38 (3), 122-125.

Pakravan, H.R., Jamshidi, M., Latifi, M. and Pacheco-Torgal, F. (2012) Evaluation of Adhesion in Polymeric Fibre Reinforced Cementitious Composites. *International Journal of Adhesion and Adhesives*, 32, 53-60.

Pakravan, H.R. and Memariyan, F. (2017a) Modification of Low-Surface Energy Fibers used as Reinforcement in Cementitious Composites: a Aeviuw. *Polymer-Plastics Technology and Engineering*, 56 (3), 227-239.

Pakravan, H.R. and Memariyan, F. (2017b) Modification of Low-surface Energy Fibers used as Reinforcement in Cementitious Composites: A Review. *Polymer-Plastics Technology & Engineering*, 56 (3), 227-239.

Pasquariello, D., Lindeberg, M., Hedlund, C. and Hjort, K. (2000) Surface energy as a function of self-bias voltage in oxygen plasma wafer bonding. *Sensors and Actuators A: Physical*, 82 (1), 239-244.

Payrow, P., Nokken, M.R. and Banu, D. (2011) Effect of Surface Treatment on the Post-Peak Residual Strength and Toughness of Polypropylene/Polyethylene-Blended Fiber-Reinforced Concrete. *Journal of Composite Materials*, 45 (20), 2047-2054.

Peled, A., Guttman, H. and Bentur, A. (1992) Treatments of Polypropylene Fibres to Optimize their Reinforcing Efficiency in Cement Composites. *Cement and Concrete Composites*, 14 (4), 277-285.

Piggott, M.R. (1993) The Single Fibre Pull-Out Method: its Advantages, Interpretation and Experimental Realization. *Composite Interface*, 1 (3), PP. 211-223.

Ping LU, X.C., Ming YANG (2015) Preparation of Ag-glass Fiber Composite by Plasma Treatment-continuous Immersion. *Chinese Journal of Materials Research*, 29 (1), 45-50.

Pisanova, E. (1997) Fracture Mechanics of Single-Fibre Pull-Out Test. *Material Science*, 32, PP. 483-490.

pisanova, E., Zhanndarov, S. and Mader, E. (2001) How can Adhesion be Determined from Micromechanical Test. *Composites Part A: Applied Science and Manufacturing*, 32, PP. 425-432.

Poletti, G., Orsini, F., Raffaele-Addamo, A., Riccardi, C. and Selli, E. (2004) Surface Morphology Changes of Poly(ethyleneterephthalate) Fabrics Induced by Cold Plasma Treatments. *Pramana*, 62 (4), 911-921.

Praveen, K.M., Thomas, S., Grohens, Y., Mozetič, M., Junkar, I., Primc, G. and Gorjanc, M. (2016) Investigations of Plasma Induced Effects on the Surface Properties of Lignocellulosic Natural Coir Fibres. *Applied Surface Science*, 368, 146-156.

Rao, K.S., Kumar, S.R. and Narayana, A.L. (2013) Comparision of Performance of Standard Concrete and Fibre Reinforced Standard Concrete Exposed to Elevated Temperatures. *American Journal of Engineering Research (AJER)*, 02 (03), PP. 20-26.

Ren, Y., Wang, C. and Qiu, Y. (2008) Aging of Surface Properties of Ultra High Modulus Polyethylene Fibers Treated with He/O₂ Atmospheric Pressure Plasma Jet. *Surface and Coatings Technology*, 202 (12), 2670-2676.

Richaud, E., Farcas, F., Divet, L. and Paul Benneton, J. (2008) Accelerated Ageing of Polypropylene Geotextiles, the Effect of Temperature, Oxygen Pressure and Aqueous Media on Fibers—Methodological Aspects. *Geotextiles and Geomembranes*, 26 (1), 71-81.

Russ, S., Pfender, E. and Strykowski, P.J. (1994) Unsteadiness and Mixing in Thermal Plasma jets. *Plasma Chemistry and Plasma Processing*, 14 (4), 425-436.

Rypla, R. and Vořechovský, M. (2017) Multiscale Probabilistic Modeling of a Crack Bridge in Glass Fiber Reinforced Concrete. *Applied and Computational Mechanics*, 11 (1), 59-68.

Sahmaran, M. and Yaman, I.O. (2007) Hybrid Fiber Reinforced Self-Compacting Concrete with a High-Volume Coarse Fly Ash. *Construction and Building Materials*, 21 (1), 150-156.

Sanaee, Z., Mohajerzadeh, S., Zand, K., Gard, F.S. and Pajouhi, H. (2011) Minimizing Permeability of PET Substrates Using Oxygen Plasma Treatment. *Applied Surface Science*, 257 (6), 2218-2225.

Sánchez Serrano, J., Ureña, A., Lazcano Ureña, S. and Blanco Varela, T. (2015) New Approach to Surface Preparation for Adhesive Bonding of Aeronautical Composites:

Atmospheric Pressure Plasma. Studies on the Pretreatment Lifetime and Durability of the Bondline. *Composite Interfaces*, 22 (8), 731-742.

Schutze, A., Jeong, J.Y., Babayan, S.E., Park, J., Selwyn, G.S. and Hicks, R.F. (1998) The Atmospheric-Pressure Plasma Jet: a Review and Comparison to other Plasma Sources. *IEEE transactions on plasma science*, 26 (6), 1685-1694.

Selwyn, G., Herrmann, H., Park, J. and Henins, I. (2001) Materials Processing Using an Atmospheric Pressure, RF-Generated Plasma Source. *Contributions to Plasma Physics*, 41 (6), 610-619.

Serna, P., Arango, S., Ribeiro, T., Núñez, A.M. and Garcia-Taengua, E. (2009) Structural Cast-in-Place SFRC: Technology, Control Criteria and Recent Applications in Spain. *Materials and Structures/Materiaux et Constructions*, 42 (9), 1233-1246.

Shah, A. and Ribakov, Y. (2011) Recent trends in Steel Fiber High-Strength Concrete. *Materials and Design*, 32 (8-9), 4122-4151.

Shahidi, S., Ghoranneviss, M. and Mozzenchi, B. (2012) Application of Plasma in Different Branches of Industries. *RMUTP International Conference: Textiles & Fashion 2012*,

Singh, S., Ransinchung, G.D. and Kumar, P. (2017) Effect of Mineral Admixtures on Fresh, Mechanical and Durability Properties of RAP Inclusive Concrete. *Construction and Building Materials*, 156, 19-27.

Singh, S., Shukla, A. and Brown, R. (2004a) Pullout Behavior of Polypropylene Fibers from Cementitious Matrix. *Cement and Concrete Research*, 34 (10), 1919-1925.

Singh, S., Shukla, A. and Brown, R. (2004b) Pullout Behaviour of Polypropylene Fibres from Cementitious Matrix. *Cement and Concrete Research*, 34 (10), 1919-1925.

Singha, K. (2012) A Short Review on Basalt Fiber. *International Journal of Textile Science*, 1 (4), pp. 19-28.

Skacelova, D., Fialova, M., Stahel, P. and Cernak, M. (2011) Improvement of Surface Properties of Reinforcing Polypropylene Fibres by Atmospheric Pressure Plasma Treatment. *30th International Conference on Phenomena in Ionized Gases (ICPIG)*,

Sørensen, B.F. and Lilholt, H. (2016) Fiber Pull-Out test and Single Fiber Fragmentation Test-Analysis and Modelling. *IOP Conference Series: Materials Science and Engineering of Conference*.

Švorčík, V., Kolářová, K., Slepíčka, P., Macková, A., Novotná, M. and Hnatowicz, V. (2006) Modification of Surface Properties of High and Low Density Polyethylene by Ar Plasma Discharge. *Polymer Degradation and Stability*, 91 (6), 1219-1225.

Tang, K. (2017) Stray Current Induced Corrosion of Steel Fibre Reinforced Concrete. *Cement and Concrete Research*, 100, 445-456.

Tendero, C., Tixier, C., Tristant, P., Desmaison, J. and Leprince, P. (2006) Atmospheric Pressure Plasmas: A Review. *Spectrochimica Acta Part B: Atomic Spectroscopy*, 61 (1), 2-30.

Tosun, K., Felekoğlu, B. and Baradan, B. (2012) Multiple Cracking Response of Plasma Treated Polyethylene Fiber Reinforced Cementitious Composites Under Flexural Loading Under Flexural Loading. *Cement and Concrete Composites*, 34 (4), 508-520.

Trejbal, J., Smilauer, V., Kromka, A., Potocky, S. and Kopecky, L. (2015) *Wettability Enhancement of Polymeric Micro Fibre Reinforcement by Plasma Treatment*. Czech Technical University, Faculty of Civil Engineering, Prague, Czech Republic. EU: Czech Academy of Science, Institute of Physics.

Tuominen, M., Lahti, J. and Kuusipalo, J. (2011) Effects of Flame and Corona Treatment on Extrusion Coated Paper Properties. *Tappi Journal*, 10 (10), 29-37.

Tyata, R.B., Subedi, D.P., Shrestha, A. and Baral, D. (2012) Development of Atmospheric Pressure Plasma Jet in Air. *Kathmandu University Journal of Science, Engineering and Technology*, 8 (1), 15-22.

Uhm, H.S., Hong, Y.C. and Shin, D.H. (2006) A Microwave Plasma Torch and its Applications. *Plasma Sources Science and Technology*, 15 (2), 183-188.

Vandewalle, L. (2007) Post Cracking Behaviour of Hybrid Steel Fibre Reinforced Concrete. In *Mechanics of Concrete and Concrete Structures- FraMCoS, Proceedings of the 6th International Conference*, 17-22

Vohrer, U., Hegemann, D. and Oehr, C. (2003) XPS, AES, and AFM as Tools for Study of Optimized Plasma Functionalization. *Analytical and Bioanalytical Chemistry*, 375 (7), 34-929.

Vrijdaghs, R., Prisco, M.d. and Vandewalle, L. (2017) Short-Term and Creep Pull-out Behavior of Polypropylene Macrofibers at Varying Embedded Lengths and Angles from a Concrete Matrix. *Construction and Building Materials*, 147, 53-61.

Wallbank, E. (1989) *The Performance of Concrete in Bridges. A survey of 200 Highway Bridges.*

Wang, C.X., Du, M., Lv, J.C., Zhou, Q.Q., Ren, Y., Liu, G.L., Gao, D.W. and Jin, L.M. (2015) Surface Modification of Aramid Fiber by Plasma Induced Vapor Phase Graft Polymerization of Acrylic Acid. I. Influence of Plasma Conditions. *Applied Surface Science*, 349, 333-342.

Wang, G.J., Liu, Y.W., Guo, Y.J., Zhang, Z.X., Xu, M.X. and Yang, Z.X. (2007) Surface Modification and Characterizations of Basalt Fibers with Non-Thermal Plasma. *Surface and Coatings Technology*, 201 (15), 6565-6568.

Wang, S., Le, H.T.N., Poh, L.H., Feng, H. and Zhang, M.H. (2016) Resistance of High-Performance Fiber-Reinforced Cement Composites Against High-Velocity Projectile Impact. *International Journal of Impact Engineering*, 95, 89-104.

Wang Xiaodong, Peng Xiaofeng and Buxuan, W. (2004) Contact Angle Hysteresis on Rough Solid Surfaces. *Heat Transfer-Asian Research*, 33 (4), 201-210.

Wei, Q.F. (2004) Surface Characterization of Plasma-Treated Polypropylene Fibers. *Materials Characterization*, 52 (3), 231-235.

Weiming Lu, Fu, X. and Chung, D. (1998) A Comparative Study of the Wettability of Steel, Carbon, and Polyethylene Fibers by Water. *Cement and Concrete Research*, 28, 783-786.

Włodarczyk, M. and Jedrzejewski, I. (2016) Concrete Slabs Strengthened with Basalt Fibres – Experimental Tests Results. *Procedia Engineering*, 153, 866-873.

Wolf, R.A. (2012) Plasmas for Surface Modifications. In: (ed.) *Atmospheric Pressure Plasma for Surface Modification*. 1st ed. Somerset, UNITED STATES: John Wiley & Sons, Incorporated. pp. 27-54.

Won, J.P., Lim, D.H. and Park, C.G. (2006) Bond Behaviour and Flexural Performance of Structural Synthetic Fibre-Reinforced Concrete. *Magazine of Concrete Research*, 58 (6), 401-410.

Xiaochun, Q., Xiaoming, L. and Xiaopei, C. (2017) The Applicability of Alkaline-Resistant Glass Fiber in Cement Mortar of Road Pavement: Corrosion Mechanism and Performance Analysis. *International Journal of Pavement Research and Technology*, 10 (6), 536-544.

Yamamoto, T., Okubo, M., Imai, N. and Mori, Y. (2004) Improvement on Hydrophilic and Hydrophobic Properties of Glass Surface Treated by Nonthermal Plasma Induced by Silent Corona Discharge. *Plasma Chemistry and Plasma Processing*, 24 (1), 1-12.

Yan, L., Jenkins, C.H. and Pendleton, R.L. (2000) Polyolefin Fiber-Reinforced Concrete Composites: Part I. Damping and Frequency Characteristics. *Cement and Concrete Research*, 30 (3), 391-401.

Yan, X., Yang, L., An, Y., Jin, W., Li, Y. and Li, B. (2015) Surface Roughness and Hydrophilicity Enhancement of Polyolefin-Based Membranes by Three Kinds of Plasma Methods. *Surface and Interface Analysis*, 47 (4), 545-553.

Yang, G., Feng, Y., Yang, Y., Wang, D. and Kou, C. (2016) A study of Surface Modification of E-glass Fiber by Low Temperature Plasma Treatment. *2016 IEEE International Conference on High Voltage Engineering and Application (ICHVE)*, 19-22 Sept. 2016 of Conference.

Yang, L. and Thomason, J.L. (2010) Interface Strength in Glass Fibre–Polypropylene Measured Using the Fibre Pull-Out and Microbond Methods. *Composites Part A: Applied Science and Manufacturing*, 41 (9), 1077-1083.

Yang, S. and Yin, H. (2007) Two Atmospheric-pressure Plasma Sources for Polymer Surface Modification. *Plasma Chemistry and Plasma Processing*, 27 (1), 23-33.

Yao, W., Li, J. and Wu, K. (2003) Mechanical Properties of Hybrid Fiber-Reinforced Concrete at Low Fiber Volume Fraction. *Cement and Concrete Research*, 33 (1), 27-30.

Yin, S., Tuladhar, R., Riella, J., Chung, D., Collister, T., Combe, M. and Sivakugan, N. (2016) Comparative Evaluation of Virgin and Recycled Polypropylene Fibre Reinforced Concrete. *Construction and Building Materials*, 114, 134-141.

Zhang, C., Gopalaratnam, V.S. and Yasuda, H.K. (1999) Plasma Treatment of Polymeric Fibres for Improved Performance in Cement Matrices *Applied Polymer Science*, 76, 1985-1996.

Zhang, C., Zhao, M., Wang, L., Qu, L. and Men, Y. (2017) Surface Modification of Polyester Fabrics by Atmospheric-Pressure Air/He Plasma for Color Strength and Adhesion Enhancement. *Applied Surface Science*, 400, 304-311.

Zhang, S., Huang, G., Wang, X., Huang, Y., Yang, J. and Li, G. (2013) Effect of Air Plasma Treatment on the Mechanical Properties of Polyphenylene Sulfide/Glass Fiber Cloth Composites. *Journal of Reinforced Plastics and Composites*, 32 (11), 786-793.

Zhang, Y., Li, E. and Wang, C. (2015) Analysis and Measurement of Radiant Wavelength of Microwave Focused Lenses. 15, 1130-1131

Zhou, Y., Fan, M. and Chen, L. (2016) Interface and Bonding Mechanisms of Plant Fibre Composites: An Overview. *Composites Part B: Engineering*, 101, 31-45.

Zhu, D., Mobasher, B., Erni, J., Bansal, S. and Rajan, S.D. (2012) Strain Rate and Gage Length Effects on Tensile Behavior of Kevlar 49 Single Yarn. *Composites Part A: Applied Science and Manufacturing*, 43 (11), 2021-2029.

Zohdi, T.I. and Steigmann, D.J. (2002) The Toughening Effect of Microscopic Filament Misalignment on Macroscopic Ballistic Fabric Response. *International Journal of Fracture*, 118 (4), 71-76.

Zong, L. and Grubb, D.T. (1994) Single Fibre Polymer Composites. *Material Science*, 29, PP. 189-202.